Leveraging Sparsity in Variational Data Assimilation

A THESIS
SUBMITTED TO THE FACULTY OF THE GRADUATE SCHOOL
OF THE UNIVERSITY OF MINNESOTA
BY

Mohammad Ebtehaj

IN PARTIAL FULFILLMENT OF THE REQUIREMENTS
FOR THE DEGREES OF
MASTER OF SCIENCE

Gilad Lerman

September, 2013

Acknowledgments

There are many people that have earned my gratitude for their contribution to my life and especially during my graduate school at the University of Minnesota. In particular, I would like to express my sincere thanks to Professor Gilad Lerman, my adviser in the school of mathematics, who showed me the way and supported my academic endeavors with patience and care. I am indebted to my PhD adviser Professor Efi Foufoula-Georgiou in the department of civil engineering. I would like to express my utmost gratitude to her, who paved the way and my academic accomplishments would not have been possible without her generous support and guidance. My appreciations are also extended to Professor Arnd Scheel, a dedicated teacher, who kindly admitted to serve as a committee member of this thesis and I owe him fundamental parts of my knowledge in linear algebra.

Dedications

To my parents: Eshrat Saffari and Ali A. Ebtehaj who scarified their youth for their children and have been the origin of my academic aspirations.

To my lovely wife: Sara Khanzadi who has been an honest and patient witness to all of the good and bad days of my academic endeavors and supported me through every step of the way.

Abstract

Nowadays data assimilation is an essential component of any effective environmental prediction system. Environmental prediction models are, indeed, initial value problems and their forecast skills highly depend on the quality of their initialization. Data assimilation (DA) seeks the best estimate of the initial condition of a (numerical) model, given observations and physical constraints coming from the underlying dynamics. This important problem is typically addressed by two major classes of methodologies, namely sequential and variational methods. The sequential methods are typically built on the theory of mathematical filtering and recursive weighted least-squares, while the variational methods are mainly rooted in the theories of mathematical optimization and batch mode weighted least-squares. The former methods, typically use observations in sequential mode to obtain the best estimate of the geophysical state of interest at present time. In this thesis, we briefly review the mathematical and statistical aspects of classic data assimilation methodologies with particular emphasis on the family of variational methods. We explore the use of regularization in variational data assimilation problem and focus on sparsity-promoting approaches in a pre-selected basis. Central results suggest that in the presence of sparsity, the ℓ_1-norm regularization in an appropriately chosen basis produces more accurate and stable solutions than the classic data assimilation methods. To motivate further developments of the proposed methodology, assimilation experiments are conducted in the wavelet and spectral domain using the linear advection-diffusion equation.

Contents

List of Tables

List of Figures

Chapter 1

An Overview

1.1 Introduction and problem statement

Prediction of a dynamical system requires a realistic representation of the underlying dynamics by properly parametrized physical and/or stochastic models. These models typically rely on a set of realistic evolutionary equations that integrate the system states over time starting from pre-specified values at initial time, called *initial condition*s. Therefore, not only a realistic representation of the underlying process is necessary but also having an accurate estimate of the initial condition is essential to produce high quality and sufficiently skillful forecasts of the future behavior of the dynamical system. Typically an inaccurate estimate of the initial condition causes divergence of the model trajectories from the ground truth values. In environmental science communities, in short, data assimilation (DA) refers to the problem of using observational knowledge to determine the best estimate of the initial conditions of a physical or stochastic model to improve environmental predictability. Originated from the demand to improve the quality of weather prediction in the early twentieth century, nowadays this area of science is an essential component in effective atmospheric, oceanic and hydrologic predictive systems. A data assimilation system typically has four essential components including: 1) data collection, 2) analysis or diagnosis , 3) initialization, and 4) forecast or prognosis. In the data collection step, massive amount of environmental observations need to be collected and their quality need to be controlled. The data may include surface stations such as ground-based weather radars, gauges, radio sounds, aircraft data, ship reports, sounding balloons, and satellite observatory networks. These sensors provide measurements such as surface pressure, temperature, wind velocity, humidity, precipitation, soil moisture, evapo-transpiration, sea surface temperature. Quality of the measured data needs to be controlled and accepted data have to be registered to the desired grid points of the numerical models. In the analysis step, this information is being combined with any *background* knowledge about the initial conditions to obtain the

best estimate of the initial states. Then this best estimate or the *analysis* at the model grid points is used to initialize the model for *prediction* of the next time step. At the next time step, when new observations become available, the *forecast* state from the previous time can then be served as the *background* information to be combined with the observations for producing new analysis state and so on. This recursion proceeds to keep the model forecasts close enough to the ground truth states. The above steps are typically referred to as a data assimilation cycle.

Figure 1.1a (reproduced from *Kalnay* (2003, p. 3)) shows the S1 forecast quality metric for 36 and 72 hours prediction of 500 hPa atmospheric pressure surface in the past fifty years over North America [1]. The historical evolution of the S1 score in Figure (1.1) shows that the forecast skill has been dramatically improved in the past 50 years. In 1950 it is clear that the 36hr S1 score was in the middle of what was known empirically as the useless (S1=70%) and perfect forecasts (S1=20%). However, nowadays we are capable of producing forecasts with a perfect quality according to the standards of the fifty years ago in this respect. Figure 1.1 also shows that for the same S1 score the quality of 72hr forecast is now almost equal to the score of the 36hr forecast in the 10-20 years ago. *Kalnay* (2003) interpreted these improvements as a results of: (a) improved parametrization of atmospheric phenomena, (b) increased computational power that allows to capture smaller scale atmospheric features and to take into account more advanced parametrization schemes, (c) improved data assimilation methodologies, and (d) increased availability of high-quality data sources either form surface stations or from spaceborne sensors.

1.2 History and Evolution

As always, the early motivation was some failures in numerical atmospheric predictions. For example, Richardson on May 20, 1922 attempted to predict 6hr changes in surface pressure by fully integrating the primitive equations of motion in central Germany. The results was a complete failure despite the fact that many small and large scale atmospheric structures had been addressed in his modeling. In a retrospect review of his attempt *Platzman* (1967) argued that a major factor in that failure was due to inaccurate characterization of the

[1] The 500 hPa represents large scale atmospheric structure from mid to upper levels of the atmosphere. Mid level wind velocity and Rossby waves can be seen in the troughs and ridges of 500 hPa surface caused by mid-latitude cyclones and anticyclones. This surface pressure is also a very important indicator of the earth surface temperature.

The S1 score is a simple metric that has been vastly used in atmospheric science community for assessing weather forecast quality. The score is defined as:

$$S1 = 100 \frac{\left\| \nabla \mathbf{x}^f - \nabla \mathbf{y} \right\|_1}{\max\left(\left\| \nabla \mathbf{x}^f \right\|_1 , \left\| \nabla \mathbf{y} \right\|_1 \right)},$$

where, $\nabla(\cdot)$ is the gradient operator. Here $\mathbf{x}^f$ and $\mathbf{y}$ denote the forecast state and observations in $\mathbb{R}^m$, and the ℓ_1-norm is $\|\mathbf{x}\|_1 = \Sigma\, |x_i|$.

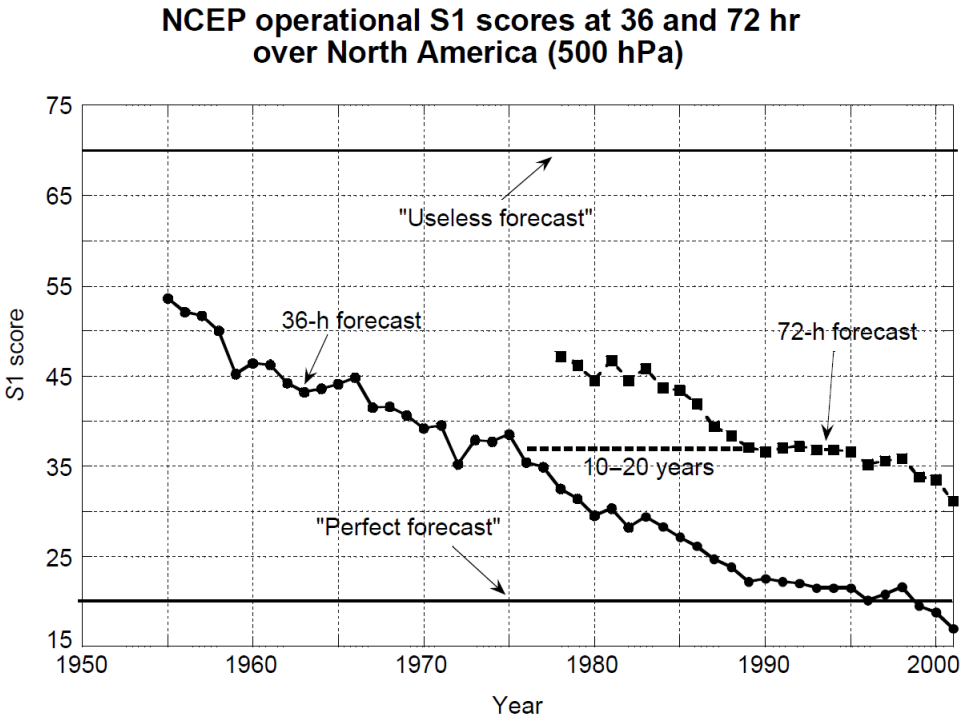

Figure 1.1: a) Historical evolution of the S1 forecast quality metric for 36 and 72hr forecasts of the 500 hPa atmospheric surface pressure in the past 50 years. The results indicate substantial improvements in forecast skills which is partly due to the advancements in the data assimilation methodologies. In this figure, the S1-score is calculated for the eastward (horizontal) direction and averaged over the area of interest. The S1=70% and 20% are empirically known as the useless and perfect forecasts, respectively (reproduced from (*Kalnay*, 2003) with data courtesy C.Vlcek at National Center for Environmental Predictions–NCEP).

initial conditions of the numerical simulation.

Complexity of initialization of environmental numerical models generally can be viewed from two different angles: (1) dimensionality and (2) sensitivity of the underlying model to its initial conditions. The dimension (number of grid points) of a synoptic or even a regional mesoscale numerical model can easily go up to the order of 10^7. Observations are typically noisy, irregularly collected, and are not completely available at all grid points of the numerical model for an accurate initialization. On the other hand, environmental prediction models are typically very sensitive to their initial conditions. In other words, a small perturbation in their initial conditions may give rise to trajectories which are drastically deviated from the true values (see the seminal work by *Lorenz*, 1963a,b, 1965, among others).

The early attempts to use observations for atmospheric model initializations had been performed by hand and were *subjective* to the knowledge of the forecaster. Isolines of temperature (isotherms), pressure (isobar), moisture, wind velocity (isotachs) were prepared

from a heterogeneous and irregularly spaced ground-based stations (point observations) to prepare diagnostic charts and maps for initialization of the numerical models. This process was tremendously tedious and time consuming, especially for large-scale (global) simulations. As a result, automated or the so-called *objective* methods gained more momentum by using spatial interpolation techniques to efficiently map scattered observations onto the regular grid points of the numerical models. The first attempts were primarily based on deterministic least squares fitting of the polynomial functions to the measurement points for producing an estimate of the initial conditions at the desired grid points (*Panofsky*, 1949; *Gilchrist and Cressman*, 1954; *Cressman*, 1959). These methods were typically local. In other words, to estimate the initial conditions in every grid point only finite number of adjacent observations were involved for least squares polynomial fitting. In addition to the available observations, *Gilchrist and Cressman* (1954) and *Bergthórsson and Döös* (1955) suggested to use a *background* field (previous forecast or climatological knowledge) for obtaining an improved estimate of the initial conditions. To combine the observations with the background field the idea was to first interpolate the available observations onto the model grid points and then subtract the background field from the interpolated observations to produce the field of *observation increments* or the so-called *innovation* field. The innovation field were then analyzed to obtain the *analysis increments* which were then added to the background field to produce the final *analysis* or *prognostic* field to be used to *forecast* the next time step. More specifically, let us assume that the interpolated observation field at initial time is an n-by-m field $\mathbf{Y} \in \mathbb{R}^{n \times m}$, while the background field is $\mathbf{X}^b \in \mathbb{R}^{n \times m}$. Then, the analysis field $\mathbf{X}^a \in \mathbb{R}^{n \times m}$ may be computed as follows:

$$\mathbf{X}^a = \mathbf{X}^b + \mathbf{K}(\mathbf{Y} - \mathbf{X}^b) \tag{1.1}$$

where, $\mathbf{K} \in \mathbb{R}^{n \times n}$ is a *weight* or *gain* matrix that encodes the relative contribution of observations in the final analysis field. In this formulation $\mathbf{Y} - \mathbf{X}^b$ is the observation increments and $\mathbf{K}(\mathbf{Y} - \mathbf{X}^b)$ denotes the analysis increments (see, *Gandin*, 1966). This idea has formed the building block of the modern data assimilation methodologies and motivated statistically driven approaches to incorporate observations based on their intrinsic error properties and proximity to the model grid points. For a through review of the historical evolution and more complete explanations, the reader is referred to (*Daley*, 1993; *Kalnay*, 2003).

1.3 Modern developments

1.3.1 Filtering Approaches

In mid 80's and early 90's, in parallel to advancements in the theories of recursive filtering and their promising applications in optimal control and aviation problems, we witnessed growing interests of using different variants of Kalman (*Kalman*, 1960) and Kalman and Bucy filters (*Kalman and Bucy*, 1961) for data assimilation problems in atmospheric and oceanic sciences. The early attempts in this area with appreciable impacts on operational practices trace back to the pioneering work by *Ghil et al.* (1981).

Basically, Kalman filter (KF) in its original formulation deals with estimating linear systems of first order stochastic differential equations. *Kalman* (1960) presented a recursive least-squares filter in a discrete space that can efficiently estimate the underlying dynamics of a first order auto-regressive Gaussian Markov process. Efficiency of the filter relies on the fact that in a first order linear dynamics, the covariance evolves in time through the linear discrete-time Lyapunov equation. Therefore, if noisy measurements are provided sequentially in time, the filter does not require to augment all of these measurements to obtain the least-squares error estimator of the state at the present time. The recursive formulation of the KF allows us to efficiently estimate large dimensional linear dynamical systems with minimal computational efforts. However, theoretically, KF only addresses linear dynamical systems in a Gaussian noise environment and is restrictive for non-linear and non-Gaussian state spaces. To tackle non-linear dynamical systems, the extended Kalman Filter (EKF)[2] was proposed that linearizes the inherent non-linearity of the system around the available best estimate of the state to exploit the basic formulation of the original Kalman filter. In its basic formulation, EKF utilizes the Jacobians or the first terms in a Taylor expansion of the involved nonlinear operators. Obviously, a higher order EKF that retains higher order Taylor expansion coefficients is plausible to be developed; however, additional complexity and convergence issues have prohibited its widespread applications in data assimilation community (*Miller et al.*, 1994; *Ghil*, 1997; *Kumar and Kaleita*, 2003, among others).

Evensen (1994a) and *Burgers et al.* (1998) introduced Ensemble Kalman Filter (EnKF), a simple but effective approach to deal with non-linearity in model and observation operators. The key idea was to approximate the posterior density function of the state by a set of samples. To this end, this filter utilizes a Monte Carlo approach to obtain an estimate of the mean and covariance of the state of interest to be used within the general context of the original formulation of the KF. It is ironic that almost more than two centuries after Johann Carl Friedrich Gauss (30 April 1777–23 February 1855) invented least-squares and

[2]The original development is known due to Stanley Smith at NASA Ames for spacecraft navigation problems (*Simon*, 2006).

more than four decades after Rudolf Kálmán who put it in a recursive context, the EnKF has received such a great deal of attention in the earth science community for data assimilation problems (*Houtekamer et al.*, 1996; *Burgers et al.*, 1998; *Houtekamer and Mitchell*, 1998; *Kepert*, 2009; *Houtekamer and Mitchell*, 2001; *Hamill et al.*, 2001; *Anderson*, 2001; *Ott et al.*, 2004; *Moradkhani et al.*, 2005b; *Zhou et al.*, 2006; *Hamill and Whitaker*, 2005; *Houtekamer et al.*, 2005; *Hunt et al.*, 2007; *Szunyogh et al.*, 2008; *Han et al.*, 2012; *Bateni and Entekhabi*, 2012, among many others).

More recently, advances in using Markov Chain Monte Carlo (MCMC) methods in target tracking and optimal control of nonlinear and non-Gaussian dynamical systems motivated applications in data assimilation problems. For nonlinear and non-Gaussian systems, typically, there is not any parametric model for the posterior density of estimate and often Monte Carlo methods are the only feasible options (*Doucet et al.*, 2001). Particle filter (e.g., *Arulampalam et al.*, 2002) is among the MCMC methods that have recently received appreciable attention in data assimilation community; although, its computational expense and degeneracy have been prohibitive for its widespread applications in large scale data assimilation problems. In particle filter, the key idea is to estimate the posterior density by drawing a sequence of sample values and their probability of occurrence from the unknown posterior density. Clearly, the accuracy of this filter heavily depends on the sample size. Generally speaking, this filter rely on the the sampling idea of Metropolis-Hasting algorithm. The samples are draw from a distribution which can be easily sampled (e.g., Gaussian) and being weighted based on a probability measure that determines their degree of membership to the posterior density. First attempts of using particle filter in data assimilation studies trace back to hydrologic data assimilation problems. For instance *Moradkhani et al.* (e.g., 2005a) used particle filter for hydrologic parameter estimation and state space uncertainty analysis, while *Zhou et al.* (2006) compared the particle filter with EnKF for land surface soil moisture data assimilation studies. More recently, in atmospheric science community, application of this filter is receiving more attention for estimation of non-linear dynamical systems (e.g., *van Leeuwen*, 2009, 2010).

1.3.2 Variational Approaches

The pioneering work by (*Sasaki*, 1970a) is among the first and the most insightful efforts to further formalize modern developments in variational data assimilation frameworks. In that work, Sasaki posed the data assimilation as a variational problem whose stationary point (the point with with zero first order derivative) is the desired analysis state. In (*Sasaki*, 1970a), a cost function is defined which encodes the Euclidean distance of the analysis only to observations, while the solution is constrained to the underlying prognostic system of equations. The presented formalism was solved for the strong and weak constraints. The strong constraints in his terminology were referred to the case where the solution is

fully constrained to the entire underlying system of prognostic equations, while in the weak constraints the solution is only partially constrained to the underlying dynamics via the so called low-pass filter in his terminology. Although, little is said about the convergence of the proposed formalisms and presented solution methods, Sasaki mentioned that " From the author's previous experiences in analysis of actual data by the variational method, it was found that adding simple low-pass filter terms to the functionals was helpful in obtaining converging solutions with less computer time. Also, it gives better results in data-sparse areas (such as over the ocean) and in noisy data areas (such as surface networks)". A closer look to the Sasaki's work reveals that the term he called "low-pass filter" is nothing but an extra cost representing the sum of squared of the first or second order derivatives of the analysis field. The motivation for extra cost was to partially constrain the solution to the unsteady or convective acceleration terms (i.e. $\partial(\cdot)/\partial t$ or $\partial(\cdot)/\partial x$) of the inertia term in primitive equations of motion. Surprisingly, the way he formulated the proposed formalism resembles the smoothing norm Tikhonov regularization (*Tikhonov et al.*, 1977), one of the most well known regularization method of all time, which has been vastly used in solving ill-posed inverse problems. Although, Sasaki empirically found that "adding a simple low-pass filter term " to the proposed variational cost function improves stability and speed of computations; nowadays we have good mathematical reasons to properly explain those advantages, which is one of the main topics of the future sections in this thesis. Note that in Sasaki's formulation of the data assimilation problem, he did not include any prior knowledge about the state of interest from the previous step of forecast and just focused on the available observations.

Another important stepping stone in the progress of the data assimilation science was due to the work by (*Lorenc*, 1981, 1986). In these works, following a Bayesian statistical approach, *Lorenc* (1986) introduced a variational cost function as follows:

$$\mathcal{J}_{3D}(\mathbf{x}_0) = (\mathbf{y} - \mathcal{H}(\mathbf{x}))^{\mathrm{T}} \mathbf{R}^{-1} (\mathbf{y} - \mathcal{H}(\mathbf{x})) + \left(\mathbf{x} - \mathbf{x}^b\right)^{\mathrm{T}} \mathbf{B}^{-1} \left(\mathbf{x} - \mathbf{x}^b\right), \tag{1.2}$$

where $\mathbf{x}_0 \in \mathbb{R}^m$ denotes the unknown initial state of interest, $\mathbf{y} \in \mathbb{R}^n$ is the observation, $\mathbf{x}^b \in \mathbb{R}^m$ is the background state, $\mathcal{H} : \mathbf{x} \rightarrow \mathbf{y}$ refers to the observation operator which maps the state space onto the observation space, and $\mathbf{R} \in \mathbb{R}^{n \times n}$ and $\mathbf{B} \in \mathbb{R}^{m \times m}$ denote the observation and background error covariance matrices, respectively. The above cost function is called the 3D-Var [3], whose minimizer is the analysis state,

$$\mathbf{x}_0^a = \underset{\mathbf{x}_0}{\operatorname{argmin}} \mathcal{J}_{3D}(\mathbf{x}_0). \tag{1.3}$$

The cost function in (1.2) encodes the weighted Euclidean distance of the unknown state

[3]This name is chosen because the cost function applies instantaneously in time and only accounts for the three spatial dimensions (x, y, z) of the problem at hand, without considering any temporal aspects (fourth dimension) aspects of the underlying prognostic equations.

$\mathbf{x}$ to the observation $\mathbf{y}$ and the background state $\mathbf{x}^b$ for ensuring that the analysis $\mathbf{x}_0^a$ is sufficiently close to both of them in the weighted least-squares sense. Note that, in the 3D-Var approach, the background state is taken into account; however, by construction it does not account for any temporal correlation or constraints coming from the underlying prognostic equations as suggested by (*Sasaki*, 1970a,b).

Primary extension of the 3D-Var scheme for constraining the solution to the temporal evolution of the underlying prognostic equations can be found in (*Thépaut et al.*, 1993; *Courtier et al.*, 1994, among others). In short, the so-called 4D-Var data assimilation is formulated as follows:

$$\begin{aligned} \mathcal{J}_{4D}(\mathbf{x}_0,\, \mathbf{x}_i) \quad &= \quad \sum_{i=0}^{k} \Big((\mathbf{y}_i - \mathcal{H}(\mathbf{x}_i))^{\mathrm{T}}\, \mathbf{R}_i^{-1}\, (\mathbf{y}_i - \mathcal{H}(\mathbf{x}_i)) \Big) + \frac{1}{2} \left\| \mathbf{x}_0^b - \mathbf{x}_0 \right\|_{\mathbf{B}^{-1}}^2 \\ &\text{s.t.} \quad \mathbf{x}_i = \mathcal{M}_{0,\,i}(\mathbf{x}_0),\ i = 0, \ldots, k, \end{aligned} \tag{1.4}$$

whose optimal solution is the analysis state. Note that, in the 4D-Var cost function, we not only use present time noisy observations of the initial state, but also we take into account a series of future discrete-time available observations of the evolved initial state under the prognostic equations. In problem (1.4), clearly, the prognostic equations are presented as a function that maps the initial state to the state at i^{th} time step, that is $\mathcal{M}_{0,\,i} : \mathbf{x}_0 \rightarrow \mathbf{x}_i$. A comprehensive treatment of the 4D-Var data assimilation and its implementation details in European Center for Median range Weather Forecast (ECMWF) center can be found in (*Courtier et al.*, 1994; *Rabier et al.*, 2000). More recently, some links between the above variational formulation of the data assimilation and Tikhonov regularization are explored and new insights are provided about the role of the Background state for stabilizing the solution of ill-conditioned data assimilation problem (*Johnson et al.*, 2005b,a). Very recently, inspired by the seminal works by *Tibshirani* (1996) and *Chen et al.* (1998) and contemporary developments in sparse regularization of inverse problems (e.g., *Hansen*, 2010; *Elad*, 2010), *Freitag et al.* (2012) and (*Ebtehaj and Foufoula-Georgiou*, 2013) proposed a regularized formulation for the 4D-Var data assimilation problem by adding an sparsity-promoting regularization term. The main motivation behind this proposed formulation was to improve the quality of data assimilation while the state of interest can be sparsely represented in a properly chosen domain.

Chapter 2 explains principles of mathematical filtering and their applications in data assimilation. The basics of recursive least-squares, Kalman filter, ensemble Kalman filter, unscented Kalman filter, and particle filter are briefly discussed. However, the central content of this chapter goes to variational data assimilation approaches, which are at the core of this thesis. The goal is establish the links between variational and filtering approaches, explain their statistical interpretations, and their roots in the theory of optimization and variational calculus. Chapter 3 is devoted to explain the concepts of regularization for solv-

ing ill-posed inverse problems and its application for variational data assimilation. This chapter focuses on recently developed sparse promoting regularization methods and their potential applications in variational data assimilation problems. In Chapter 4, a new regularized formulation is presented for variational data assimilation problem, which allows to incorporate potential sparsity of the state space in a pre-selected basis. This chapter presents the results of an sparse promoting regularized data assimilation approach and emphasize on its advantages. In particular, we extend the previous studies (*Freitag et al.*, 2012) in this area by: (a) proposing a generalized regularization framework for assimilating low-resolution and noisy observations while the initial state of interest exhibits sparse representation in a pre-selected basis (i.e., wavelet, discrete cosine transform); (b) extending the promise of the methodology to an advection-diffusion dynamics; and (c) proposing a new and efficient solution method for large-scale data assimilation problems. In this chapter, I show that if sparsity in a pre-selected basis holds, this prior information can serve to improve the accuracy and stability of data assimilation problems. To this end, using prototype studies, different initial conditions are selected, which are sparse under the wavelet and discrete cosine transformation (DCT). The promise of the ℓ_1-norm RVDA is demonstrated via assimilating down-sampled and noisy observations in a 4D-Var setting while strongly constraining the solution to the governing advection-diffusion equation. Chapter 5 concludes and delineates the roadmap for future studies. Specifically, it is explained that how we may exploit sparsity, while the underlying dynamics and observation operator might be nonlinear. Particular attention is given to explain Monte Carlo based approaches that can incorporate sparsity prior in the context of ensemble data assimilation.

Chapter 2

Mathematical Concepts of Data Assimilation

As previously explained data assimilation (DA) seeks the best estimate of the initial conditions of a (numerical) model given observations, background prior knowledge of the system state, and physical constraints coming from the underlying dynamics. In other words, at present time we have a set of noisy and incomplete observations together with a *Background* state, which typically is the previous forecast provided by the underlying model. The goal is to develop a mechanism to optimally combine all of this information to obtain the best estimate or *analysis* of the present state of the environmental system, while the analysis is consistent with the underlying prognostic model. This important problem is typically addressed by two major classes of methodologies, namely sequential and variational methods (*Ide et al.*, 1997), which are the subjects of the following subsections. We first briefly explain the sequential methods which are rooted in the theory of mathematical filtering and then devote our particular attention to the variational approaches which are mostly rooted in variational calculus and batch mode estimation.

2.1 Filtering Approaches

2.1.1 Weighted least squares

Recursive least squares is the building block of the Kalman Filter (KF), which we take this opportunity to briefly explain it in this subsection. The story begins with a simple weighted least squares (WLS) estimate of an unknown state from the following observation model. Let us suppose that $\mathbf{x} \in \mathbb{R}^m$ is a *constant parameter* or say a *fixed* quantity which is related

to our noisy observation $\mathbf{y} \in \mathbb{R}^n$ through the following linear (observation) model:

$$\mathbf{y} = \mathbf{H}\mathbf{x} + \mathbf{v} \tag{2.1}$$

where $\mathbf{H} \in \mathbb{R}^{n \times m}$ $(n > m)$ is called observation operator, $\mathbf{v} \sim \mathcal{N}(0, \mathbf{R})$ is an additive observation error coming from a zero mean Gaussian density uncorrelated with $\mathbf{x}$. Naturally, the minimum weighted least-squares estimate of $\mathbf{x}$, given the observations, amounts to minimizing the following cost function which is the weighted sum of squared error:

$$\begin{aligned} \mathcal{J}(\mathbf{x}) &= \mathbf{e}^{\mathrm{T}}\mathbf{R}^{-1}\mathbf{e} \\ &= (\mathbf{y} - \mathbf{H}\mathbf{x})^{\mathrm{T}} \mathbf{R}^{-1} (\mathbf{y} - \mathbf{H}\mathbf{x}) . \end{aligned} \tag{2.2}$$

Taking the partial derivative with respect to $\mathbf{x}$

$$\nabla_{\mathbf{x}} \mathcal{J} = \mathbf{H}^{\mathrm{T}}\mathbf{R}^{-1}(\mathbf{y} - \mathbf{H}\mathbf{x}), \tag{2.3}$$

we obtain the WLS estimate of the unknown parameter as follows:

$$\hat{\mathbf{x}} = \left(\mathbf{H}^{\mathrm{T}}\mathbf{R}^{-1}\mathbf{H}\right)^{-1} \mathbf{H}^{\mathrm{T}}\mathbf{R}^{-1}\mathbf{y}. \tag{2.4}$$

The above WLS has a unique solution while $\mathbf{R} \succ 0$ is positive definite and $\mathbf{H}$ is full (column) rank.

In the most simplest case where the observation operator is a square identity matrix in $\mathbb{R}^{m \times m}$ and the observation error is an uncorrelated Gaussian white noise, we get:

$$\hat{\mathbf{x}} = \left(\sum_i^m 1/\sigma_i^2 \right)^{-1} \sum_i^m \left(\frac{y_i}{\sigma_i^2} \right) \tag{2.5}$$

where y_i are elements of observation vector $\mathbf{y} \in \mathbb{R}^m$, $\mathbf{R} = \mathrm{diag}\left(\sigma_1^2, \ldots, \sigma_m^2\right)$ with $\mathbb{E}\left(v_i^2\right) = \sigma_i^2$ for $i = 1, \ldots, m$. This is reminiscent of the scalar weighted least-squares, we learned in high-school physics, to obtain the weighted mean of a data set while the weights are determined by the inverse of their variances.

Now assume that we are obtaining measurements sequentially in time and would like to update the best estimate of the state variable of interest $\mathbf{x}$, given the entire set of the past observations. In this case, using the above batch mode WLS solution, we need to augment all of the observation vectors, the observation operators, and then recompute our estimate at every time a new observation become available. It is clear that the computational cost of this problem can outgrow our computation resources quickly as the inversion of Hessian in (2.2), that is $\left(\mathbf{H}^{\mathrm{T}}\mathbf{R}^{-1}\mathbf{H}\right)^{-1}$, becomes computationally prohibitive.

2.1.2 Recursive weighted least squares

The key idea is to devise a methodology to obtain the best estimate of $\mathbf{x}$ recursively, without the need to keep and augment all of the available observations through time. To this end, we first focus on explaining the conditional expectation and its covariance of estimate in a Gaussian domain and then conclude about the linear least-squares recursive estimator, accordingly. Then, we dwell into a brief explanation of the Kalman Filter, Extended Kalman filter, ensemble Kalman filter, unscented Kalman filter, and particle filter.

2.1.2.1 Jointly Gaussian random variates

Let us assume that $\mathbf{x} \in \mathbb{R}^m$ and $\mathbf{y} \in \mathbb{R}^n$ are jointly Gaussian

$$\begin{bmatrix} \mathbf{x} \\ \mathbf{y} \end{bmatrix} \sim \mathcal{N}(\mathbf{m}, \mathbf{K})$$

where

$$\mathbf{m} = \begin{bmatrix} \mathbf{m_x} \\ \mathbf{m_y} \end{bmatrix} = \begin{bmatrix} \mathbb{E}(\mathbf{x}) \\ \mathbb{E}(\mathbf{y}) \end{bmatrix}$$

and

$$\mathbf{K} = \begin{bmatrix} \mathbf{C_x} & \mathbf{C_{xy}} \\ \mathbf{C_{yx}} & \mathbf{C_y} \end{bmatrix}$$

denotes the joint mean and covariance matrix. Here, the expected value of $\mathbf{x}$, its auto-covariance, and the cross-covariance matrices are:

$$\begin{aligned} \mathbb{E}(\mathbf{x}) &= \sum_{\mathbf{x} \in \mathcal{X}} \mathbf{x} p_{\mathbf{X}}(\mathbf{x}) \\ \mathbf{C_x} &= \mathbb{E}\left[(\mathbf{x} - \mathbb{E}(\mathbf{x}))(\mathbf{x} - \mathbb{E}(\mathbf{x}))^{\mathrm{T}} \right] \in \mathbb{R}^{m \times m} \\ \mathbf{C_{xy}} &= \mathbb{E}\left[(\mathbf{x} - \mathbb{E}(\mathbf{x}))(\mathbf{y} - \mathbb{E}(\mathbf{y}))^{\mathrm{T}} \right] \in \mathbb{R}^{m \times n}. \end{aligned}$$

In the above setting, the conditional density of $\mathbf{x}$ given $\mathbf{y}$ is as follows:

$$p_{\mathbf{x}|\mathbf{y}}(\mathbf{x}|\mathbf{y}) = \frac{1}{(2\pi)^{m/2} \left| \mathbf{C_{x|y}} \right|^{1/2}} \cdot \exp\left(-\frac{1}{2} (\mathbf{x} - \mathbf{m_{x|y}})^{\mathrm{T}} \mathbf{C}_{\mathbf{x}|\mathbf{y}}^{-1} (\mathbf{x} - \mathbf{m_{x|y}}) \right)$$

where

$$\mathbf{m_{x|y}} = \mathbf{m_x} + \mathbf{C_{xy}} (\mathbf{C_y})^{-1} (\mathbf{y} - \mathbf{m_y}), \tag{2.6}$$

and

$$\mathbf{C}_{\mathbf{x}|\mathbf{y}} = \mathbf{C}_{\mathbf{x}} - \mathbf{C}_{\mathbf{xy}}\mathbf{C}_{\mathbf{y}}^{-1}\mathbf{C}_{\mathbf{yx}}. \tag{2.7}$$

Given the observation model in (2.1), equations (2.6) and (2.7) can be further expanded and simplified. In other words, since the observation noise is uncorrelated with $\mathbf{x}$, we get

$$\begin{aligned}
\mathbf{C}_{\mathbf{xy}} &= \mathbb{E}\left[(\mathbf{x}-\mathbf{m}_{\mathbf{x}})(\mathbf{y}-\mathbf{m}_{\mathbf{y}})^{\mathrm{T}}\right] \\
&= \mathbb{E}\left[(\mathbf{x}-\mathbf{m}_{\mathbf{x}})(\mathbf{H}\mathbf{x}-\mathbf{H}\mathbf{m}_{\mathbf{x}})^{\mathrm{T}}\right] \\
&= \mathbb{E}\left[(\mathbf{x}-\mathbf{m}_{\mathbf{x}})(\mathbf{x}-\mathbf{m}_{\mathbf{x}})^{\mathrm{T}}\right]\mathbf{H}^{\mathrm{T}} \\
&= \mathbf{C}_{\mathbf{x}}\mathbf{H}^{\mathrm{T}}
\end{aligned} \tag{2.8}$$

and,

$$\begin{aligned}
\mathbf{C}_{\mathbf{y}} &= \mathbb{E}\left[(\mathbf{y}-\mathbf{m}_{\mathbf{y}})(\mathbf{y}-\mathbf{m}_{\mathbf{y}})^{\mathrm{T}}\right] \\
&= \mathbf{H}\mathbb{E}\left[(\mathbf{x}-\mathbf{m}_{\mathbf{x}})(\mathbf{x}-\mathbf{m}_{\mathbf{x}})^{\mathrm{T}}\right]\mathbf{H}^{\mathrm{T}} + \mathbb{E}\left[\mathbf{v}\mathbf{v}^{\mathrm{T}}\right] \\
&= \mathbf{H}\mathbf{C}_{\mathbf{x}}\mathbf{H}^{\mathrm{T}} + \mathbf{R}.
\end{aligned} \tag{2.9}$$

Therefore, given that $\mathbf{m}_{\mathbf{y}} = \mathbf{H}\mathbf{m}_{\mathbf{x}}$ in (2.1), the conditional expectation in equation (2.6) can be further simplified as,

$$\mathbf{m}_{\mathbf{x}|\mathbf{y}} = \mathbf{m}_{\mathbf{x}} + \mathbf{C}_{\mathbf{x}}\mathbf{H}^{\mathrm{T}}\left(\mathbf{H}\mathbf{C}_{\mathbf{x}}\mathbf{H}^{\mathrm{T}} + \mathbf{R}\right)^{-1}(\mathbf{y}-\mathbf{m}_{\mathbf{y}}). \tag{2.10}$$

On the other hand, it is easy to conclude that the conditional covariance in (2.7) can be expressed as follows:

$$\mathbf{C}_{\mathbf{x}|\mathbf{y}} = \mathbf{C}_{\mathbf{x}} - \mathbf{C}_{\mathbf{x}}\mathbf{H}^{\mathrm{T}}\mathbf{C}_{\mathbf{y}}^{-1}\mathbf{H}\mathbf{C}_{\mathbf{x}}. \tag{2.11}$$

2.1.2.2 Linear recursive least squares

Now let us get back to the key idea of designing a recursive least-squares estimator for a Gaussian random variable. Assuming that we are in the Gaussian domain, and the observation model is

$$\mathbf{y}_k = \mathbf{H}_k\mathbf{x}_k + \mathbf{v}_k. \tag{2.12}$$

In the above equation, we no longer assume that the state is a fixed quantity. On the other hand, we assume that it is a random process that can be explained by a probability density function. To put the estimation in a recursive context, let us suppose that we have the least squares estimate $\hat{\mathbf{x}}_{k-1}$ after $k-1$ measurements with covariance $\mathbf{C}_{k-1}$. The question is how can we devise a recursive estimator that allows us to obtain the least squares estimate $\hat{\mathbf{x}}_k$ only based on $\hat{\mathbf{x}}_{k-1}$ and the new measurement $\mathbf{y}_k$?

Following the expression in (2.10), one can cast a linear recursive least squares in the following form:

$$\hat{\mathbf{x}}_k = \hat{\mathbf{x}}_{k-1} + \mathbf{K}_k \left(\mathbf{y}_k - \mathbf{H}_k \hat{\mathbf{x}}_{k-1} \right), \tag{2.13}$$

where the gain matrix can be rewritten as,

$$\mathbf{K}_k = \mathbf{C}_{k-1} \mathbf{H}_k^{\mathrm{T}} \left(\mathbf{H}_k \mathbf{C}_{k-1} \mathbf{H}_k^{\mathrm{T}} + \mathbf{R}_k \right)^{-1}. \tag{2.14}$$

Given the recursive least squares estimator in (2.13), we can also obtain a recursive formulation for evolution the covariance as follows:

$$\begin{aligned} \mathbf{C}_k &= \mathbb{E}\left[\left(\hat{\mathbf{x}}_k - \mathbf{x}_k \right) \left(\hat{\mathbf{x}}_k - \mathbf{x}_k \right)^{\mathrm{T}} \right] \\ &= \left(\mathbf{I} - \mathbf{K}_k \mathbf{H}_k \right) \mathbf{C}_{k-1} \left(\mathbf{I} - \mathbf{K}_k \mathbf{H}_k \right)^{\mathrm{T}} + \mathbf{K}_k \mathbf{R}_k \mathbf{K}_k^{\mathrm{T}}. \end{aligned} \tag{2.15}$$

Note that, the above three expressions are key to the derivation of Kalman Filter which is the subject of the next sub-section. Therefore, in the above formulations it is clear that the present least squares estimator and its covariance can be computed efficiently based on the previous time estimates and new observations.

By substituting for $\mathbf{K}_k$ from expression (2.14) into (2.15) we can also derive the following alternative expression for evolution of $\mathbf{C}_{k-1}$:

$$\mathbf{C}_k = \left(\mathbf{I} - \mathbf{K}_k \mathbf{H}_k \right) \mathbf{C}_{k-1}. \tag{2.16}$$

In addition, we can also use Woodbury matrix identity lemma to obtain another alternative for expression (2.15) as follows:

$$\mathbf{C}_k = \left(\mathbf{C}_{k-1}^{-1} + \mathbf{H}_k^{\mathrm{T}} \mathbf{R}_k^{-1} \mathbf{H}_k \right)^{-1}, \tag{2.17}$$

which is computational prohibitive for large scale problems.

2.1.3 Kalman Filter (KF)

Kalman filter in discrete space is a recursive least squares estimator for optimal estimating the following first order Gauss Markovian stochastic process

$$\mathbf{x}_k = \mathbf{A}_k \mathbf{x}_{k-1} + \mathbf{G}_k \mathbf{u}_{k-1} + \mathbf{w}_k, \tag{2.18}$$

while we have the following observation model:

$$\mathbf{y}_k = \mathbf{H}_k \mathbf{x}_k + \mathbf{v}_k. \tag{2.19}$$

In the above two equations, the model error $\mathbf{w}_k \sim \mathcal{N}(0, \mathbf{B}_k)$ and the observation noise $\mathbf{v}_k \sim \mathcal{N}(0, \mathbf{R}_k)$ are considered to be zero mean and temporarily uncorrelated Gaussian processes such that $\mathbb{E}\left(\mathbf{w}_k \mathbf{w}_l^{\mathrm{T}}\right) = \mathbf{B}_k \delta_{k-l}$ and $\mathbb{E}\left(\mathbf{v}_k \mathbf{v}_l^{\mathrm{T}}\right) = \mathbf{R}_k \delta_{k-l}$. The elements $\mathbf{G}_k$ and $\mathbf{u}_{k-1}$ are deterministic drift elements which are often called control-input models.

Only from the existing Morkovian model in (2.18), we have the following recursions

$$\begin{aligned} \hat{\mathbf{x}}_k &= \mathbb{E}(\mathbf{x}_k) \\ &= \mathbf{A}_k \hat{\mathbf{x}}_{k-1} + \mathbf{G}_k \mathbf{u}_{k-1}, \end{aligned} \tag{2.20}$$

and the Lyapunov linear evolution of the covariance

$$\mathbf{C}_k = \mathbf{A}_k \mathbf{C}_{k-1} \mathbf{A}_k^{\mathrm{T}} + \mathbf{B}_k. \tag{2.21}$$

Clearly, in the above setting the quality of estimate of $\hat{\mathbf{x}}_k$ at k^{th} time step depends on the availability of observations which is only a prior information that can be updated in the light of available observations. In other words, when observations become available up to time $k-1$, the conditional expectation $\hat{\mathbf{x}}_{k|k-1} = \mathbb{E}(\mathbf{x}_k | \mathbf{y}_{1:k-1})$ and its covariance $\mathbf{C}_{k|k-1}$ at time step k are called *prior* estimates. However, the updated estimates, in light of new observations at time step k, are called a *posterior* estimates and are denoted by $\hat{\mathbf{x}}_{k|k}$ and $\mathbf{C}_{k|k}$.

Therefore, in the presence of observations up to previous time step $k-1$, the above recursions in (2.20) and (2.21) can be expressed as:

$$\hat{\mathbf{x}}_{k|k-1} = \mathbf{A}_k \hat{\mathbf{x}}_{k-1|k-1} + \mathbf{G}_k \mathbf{u}_{k-1} \tag{2.22}$$

and

$$\mathbf{C}_{k|k-1} = \mathbf{A}_k \mathbf{C}_{k-1|k-1} \mathbf{A}_k^{\mathrm{T}} + \mathbf{B}_k, \tag{2.23}$$

where $\hat{\mathbf{x}}_{k-1|k-1}$ and $\mathbf{C}_{k-1|k-1}$ are posterior estimates at time step $k-1$ and $\hat{\mathbf{x}}_{k|k-1}$ and $\mathbf{C}_{k|k-1}$ are the prior estimates at time step k.

Now, given new observations at k^{th} time step, we can obtain the posterior estimate $\mathbf{x}_{k|k}$ and its covariance $\mathbf{C}_{k|k}$ by adopting the explained expressions for the recursive least-squares in (2.13), (2.14), and (2.15). Accordingly we have,

$$\hat{\mathbf{x}}_{k|k} = \hat{\mathbf{x}}_{k|k-1} + \mathbf{K}_k \left(\mathbf{y}_k - \mathbf{H}_k \hat{\mathbf{x}}_{k|k-1}\right), \tag{2.24}$$

and

$$\begin{aligned}\mathbf{C}_{k|k} &= (\mathbf{I}-\mathbf{K}_k\mathbf{H}_k)\,\mathbf{C}_{k|k-1}\,(\mathbf{I}-\mathbf{K}_k\mathbf{H}_k)^{\mathrm{T}}+\mathbf{K}_k\mathbf{R}_k\mathbf{K}_k^{\mathrm{T}}\\ &= (\mathbf{I}-\mathbf{K}_k\mathbf{H}_k)\,\mathbf{C}_{k|k-1}\\ &= \left(\left(\mathbf{C}_{k|k-1}\right)^{-1}+\mathbf{H}_k^{\mathrm{T}}\mathbf{R}_k^{-1}\mathbf{H}_k\right)^{-1},\end{aligned} \tag{2.25}$$

where the Kalman gain $\mathbf{K}_k$ at k^{th} time-step is the following:

$$\mathbf{K}_k=\mathbf{C}_{k|k-1}\mathbf{H}_k^{\mathrm{T}}\left(\mathbf{H}_k\mathbf{C}_{k|k-1}\mathbf{H}_k^{\mathrm{T}}+\mathbf{R}_k\right)^{-1}. \tag{2.26}$$

If all of the restrictive assumptions, especially about linearity and Gaussianity hold, the Kalman filter is the minimum mean squared least squares estimator (MMSE) and no other estimators can work better than this filter in the mean squared sense. Note that, violating only the Gaussian assumption, all of the above formulations remain the same; however, the filter is no longer optimal. In effect, assuming that the observations are unbiased, the filter can evolve the posterior mean and covariance in time and can provide a second order suboptimal approximation for an arbitrary non-Gaussian posterior density and called the best linear least squares estimator (LLSE).

Notice that, from probabilistic point of view, the Kalman filter can be viewed as the recursive evolution of the prior and posterior Gaussian density of the state with the following prior density is denoted by

$$p(\mathbf{x}_k|\mathbf{y}_{1:k-1}) \;\sim\; \mathcal{N}\left(\hat{\mathbf{x}}_{k|k-1},\,\mathbf{C}_{k|k-1}\right) \tag{2.27}$$

while the posterior density is:

$$p(\mathbf{x}_k|\mathbf{y}_{1:k})\sim\mathcal{N}\left(\hat{\mathbf{x}}_{k|k},\,\mathbf{C}_{k|k}\right). \tag{2.28}$$

2.1.4 Extended Kalman Filter

In a general form, we may explain the model and observation equations as follows:

$$\begin{aligned}\mathbf{x}_k &= \mathcal{A}_k\left(\mathbf{x}_{k-1}\right)+\mathbf{v}_k\\ \mathbf{y}_k &= \mathcal{H}_k\left(\mathbf{x}_k\right)+\mathbf{w}_k\end{aligned} \tag{2.29}$$

where $\mathcal{A}_k:\mathbb{R}^m\to\mathbb{R}^m$ is a possible nonlinear model operator that maps the state $\mathbf{x}_{k-1}\in\mathbb{R}^m$ from the previous time step to the state at the current time step $\mathbf{x}_k\in\mathbb{R}^m$ and $\mathcal{H}_k:\mathbb{R}^m\to\mathbb{R}^n$ is a nonlinear observation operator that maps the current state $\mathbf{x}_k\in\mathbb{R}^m$ onto the observation space $\mathbf{y}_k\in\mathbb{R}^n$, where $\mathbf{v}_k\sim\mathcal{N}\left(0,\,\mathbf{R}_k\right)$ and $\mathbf{w}_k\sim\mathcal{N}\left(0,\,\mathbf{B}_k\right)$ are uncorrelated Gaussian error.

Given the above representation of the system dynamics, obviously the linear formulation of the original Kalman filter is no longer valid. To recast the above nonlinear dynamics into a linear least-squares formulation, the basic idea of the extended Kalman filter is to linearize the above nonlinear operators as follows:

$$\begin{aligned}
\hat{\mathbf{x}}_{k|k-1} &= \mathcal{A}_k\left(\hat{\mathbf{x}}_{k-1|k-1}\right) && (2.30)\\
\hat{\mathbf{x}}_{k|k} &= \hat{\mathbf{x}}_{k|k-1} + \mathbf{K}_k\left(\mathbf{y}_k - \dot{\mathbf{H}}_k\hat{\mathbf{x}}_{k|k-1}\right) && (2.31)\\
\mathbf{C}_{k|k-1} &= \dot{\mathbf{A}}_k\mathbf{C}_{k-1|k-1}\dot{\mathbf{A}}_k^{\mathrm{T}} + \mathbf{B}_k && (2.32)\\
\mathbf{C}_{k|k} &= \left(\mathbf{I} - \mathbf{K}_k\dot{\mathbf{H}}_k\right)\mathbf{C}_{k|k-1}\left(\mathbf{I} - \mathbf{K}_k\dot{\mathbf{H}}_k\right)^{\mathrm{T}} + \mathbf{K}_k\mathbf{R}_k\mathbf{K}_k^{\mathrm{T}} && (2.33)
\end{aligned}$$

where

$$\dot{\mathbf{A}}_k = \frac{d\mathcal{A}_k(x)}{d\mathbf{x}}|_{\mathbf{x}=\hat{\mathbf{x}}_{k-1|k-1}} \quad (2.34)$$

$$\dot{\mathbf{H}}_k = \frac{d\mathcal{H}_k(x)}{d\mathbf{x}}|_{\mathbf{x}=\hat{\mathbf{x}}_{k|k-1}} \quad (2.35)$$

are the related Jacobians and the Kalman gain is

$$\mathbf{K}_k = \mathbf{C}_{k|k-1}\dot{\mathbf{H}}_k^{\mathrm{T}}\left(\dot{\mathbf{H}}_k\mathbf{C}_{k|k-1}\dot{\mathbf{H}}_k^{\mathrm{T}} + \mathbf{R}_k\right)^{-1}. \quad (2.36)$$

The described EKF requires computation of the first order terms in the Taylor expansions or the Jacobians of the involved non-linear operators, which is often prohibitive and closed form expressions can not be easily obtained for very large scale nonlinear systems. Beyond using first order Jacobians, higher order expansion terms have also been proposed but because of the existing computational complexities, their practical use have not been widespread. In addition, the EKF also assumes Gaussianity in the tangent space and evolves the posterior density under this assumption. Clearly, when the state of interest is not Gaussian, EKF is just a an approximate filter and maybe unsuccessful to capture the underlying non-Gaussianity. To tackle non-linearity and non-Gaussianity of the underlying state, Monte Carlo approaches are proposed to improve the performance of EKF including ensemble Kalman filter (EnKF) by *Evensen* (1994a), unscented Kalman Filter (UKF) by *Uhlmann* (1995) and particle filter for which a lucid explanation can be found in (*Doucet et al.*, 2000).

2.1.5 Ensemble Kalman Filter

Ensemble Kalman filter (EnKF) is a very brute force Monte Carlo extension to the original KF idea to tackle non-linearity of the model operator, while the observation model is considered to be linear in its original formulation and the error terms are additive (e.g., *Evensen*, 1994a; *Burgers et al.*, 1998; *Houtekamer and Mitchell*, 1998; *Evensen*, 2003). An

extension of the filter to account for the nonlinear observation operator can also be found in (*Hamill*, 2006).

In a nonlinear model operator, clearly, we are no in the Gaussian domain and can not fully explain the evolution of the density of $\mathbf{x}$ via a Gaussian parametric model. In addition, the linear Lyapunov equation is no longer valid for evolving the covariance of estimate in time, because the evolution depends on higher statistical moments. The main proposal of the EnKF builds upon a brute force randomization strategy. In other words, the idea is to properly generate a set of random realizations or *ensembles* of the state variable of interest to approximate its prior and posterior density via sample mean and covariance.

Specifically, let us assume that given observations up to time step $k-1$, we have N ensembles (realizations) of the posterior estimates $\left\{\hat{\mathbf{x}}^i_{k-1|k-1}\right\}_{i=1}^N$. At this moment, these ensembles may be considered as multiple posterior realizations of the system dynamics obtained from a proper randomization strategy. The prior ensembles at k^{th} time-step is the can be produced by propagating the previous time posterior ensembles throughout the underlying nonlinear model operator as follows:

$$\hat{\mathbf{x}}_{k|k-1} = \mathcal{A}_k\left(\hat{\mathbf{x}}_{k-1|k-1}\right). \tag{2.37}$$

Note that, given model equation in (2.29), this ensembles are conditional expectation or mean of the prior distribution, that is $\hat{\mathbf{x}}_{k|k-1} = \mathbb{E}\left(\hat{\mathbf{x}}_k|\mathbf{y}_{1:k-1}\right)$. Let us assume that at time step k, we have N prior ensembles and thus their prior ensemble mean can be computed as,

$$\hat{\mathbf{x}}^e_{k|k-1} = \frac{1}{N}\sum_{i=1}^{N}\hat{\mathbf{x}}^i_{k|k-1}, \tag{2.38}$$

where the ensemble covariance is:

$$\mathbf{C}^e_{k|k-1} = \frac{1}{N-1}\sum_{i=1}^{N}\left(\hat{\mathbf{x}}^i_{k|k-1} - \hat{\mathbf{x}}^e_{k|k-1}\right)\left(\hat{\mathbf{x}}^i_{k|k-1} - \hat{\mathbf{x}}^e_{k|k-1}\right)^{\mathrm{T}}. \tag{2.39}$$

To obtain the posterior estimates after obtaining the observations at time k, it is suggested by *Burgers et al.* (1998) to perturb the observations $\mathbf{y}^i_k = \mathbf{y}_k + \eta^i_k$, where $\eta^i_k \sim \mathcal{N}\left(0,\, \mathbf{R}_k\right)$ and $i = 1 \cdots N$. Then, for each ensemble prior $\hat{\mathbf{x}}^i_{k|k-1}$ and perturbed observation $\mathbf{y}^i_k$, we can compute posterior ensembles as follows:

$$\hat{\mathbf{x}}^i_{k|k} = \hat{\mathbf{x}}^i_{k|k-1} + \mathbf{K}^e_k\left(\mathbf{y}^i_k - \mathbf{H}_k\hat{\mathbf{x}}^i_{k|k-1}\right), \tag{2.40}$$

$$\mathbf{C}^e_{k|k} = \left(\mathbf{I} - \mathbf{K}^e_k\mathbf{H}_k\right)\mathbf{C}^e_{k|k-1}\left(\mathbf{I} - \mathbf{K}^e_k\mathbf{H}_k\right)^{\mathrm{T}} + \mathbf{K}^e_k\mathbf{R}_k\mathbf{K}^{e\mathrm{T}}_k \tag{2.41}$$

$$= \left(\mathbf{I} - \mathbf{K}^e_k\mathbf{H}_k\right)\mathbf{C}^e_{k|k-1} \tag{2.42}$$

where the gain matrix is

$$\mathbf{K}_k^e = \mathbf{C}_{k|k-1}^e \mathbf{H}_k^{\mathrm{T}} \left(\mathbf{H}_k \mathbf{C}_{k|k-1}^e \mathbf{H}_k^{\mathrm{T}} + \mathbf{R}_k \right)^{-1}. \tag{2.43}$$

As a results, the ensemble (sample) posterior mean

$$\hat{\mathbf{x}}_{k|k}^e = \frac{1}{N} \sum_{i=1}^{N} \hat{\mathbf{x}}_{k|k}^i, \tag{2.44}$$

can be computed at time-step k, as shown in (2.44). The explained process can then be recursively repeated and the filter can evolve each ensemble member recursively in time to obtain the sample mean and covariance of the full nonlinear posterior density.

The EnKF has gone through several modifications and extensions, which their explanations are not in the scope of this thesis. However, mathematically speaking, the original formulation of the EnKF seems to sample the distribution of the prior and posterior mean and not the entire density.

Specifically, given the N posterior ensembles $\mathbf{x}_{k-1|k-1}^i$ at previous time $k-1$, the prior ensembles can be produced as follows:

$$\hat{\mathbf{x}}_{k|k-1}^i = \mathcal{A}_k \left(\hat{\mathbf{x}}_{k-1|k-1}^i + \zeta_{k-1}^i \right), \tag{2.45}$$

where $\zeta_{k-1}^i \sim \mathcal{N}\left(0, \mathbf{C}_{k-1|k-1}^e\right)$, and $\mathbf{C}_{k-1|k-1}^e$ is the best ensemble (sample) estimator of the posterior covariance matrix at time step $k-1$. Having the prior ensembles at k^{th} time step we then can compute the prior ensemble mean and covariance as follows:

$$\hat{\mathbf{x}}_{k|k-1}^e = \frac{1}{N} \sum_{i=1}^{N} \hat{\mathbf{x}}_{k|k-1}^i \tag{2.46}$$

$$\mathbf{C}_{k|k-1}^e = \frac{1}{N-1} \sum_{i=1}^{N} \left(\hat{\mathbf{x}}_{k|k-1}^i - \hat{\mathbf{x}}_{k|k-1}^e \right) \left(\hat{\mathbf{x}}_{k|k-1}^i - \hat{\mathbf{x}}_{k|k-1}^e \right)^{\mathrm{T}} + \mathbf{B}_k, \tag{2.47}$$

where $\mathbf{B}_k$ is the process error. The update part remains the same as presented in (2.40)-(2.44) and the recursion continues by reloading equation (2.45) at the next time step [1].

Obviously, the accuracy of this filter depends on the number of ensembles and it is clear that in the Gaussian case when the number of ensembles goes to infinity the solution of EnKF converges to the solution of the classic KF. As is evident, the Gaussian assumptions are at the core of EnKF, which is clearly prohibitive for proper capturing of the possible non-Gaussianity (multi-modal density) and heavy tailed structure of the underlying state.

[1] Note that the above formulations are slightly different than the originally proposed EnKF (*Evensen*, 2003) in which the sample covariance matrix $\mathbb{E}\left(\eta_{\mathbf{k}} \eta_{\mathbf{k}}^{\mathrm{T}}\right) = \mathbf{R}_k^e$ is used instead of population observation error covariance $\mathbf{R}_k$.

However, because of addressing the underlying non-linearity via Monte Carlo sampling, we have the opportunity to obtain an empirical posterior distribution of the state ensembles at each time step and partially track the existing non-Gaussianity in the state space. Although, this filter has received a great deal of attention in geophysical communities, the sampling strategy in the original development is completely naive and unsupervised. Theoretically speaking, the unscented Kalman filter and especially particle filter offer a much more sophisticated approaches to tackle the explained deficiencies.

2.1.6 Unscented Kalman Filter

As previously explained, when a probability density function undergoes a nonlinear transformation, its mean and covariance also evolve non-linearly and become a function of higher order moments. To recursively estimate nonlinear systems, EKF requires characterization of the Jacobians which is computationally prohibitive in practice. Using EnKF with small number of ensembles may also lead to inaccurate estimation of the mean and covariance and thus divergence of the filter. Unscented Kalman Filter (UKF) is similar to EnKF in the sense that both use samples or ensembles to approximate the evolution of the mean and covariance of the probability distribution without any need to direct characterization of the Jacobians. Although UKF resembles Monte Carlo-type methods such as EnKF, there is an extremely important and subtle difference. In the UKF, the samples are not drawn at random but rather according to a deterministic algorithm. The UKF seeks minimal number of ensembles (called sigma points) to provide a certain degree of accuracy for estimating nonlinear evolution of the mean and covariance (e.g., *Uhlmann*, 1995; *Julier and Uhlmann*, 1997; *Wan and Van der Merwe*, 2000; *Julier and Uhlmann*, 2004; *Simon*, 2006). Consequently, because of the ensemble based nature of the filter, high order information about the distribution can also be inferred empirically.

In particular, *Uhlmann* (1995) showed that, when the density of $\mathbf{x} \in \mathbb{R}^n$ undergoes a nonlinear transformation, at least $n+1$ number of specifically sampled points (called minimal simplex sigma points) are necessary and sufficient to obtain a third order accurate estimate of its transformed mean and covariance (*Julier and Uhlmann*, 2002, 2004). However, empirical analysis suggests that $2n$ symmetrically and regularly spaced sigma points typically lead to significantly more accurate estimates of the nonlinear evolution of the mean and covariance. The core idea of the UKF relies on a particular transformation, the so called unscented transform.

Unscented Transform

1. Let us assume that $\mathbf{x} \in \mathbb{R}^m$ with a known mean $\bar{\mathbf{x}}$ and covariance $\mathbf{C}_{\mathbf{x}}$. Given a nonlinear function $\mathbf{y} = f(\mathbf{x})$, we are interested to obtain an estimate of $\bar{\mathbf{y}}$ and $\mathbf{C}_{\mathbf{y}}$.

2. Form $2m$ sigma point ensembles $\mathbf{x}^i$ as follows:

$$\begin{aligned} \mathbf{x}^i &= \bar{\mathbf{x}} + \mathbf{c}^i \quad i = 1, \ldots, 2m \\ \mathbf{c}^i &= \left(m\mathbf{C}_{\mathbf{x}}\right)_i^{1/2} \quad i = 1, \ldots, m \\ \mathbf{c}^{(m+i)} &= -\left(m\mathbf{C}_{\mathbf{x}}\right)_i^{1/2} \quad i = 1, \ldots, m \end{aligned} \tag{2.48}$$

where $\mathbf{c}^i$ is the i^{th} column of $\left(m\mathbf{C}_{\mathbf{x}}\right)^{1/2}$.

3. Propagate sigma point ensembles through the nonlinear transform $\mathbf{y}^i = f\left(\mathbf{x}^i\right)$, where $i = 1, \ldots, 2m$.

4. Approximate the ensemble mean and covariance of $\mathbf{y}$ as follows:

$$\bar{\mathbf{y}}^e = \frac{1}{2m}\sum_{i=1}^{2m}\mathbf{y}^i \tag{2.49}$$

$$\mathbf{C}_{\mathbf{y}}^e = \frac{1}{2m-1}\sum_{i=1}\left(\mathbf{y}^i - \bar{\mathbf{y}}^e\right)\left(\mathbf{y}^i - \bar{\mathbf{y}}^e\right)^{\mathrm{T}}. \tag{2.50}$$

Note that, it turns out that having the $2m$ sigma points, we can obtain a *fourth order* accurate estimate of the transformed mean and covariance. Here, we only explained the very basic and primitive version of the unscented transform. There are more advanced unscented transformations for which empirical and theoretical studies suggest significant improvements.

Unscented Kalman Filter

Let us assume a nonlinear system of model and observation equations with additive errors as follows:

$$\begin{aligned} \mathbf{x}_{k+1} &= \mathcal{A}\left(\mathbf{x}_k\right) + \mathbf{w}_k \\ \mathbf{y}_k &= \mathcal{H}\left(\mathbf{x}_k\right) + \mathbf{v}_k \end{aligned} \tag{2.51}$$

where $\mathbf{w}_k \sim \mathcal{N}\left(0,\, \mathbf{B}_k\right)$ and $\mathbf{v}_k \sim \mathcal{N}\left(0,\, \mathbf{R}_k\right)$ are independent Gaussian densities. Given a posterior estimate $\hat{\mathbf{x}}_{k-1|k-1}$ of the state of interest and its covariance $\mathbf{C}_{k-1|k-1}$ at time step $k-1$, the steps of estimating the mean and covariance of the prior and posterior density at time step k can be summarized as follows:

1. **Prior estimates**:

   (a) Generate $2m$ sigma point ensembles using the explained unscented transforma-

tion in equation (2.48)

$$\begin{aligned}
\hat{\mathbf{x}}^i_{k-1|k-1} &= \hat{\mathbf{x}}_{k-1|k-1} + \mathbf{c}^i_{k-1|k-1} \quad i = 1, \ldots, 2m \\
\mathbf{c}^i_{k-1|k-1} &= \left(m\mathbf{C}_{k-1|k-1}\right)^{1/2}_i \quad i = 1, \ldots, m \\
\mathbf{c}^{(m+i)}_{k-1|k-1} &= -\left(m\mathbf{C}_{k-1|k-1}\right)^{1/2}_i \quad i = 1, \ldots, m.
\end{aligned} \tag{2.52}$$

(b) Propagate the ensembles of sigma points through the nonlinear model equation as follows:

$$\hat{\mathbf{x}}^i_{k|k-1} = \mathcal{A}\left(\mathbf{x}^i_{k-1|k-1}\right) \tag{2.53}$$

(c) Obtain the prior ensemble mean and covariance as,

$$\hat{\mathbf{x}}^e_{k|k-1} = \frac{1}{2m}\sum_{i=1}^{2m} \hat{\mathbf{x}}^i_{k|k-1} \tag{2.54}$$

$$\mathbf{C}^e_{k|k-1} = \frac{1}{2m-1}\sum_{i=1}^{2m} \left(\hat{\mathbf{x}}^i_{k|k-1} - \hat{\mathbf{x}}^e_{k|k-1}\right)\left(\hat{\mathbf{x}}^i_{k|k-1} - \hat{\mathbf{x}}^e_{k|k-1}\right)^{\mathrm{T}} + \mathbf{B}_k \tag{2.55}$$

2. **Posterior estimates:**

(a) As the current best estimates of the state are encoded in the prior mean and covariance, new sigma points need to be generated as follows:

$$\begin{aligned}
\hat{\mathbf{x}}^i_{k|k-1} &= \hat{\mathbf{x}}^e_{k|k-1} + \mathbf{c}^i_{k|k-1} \quad i = 1, \ldots, 2m \\
\mathbf{c}^i_{k|k-1} &= \left(m\mathbf{C}_{k|k-1}\right)^{1/2}_i \quad i = 1, \ldots, m \\
\mathbf{c}^{(n+i)}_{k|k-1} &= -\left(m\mathbf{C}_{k|k-1}\right)^{1/2}_i \quad i = 1, \ldots, m.
\end{aligned} \tag{2.56}$$

(b) Use the nonlinear observation operator to transform the prior ensemble sigma points $\hat{\mathbf{x}}^i_{k|k-1}$ to observations $\mathbf{y}^i_k$ as follows:

$$\hat{\mathbf{y}}^i_k = \mathcal{H}\left(\hat{\mathbf{x}}^i_{k|k-1}\right). \tag{2.57}$$

Obtain the ensemble observation mean, covariance and cross-covariance as fol-

lows:

$$\begin{aligned}
\hat{\mathbf{y}}_k^e &= \frac{1}{2m}\sum_{i=1}^{2m}\hat{\mathbf{y}}_k^i && (2.58)\\
\mathbf{C}_{\mathbf{y}}^e &= \frac{1}{2m-1}\sum_{i=1}^{2m}\left(\hat{\mathbf{y}}_k^i-\hat{\mathbf{y}}_k^e\right)\left(\hat{\mathbf{y}}_k^i-\hat{\mathbf{y}}_k^e\right)^{\mathrm{T}}+\mathbf{R}_k && (2.59)\\
\mathbf{C}_{\mathbf{xy}}^e &= \frac{1}{2m-1}\sum_{i=1}^{2m}\left(\hat{\mathbf{x}}_{k|k-1}^i-\hat{\mathbf{x}}_{k|k-1}^e\right)\left(\hat{\mathbf{y}}_k^i-\hat{\mathbf{y}}_k^e\right)^{\mathrm{T}} && (2.60)
\end{aligned}$$

(c) Obtain the posterior estimate using classic KF formulation

$$\begin{aligned}
\mathbf{K}_k^e &= \mathbf{C}_{\mathbf{xy}}^e\left(\mathbf{C}_{\mathbf{y}}^e\right)^{-1}\\
\hat{\mathbf{x}}_{k|k}^e &= \hat{\mathbf{x}}_{k|k-1}^e+\mathbf{K}_k^e\left(\mathbf{y}_k-\hat{\mathbf{y}}_k^e\right)\\
\mathbf{C}_{k|k}^e &= \mathbf{C}_{k|k-1}^e-\mathbf{K}_k\mathbf{C}_{\mathbf{y}}^{\mathbf{e}}\mathbf{K}_k^{\mathrm{T}}. && (2.61)
\end{aligned}$$

Despite the fact that the UKF algorithm includes a sophisticated and minimal sampling strategy compared to the EnKF, it has not yet well received for data assimilation problems in earth science community and there are only a few papers (e.g., *Ambadan and Tang*, 2009) in this respect. The main reasons might be: (1) more implementation complexity of the UKF compared to the EnKF; (2) the need for computation of the root mean squared error of the covariance matrix at each step which might be computationally very prohibitive for high dimensional geophysical data assimilation problems; (3) the large number of the suggested ensemble sigma points, that is at least $m+1$ for a problem in $\mathbb{R}^m$. The last two issues are indeed serious for operational data assimilation problems whose dimension may easily exceeds 10^7.

2.1.7 Particle Filter

Particle filter is another brute force Monte Carlo approach for nonlinear and non-Gaussian state space estimation problem in the following general form:

$$\begin{aligned}
\mathbf{x}_k &= \mathcal{A}_k\left(\mathbf{x}_{k-1},\,\mathbf{v}_k\right)\\
\mathbf{y}_k &= \mathcal{H}_k\left(\mathbf{x}_k,\,\mathbf{w}_k\right). && (2.62)
\end{aligned}$$

The particle filter is a probability based estimator and often works well, where the explained strict linearity and Gaussian assumptions are no longer valid. It uses a Monte Carlo approach to sample the conditional density of the state space, given observations, to obtain an empirical approximation of the posterior density function of the state. This approach

is advantageous compared to the parametric second order filtering methods which only estimate the mean and covariance of posterior probability, especially for the multi-modal probability density functions. Given an empirical estimate of the entire posterior, one can easily obtain any desired statistics such the mean, mode or other higher order ones. Due to its Monte Carlo nature, this filter can be computationally very demanding and its practical usage often requires a trade off analysis between computational cost and estimation accuracy. Depends on the employed sampling strategy, particle filter is known with different names such as sequential importance sampling (SIS) (*Doucet et al.*, 2001, chap. 11), sampling importance resampling (SIR) (*Gordon et al.*, 1993), auxiliary sampling importance resampling (ASIR) (*Pitt and Shephard*, 1999), and regularized particle filter (*Doucet et al.*, 2001, chap. 12). For an alaborate discussion on Unscented Kalman Filter please see *Simon* (2006, p. 433)

By all means, particle filter is rooted in original work by Nicholas Metropolis and later Metropolis and Hasting. In their seminal work, a Markov chain Monte Calro (MCMC) method is proposed to draw a sequence of random samples from an arbitrary density for which direct sampling is unknown or is extremely difficult. In other words, in particle filter methods, we typically seek methodologies that allow us to draw samples from the posterior density based on an acceptance-rejection criteria which relies on Markovian properties of the state variable of interest. In this filtering approach, the target is to approximate the entire posterior density and not only certain number of its important moments. In this subsection, we briefly explain the concept of the Bayesian filtering and explain a specific type of the Particle Filter.

Bayesian State Estimation

The Bayesian view to the filtering seeks methodologies to obtain sequential approximations to the full posterior density in light of new available observations in time. In particular given the entire history of observations throughout the time $\mathbf{y}_{1:k} = \{\mathbf{y}_1, \mathbf{y}_2, \ldots, \mathbf{y}_k\}$, the Bayesian view attempts to recursively approximate the posterior conditional density $p(\mathbf{x}_k|\mathbf{y}_{1:n})$ as follows:

$$p(\mathbf{x}_k|\mathbf{y}_{1:k}) = \frac{p(\mathbf{y}_{1:k}|\mathbf{x}_k)\, p(\mathbf{x}_k)}{p(\mathbf{y}_{1:k})} \tag{2.63}$$

In the above Bayes rule the probability $p(\mathbf{x}_k)$ is not obviously available to us. To put the above Bayes rule in a recursive way, we need to rearrange it in a way that we can update the prior $p(\mathbf{x}_k)$ in terms of the previous time available observations $\mathbf{y}_{1:n-1}$and in particular the prior probability model $p(\mathbf{x}_k|\mathbf{y}_{1:k-1})$ as follows:

$$p(\mathbf{x}_k) = \frac{p(\mathbf{x}_k|\mathbf{y}_{1:k-1})\, p(\mathbf{y}_{1:k-1})}{p(\mathbf{y}_{1:k-1}|\mathbf{x}_k)} = \frac{p(\mathbf{x}_k, \mathbf{y}_{1:k-1})\, p(\mathbf{y}_{1:k-1})}{p(\mathbf{y}_{1:k-1})\, p(\mathbf{y}_{1:k-1}|\mathbf{x}_k)}. \tag{2.64}$$

From Byes rule we also know that,

$$p\left(\mathbf{y}_{1:k}|\mathbf{x}_k\right) = \frac{p\left(\mathbf{x}_k,\, \mathbf{y}_{1:k}\right)}{p\left(\mathbf{x}_k\right)} = \frac{p\left(\mathbf{x}_k,\, \mathbf{y}_k,\, \mathbf{y}_{1:k-1}\right)}{p\left(\mathbf{x}_k\right)}. \tag{2.65}$$

Plugging in (2.64) and (2.65) into (2.63) and multiplying both the numerator and denominator by $p\left(\mathbf{x}_k,\, \mathbf{y}_k\right)$ we get

$$\begin{aligned} p\left(\mathbf{x}_k|\mathbf{y}_{1:k}\right) &= \frac{p\left(\mathbf{x}_k,\, \mathbf{y}_k,\, \mathbf{y}_{1:k-1}\right)}{p\left(\mathbf{x}_k\right)} \frac{p\left(\mathbf{x}_k,\, \mathbf{y}_{1:k-1}\right) p\left(\mathbf{y}_{1:k-1}\right)}{p\left(\mathbf{y}_{1:k-1}\right) p\left(\mathbf{y}_{1:k-1}|\mathbf{x}_k\right)} \frac{1}{p\left(\mathbf{y}_k,\, \mathbf{y}_{1:k-1}\right)} \frac{p\left(\mathbf{x}_k,\, \mathbf{y}_k\right)}{p\left(\mathbf{x}_k,\, \mathbf{y}_k\right)} \\ &= \frac{p\left(\mathbf{x}_k,\, \mathbf{y}_k,\, \mathbf{y}_{1:k-1}\right)}{p\left(\mathbf{x}_k,\, \mathbf{y}_k\right)} \frac{p\left(\mathbf{x}_k,\, \mathbf{y}_k\right)}{p\left(\mathbf{x}_k\right)} \frac{p\left(\mathbf{x}_k,\, \mathbf{y}_{1:k-1}\right)}{p\left(\mathbf{y}_{1:k-1}\right)} \frac{p\left(\mathbf{y}_{1:k-1}\right)}{p\left(\mathbf{y}_k,\, \mathbf{y}_{1:k-1}\right)} \frac{1}{p\left(\mathbf{y}_{1:k-1}|\mathbf{x}_k\right)} \\ &= \frac{p\left(\mathbf{y}_{1:k-1}|\mathbf{x}_k,\, \mathbf{y}_k\right) p\left(\mathbf{y}_k|\mathbf{x}_k\right) p\left(\mathbf{x}_k|\mathbf{y}_{1:k-1}\right)}{p\left(\mathbf{y}_k|\mathbf{y}_{1:k-1}\right) p\left(\mathbf{y}_{1:k-1}|\mathbf{x}_k\right)}. \end{aligned} \tag{2.66}$$

Given that $\mathbf{y}_k$ is a function of $\mathbf{x}_k$, we have $p\left(\mathbf{y}_{1:k-1}|\mathbf{x}_k,\, \mathbf{y}_k\right) = p\left(\mathbf{y}_{1:k-1}|\mathbf{x}_k\right)$ and thus,

$$p\left(\mathbf{x}_k|\mathbf{y}_{1:k}\right) = \frac{p\left(\mathbf{y}_k|\mathbf{x}_k\right) p\left(\mathbf{x}_k|\mathbf{y}_{1:k-1}\right)}{p\left(\mathbf{y}_k|\mathbf{y}_{1:k-1}\right)} \tag{2.67}$$

The above derivation is the key to obtain the posterior estimate of the probability density function in a Bayesian setting. The first density in the numerator , called likelihood function, which is known to us from the observation equation and prior knowledge of the noise properties. For example given the observation model as

$$\mathbf{y}_k = \mathcal{H}\left(\mathbf{x}_k\right) + \mathbf{w}_k, \tag{2.68}$$

where $\mathbf{w} \sim \mathcal{N}\left(0,\, \mathbf{R}_k\right)$, then the likelihood function is

$$p\left(\mathbf{y}_k|\mathbf{x}_k\right) = \frac{1}{\left(2\pi\right)^{n/2} \left|\mathbf{R}_k\right|^{1/2}} \exp\left(-\frac{1}{2}\left[\mathbf{y}_k - \mathcal{H}\left(\mathbf{x}_k\right)\right]^{\mathrm{T}} \mathbf{R}^{-1} \left[\mathbf{y}_k - \mathcal{H}\left(\mathbf{x}_k\right)\right]\right). \tag{2.69}$$

However, other conditional probability density functions in (2.67), including $p\left(\mathbf{x}_k|\mathbf{y}_{1:k-1}\right)$and $p\left(\mathbf{y}_k|\mathbf{y}_{1:k-1}\right)$, are not directly available. To this end, let us first focus on the prior probability $p\left(\mathbf{x}_k|\mathbf{y}_{1:k-1}\right)$. Using the probability sum rule, we have,

$$\begin{aligned} p\left(\mathbf{x}_k|\mathbf{y}_{1:k-1}\right) &= \int p\left(\mathbf{x}_k,\, \mathbf{x}_{k-1}|\mathbf{y}_{1:k-1}\right) d\mathbf{x}_{k-1} \\ &= \int p\left(\mathbf{x}_k|\mathbf{x}_{k-1},\, \mathbf{y}_{1:k-1}\right) p\left(\mathbf{x}_{k-1}|\mathbf{y}_{1:k-1}\right) d\mathbf{x}_{k-1} \\ &= \int p\left(\mathbf{x}_k|\mathbf{x}_{k-1}\right) p\left(\mathbf{x}_{k-1}|\mathbf{y}_{1:k-1}\right) d\mathbf{x}_{k-1}. \end{aligned} \tag{2.70}$$

The $p\left(\mathbf{x}_k|\mathbf{x}_{k-1}\right)$ in (2.70) is available to us from model equation and $p\left(\mathbf{x}_{k-1}|\mathbf{y}_{1:k-1}\right)$ is the posterior probability at previous time that is assumed to be available at each recursion.

The conditional density $p\left(\mathbf{y}_k|\mathbf{y}_{1:k-1}\right)$ in denominator of (2.67) can be expanded using the sum and product rules as follows:

$$\begin{aligned} p\left(\mathbf{y}_k|\mathbf{y}_{1:k-1}\right) &= \int p\left(\mathbf{y}_k,\, \mathbf{x}_k|\mathbf{y}_{1:k-1}\right) d\mathbf{x}_k \\ &= \int p\left(\mathbf{y}_k,\, |\mathbf{x}_k,\, \mathbf{y}_{1:k-1}\right) p\left(\mathbf{x}_k|\mathbf{y}_{1:k-1}\right) d\mathbf{x}_k \\ &= \int p\left(\mathbf{y}_k,\, |\mathbf{x}_k\right) p\left(\mathbf{x}_k|\mathbf{y}_{1:k-1}\right) d\mathbf{x}_k, \end{aligned} \tag{2.71}$$

which is completely known to us. The first likelihood term is available to us from the measurement equation and the prior probability is defined in (2.70). Therefore, the a posteriori probability density function in (2.67) can be written as follows:

$$p\left(\mathbf{x}_k|\mathbf{y}_{1:k}\right) = \frac{p\left(\mathbf{y}_k|\mathbf{x}_k\right) p\left(\mathbf{x}_k|\mathbf{y}_{1:k-1}\right)}{\int p\left(\mathbf{y}_k,\, |\mathbf{x}_k\right) p\left(\mathbf{x}_k|\mathbf{y}_{1:k-1}\right) d\mathbf{x}_k}. \tag{2.72}$$

Now we have all necessary ingredients in our repository to run a recursive Bayesian estimator, which has been summarized as follows:

Bayesian Filtering

In brief, the Bayesian filtering can be summarized as follows:

1. The model and observation equations are:

$$\begin{aligned} \mathbf{x}_k &= \mathcal{A}_k\left(\mathbf{x}_{k-1},\, \mathbf{v}_k\right) \\ \mathbf{y}_k &= \mathcal{H}_k\left(\mathbf{x}_k,\, \mathbf{w}_k\right). \end{aligned} \tag{2.73}$$

   where the errors are zero mean white Gaussian noise with known covariance.

2. Assume that the initial posterior density is given by $p\left(\mathbf{x}_0|\mathbf{y}_0\right)$.

3. **For** $k = 1, 2, \ldots,$

   (a) Obtain the prior probability density function as follows:

$$p\left(\mathbf{x}_k|\mathbf{y}_{1:k-1}\right) = \int p\left(\mathbf{x}_k|\mathbf{x}_{k-1}\right) p\left(\mathbf{x}_{k-1}|\mathbf{y}_{1:k-1}\right) d\mathbf{x}_{k-1}. \tag{2.74}$$

   (b) Obtain the posterior probability density function as follows:

$$p\left(\mathbf{x}_k|\mathbf{y}_{1:k}\right) = \frac{p\left(\mathbf{y}_k|\mathbf{x}_k\right) p\left(\mathbf{x}_k|\mathbf{y}_{1:k-1}\right)}{\int p\left(\mathbf{y}_k,\, |\mathbf{x}_k\right) p\left(\mathbf{x}_k|\mathbf{y}_{1:k-1}\right) d\mathbf{x}_k} \tag{2.75}$$

All of the components in (2.75) are mathematically available to compute; however, in reality, there is not any closed form solution for this expression; except for strict Gaussian and linear assumptions described in derivation of the Kalman Filter. To numerically approximate the above a posteriori probability density function, there are many heuristic approaches, which have been developed in the past decades and nowadays are known as different variants of the particle filter (see, *Simon*, 2006).

Particle Filter

Particle filter is typically referred to the class of methodologies to implement the Bayesian filtering, explained in the previous subsection. As previously explained, there are multiple variants of the particle filters. Here, we only restrict our attention to explain a very simple one proposed in (*Ristic et al.*, 2004). In particle filters, we typically obtain a set of samples to characterize the density of the state variable of interest. This random samples, called *particles*, are a set of support points that associated to them there are a set of probability measures or weights $\left\{q_{k-1}^i,\, i = 1, \ldots, N\right\}$, which represent their probability of occurrence. In particular, let us assume that at time step $k-1$, a posteriori estimate of the empirical density $p\left(\mathbf{x}_{k-1}|\mathbf{y}_{1:k-1}\right)$ is characterized by a set of N particles $\left\{\mathbf{x}_{k-1|k-1}^i,\, i = 1, \ldots, N\right\}$ such that:

$$p\left(\mathbf{x}_{k-1}|\mathbf{y}_{1:k-1}\right) \approx \sum_{i}^{N} q_{k-1}^i \delta\left(\mathbf{x}_{k-1} - \mathbf{x}_{k-1|k-1}^i\right), \tag{2.76}$$

where $\sum_{i=1}^{N} q^i = 1$.

Using the model equation in (2.73), these posterior particles at time step $k-1$ can be evolved in time to produce the prior estimate of the state at time step k, as follows:

$$\mathbf{x}_{k|k-1}^i = \mathcal{A}_k\left(\mathbf{x}_{k-1|k-1}^i,\, \mathbf{w}_k^i\right). \tag{2.77}$$

After we receive the measurements at time step k, we need to update the above prior particles using equation (2.75) and sequentially march in time.

For the updating step, there are multiple methodologies, which we can not fully explain them in this document. As previously mentioned, here we restrict our considerations only to the method proposed by *Ristic et al.* (2004). To this end, given the observation model, we can compute the likelihood values of the given prior particles. For example in an additive measurement noise, similar to equation (2.69), we have

$$p\left(\mathbf{y}_k|\mathbf{x}_{k|k-1}^i\right) = \frac{1}{(2\pi)^{n/2}\left|\mathbf{R}_k\right|^{1/2}} \exp\left(-\frac{1}{2}\left[\mathbf{y}_k - \mathcal{H}\left(\mathbf{x}_{k|k-1}^i\right)\right]^{\mathrm{T}} \mathbf{R}^{-1}\left[\mathbf{y}_k - \mathcal{H}\left(\mathbf{x}_{k|k-1}^i\right)\right]\right). \tag{2.78}$$

Given the prior particles, the above likelihood function provides a measure that how likely

are those particles. Naturally, if one particle is relatively more likely than another particle, we need to consider it as more probable one with larger contribution or weight for characterization of the posterior density. To simply obtain these likelihood or relative weights, we may only obtain the functional values proportional to expression (2.78) as follows:

$$q_i \propto \exp\left(-\frac{1}{2}\left[\mathbf{y}_k - \mathcal{H}\left(\mathbf{x}^i_{k|k-1}\right)\right]^{\mathrm{T}} \mathbf{R}^{-1}\left[\mathbf{y}_k - \mathcal{H}\left(\mathbf{x}^i_{k|k-1}\right)\right]\right). \tag{2.79}$$

and then normalize them

$$q_i = \frac{q_i}{\sum_i^N q_i}, \tag{2.80}$$

such that $\sum_{i=1}^N q_i = 1$.

Now, we need to update the prior weights to generate the posterior weights at time k. The following straightforward updating step is proposed in (*Ristic et al.*, 2004) which might not be always the best updating rule.

For $i = 1, \ldots, N$, perform the following two steps:

1. Draw a random number r from a uniform probability density function $r_i \sim \mathcal{U}[0, 1]$, bounded between 0 and 1.

2. Compute the probability of non-exceedance for the likelihood probabilities q_i by accumulating them into a sum till the probability of non-exceedance is greater than r_i, that is $\sum_{i=1}^{j-1} q_i < r_i$ and $\sum_{i=1}^{j} q_i \geq r_i$.

3. Set the i^{th} posterior particle $\mathbf{x}^i_{k|k} = \mathbf{x}^j_{k|k-1}$ with probability q^j.

It turns out that if $N \to \infty$, the empirical approximation of the posterior density will tend to the true probability density function. The above updating scheme has a very simple interpretation. A closer look shows that indeed we are resampling the prior particles with replacement and label those as posterior particles whose probability exceed 0.5 in an average sense. The readers are referred to *Arulampalam et al.* (2002) for a quick tutorial on particle filter and other more efficient and effective updating schemes.

Obtaining posterior particles allow us to have an empirical estimate of the probability density function and obtain any desired statistics of that empirical distribution such as the mean, mode or other higher order statistics. However, computational cost of the particle filter is always a major issue for practical implementation of this filter. When the number of particles is large, the computational expense to forward those particles in time may be computationally prohibitive for large scale geophysical problems. In addition, the classic algorithms for particle filter often collapse to a set of particles with very small variability. This problem is often referred to as *sample impoverishment* problem. This problem often

occurs when likelihood function $p(\mathbf{y}_k|\mathbf{x}_k)$ has small overlapping region with the prior probability $p(\mathbf{x}_k|\mathbf{y}_{k-1})$ and thus resampled posteriori particles will be very close to each other (see, for more infromation *Doucet et al.*, 2000; *Arulampalam et al.*, 2002; *Simon*, 2006).

2.2 Data assimilation via Variational Approaches

In this section, we introduce basic mathematical concepts in variational data assimilation. Both 3D and 4D-Var data assimilation are reviewed. Let us recall that at the time of model initialization t_0, the goal of data assimilation can be stated as that of obtaining the *analysis* state as the best estimate of the true initial state, under given noisy *observations* and the *background* state. The background state in data assimilation is often referred to the previous-time forecast provided by underlying (physically-based) model. Solving the data assimilation problem, then the analysis is being used as the initial condition of the underlying model for forecasting of the next time step and this recursion continues.

2.2.1 Three Dimensional Variational Data Assimilation (3D-Var)

Let us assume that the unknown true state of interest at the initial time t_0 is an m-element column vector in discrete space denoted by $\mathbf{x}_0 = [x_{0,1}, \ldots, x_{0,m}]^{\mathrm{T}} \in \mathbb{R}^m$, the noisy and low-resolution observations at intial time t_0 is $\mathbf{y}_0 \in \mathbb{R}^n$, where $n \ll m$. Suppose that the observations are related to the true initial state by the following observation model

$$\mathbf{y}_0 = \mathcal{H}(\mathbf{x}_0) + \mathbf{v}_0, \tag{2.81}$$

where $\mathcal{H} : \mathbb{R}^m \to \mathbb{R}^n$ denotes the nonlinear observation operator that maps the state space into the observation space, and $\mathbf{v}_0 \sim \mathcal{N}(0, \mathbf{R}_0)$ is the Gaussian observation error with zero mean and covariance $\mathbf{R}_0$.

The problem of linear 3D-Var amounts to finding the minimum point of the following weighted least squares (WLS) cost function:

$$\mathcal{J}_{3D}(\mathbf{x}_0) = \frac{1}{2} \|\mathbf{y}_0 - \mathcal{H}(\mathbf{x}_0)\|^2_{\mathbf{R}^{-1}} + \frac{1}{2} \left\|\mathbf{x}_0^b - \mathbf{x}_0\right\|^2_{\mathbf{B}^{-1}}, \tag{2.82}$$

where, $\|\mathbf{x}\|^2_{\mathbf{R}^{-1}} = \mathbf{x}^{\mathrm{T}}\mathbf{R}^{-1}\mathbf{x}$ denotes the *quadratic-norm,* while $\mathbf{R}$ is a positive definite matrix and $\mathbf{B} \in \mathbb{R}^{m\times m}$ denotes the background error covariance matrix $\mathbb{E}\left[\left(\mathbf{x}_0 - \mathbf{x}_0^b\right)\left(\mathbf{x}_0 - \mathbf{x}_0^b\right)^{\mathrm{T}}\right] = \mathbf{B}$. Clearly, the 3D-Var analysis is the minimizer of the WLS cost function (2.82) as follows:

$$\mathbf{x}_0^a = \underset{\mathbf{x}_0}{\operatorname{argmin}} \left\{\mathcal{J}_{3D}(\mathbf{x}_0)\right\}.$$

As is evident, the 3D-Var is a moneyless data assimilation methodology and there is not any component that encodes the temporal dependency of the underlying state. At every instant of time, we obtain the best estimate of the initial state of interest given observations and background state and their covariance matrices. This best estimate or analysis is then being used for re-initializing the underlying (physically-based) model to obtaining the forecast state in the next time step and so on.

2.2.2 Four Dimensional Variational Data Assimilation (4D-Var)

The classic 4D-Var is an extension to the explained 3D-Var which constrains the solution to the underlying dynamics in a time interval of available observations. Taking into account the sequence of available observations in a window of time $[t_0, \dots t_k]$, $\mathbf{y}_i \in \mathbb{R}^n$, $i = 0, \dots k$, and denoting the background state and its error covariance by $\mathbf{x}_0^b \in \mathbb{R}^m$ and $\mathbf{B} \in \mathbb{R}^{m \times m}$; the 4D-Var problem amounts to obtaining the analysis as the minimizer of the following WLS cost function:

$$\mathcal{J}_{4D}(\mathbf{x}_0,\, \mathbf{x}_1,\, \dots,\, \mathbf{x}_k) = \sum_{i=0}^{k} \left(\frac{1}{2} \left\| \mathbf{y}_i - \mathcal{H}\left(\mathbf{x}_i\right) \right\|^2_{\mathbf{R}_i^{-1}} \right) + \frac{1}{2} \left\| \mathbf{x}_0^b - \mathbf{x}_0 \right\|^2_{\mathbf{B}^{-1}}, \tag{2.83}$$

while the solution is constrained to the underlying prognostic equations in the following functional form:

$$\mathbf{x}_i = \mathcal{M}_{0,\,i}(\mathbf{x}_0),\ i = 0, \dots, k. \tag{2.84}$$

Here the function $\mathcal{M}_{0,\,i} : \mathbb{R}^m \to \mathbb{R}^m$ is a nonlinear model operator that evolves the initial state in time from t_0 to t_i.

Let us define $\mathbf{M}_{0,\,i}$ to be the Jacobain of $\mathcal{M}_{0,\,i}$ and restrict our consideration only to a linear observation operator, that is $\mathcal{H}\left(\mathbf{x}_i\right) = \mathbf{H}\mathbf{x}_i$, then the 4D-Var cost function reduces to

$$\mathcal{J}_{4D}(\mathbf{x}_0) = \sum_{i=0}^{k} \left(\frac{1}{2} \left\| \mathbf{y}_i - \mathbf{H}\mathbf{M}_{0,\,i}\, \mathbf{x}_0 \right\|^2_{\mathbf{R}_i^{-1}} \right) + \frac{1}{2} \left\| \mathbf{x}_0^b - \mathbf{x}_0 \right\|^2_{\mathbf{B}^{-1}}. \tag{2.85}$$

By defining $\underline{\mathbf{y}} = \left[\mathbf{y}_0^{\mathrm{T}}, \dots, \mathbf{y}_k^{\mathrm{T}}\right]^{\mathrm{T}} \in \mathbb{R}^N$, where $N = n(k{+}1)$, $\underline{\mathbf{H}} = \left[\left(\mathbf{H}\mathbf{M}_{0,\,0}\right)^{\mathrm{T}}, \dots, \left(\mathbf{H}\mathbf{M}_{0,\,k}\right)^{\mathrm{T}} \right]^{\mathrm{T}}$, and

$$\underline{\mathbf{R}} = \begin{bmatrix} \mathbf{R}_0 & 0 & \cdots & 0 \\ 0 & \mathbf{R}_1 & \ddots & \vdots \\ \vdots & \ddots & \ddots & 0 \\ 0 & \cdots & 0 & \mathbf{R}_k \end{bmatrix},$$

the 4D-Var problem (2.85) further reduces to minimization of the following cost function:

$$\mathcal{J}_{4D}(\mathbf{x}_0) = \frac{1}{2}\left\|\underline{\mathbf{y}} - \underline{\mathbf{H}}\mathbf{x}_0\right\|^2_{\underline{\mathbf{R}}^{-1}} + \frac{1}{2}\left\|\mathbf{x}_0^b - \mathbf{x}_0\right\|^2_{\mathbf{B}^{-1}}, \tag{2.86}$$

which is a smooth quadratic function of the initial state of interest $\mathbf{x}_0$. Therefore, by setting the derivative to zero, it has the following analytic minimizer as the analysis state,

$$\mathbf{x}_0^a = \left(\underline{\mathbf{H}}^{\mathrm{T}}\underline{\mathbf{R}}^{-1}\underline{\mathbf{H}} + \mathbf{B}^{-1}\right)^{-1}\left(\underline{\mathbf{H}}^{\mathrm{T}}\underline{\mathbf{R}}^{-1}\underline{\mathbf{y}} + \mathbf{B}^{-1}\mathbf{x}_0^b\right). \tag{2.87}$$

Throughout this study, we used Matlab built-in function `pcg.m`, described by *Bai et al.* (1987), for obtaining classic solutions of the 4D-Var in equation (2.87).

Accordingly, the analysis error covariance is the inverse of the Hessian in expression (2.86) as follows:

$$\mathbb{E}\left[\left(\mathbf{x}_0^a - \mathbf{x}_0\right)\left(\mathbf{x}_0^a - \mathbf{x}_0\right)^{\mathrm{T}}\right] = \left(\underline{\mathbf{H}}^{\mathrm{T}}\underline{\mathbf{R}}^{-1}\underline{\mathbf{H}} + \mathbf{B}^{-1}\right)^{-1}. \tag{2.88}$$

It can be shown that the analysis in the above classic 4D-Var is the conditional expectation of the true state given observations and the background state. Therefore, the analysis in the classic 4D-Var problem is the best unbiased minimum mean squared error (MMSE) estimator of the true state (*Levy*, 2008, chap.4).

Chapter 3

Regularization and Sparsity

3.1 Introduction

Regularization is typically referred to those mathematical methodologies that allow us to properly solve ill-posed inverse problems. Inverse problems are those in which we are interested to obtain the internal variability of a system by an eternal set of often incomplete observations. Inverse problems are in the class of ill-posed problems. By definition a problem is ill-posed if it does not satisfy one of the following conditions: (a) Existence: the problem must have at least a solution; (b) Uniqueness: there must be only one solution; and (c) Stability: the problem solution must be continuously depend on the observations. For instance, let us focus on an underdetermined linear system of equation as follows:

$$\mathbf{y} = \mathbf{H}\mathbf{x} \tag{3.1}$$

where $\mathbf{H} \in \mathbb{R}^{n \times m}$, $\mathbf{y} \in \mathbb{R}^{n}$, $\mathbf{x} \in \mathbb{R}^{m}$, and $m \gg n$. For this linear system of equations infinite number of solutions exist as the number of unknowns are more than the number of equations. Therefore, this problem is ill-posed as it violates the second condition about the uniqueness of the solution. On the other hand, for an overdetermined system of equations when $m \ll n$, one may seek to obtain the least squares solution as follows:

$$\mathbf{x} = \left(\mathbf{H}^{\mathrm{T}}\mathbf{H}\right)^{-1}\mathbf{H}^{\mathrm{T}}\mathbf{y}. \tag{3.2}$$

The above solution requires that the matrix $\mathbf{H}^{\mathrm{T}}\mathbf{H}$ be invertible and the inverse be sufficiently stable. For overdetermined systems, when $\mathbf{H}$ is full rank, $\mathbf{H}^{\mathrm{T}}\mathbf{H}$ is invertible; however, might be unstable depending on its condition number. Recall that the condition number is the ratio between the largest and smallest singular values of a matrix. It can be

shown that when the condition number of a matrix is sufficiently large, the inverse matrix may contain very large elements that can potentially spoil the solution in (3.2).

Specifically, in the simplest term, let us assume that the true observation $\mathbf{y}^{true}$ is corrupted with a white Gaussian noise $\mathbf{e} \sim \mathcal{N}\left(0,\, \nu^2\mathbf{I}\right)$, that is $\mathbf{y} = \mathbf{y}^{true} + \mathbf{e}$, and thus we get

$$\begin{aligned} \mathbf{x} &= \mathbf{H}^{\dagger^{-1}}\mathbf{y} \\ &= \mathbf{H}^{\dagger^{-1}}\left(\mathbf{y}^{true} + \mathbf{e}\right) \\ &= \mathbf{x}^{true} + \mathbf{H}^{\dagger^{-1}}\mathbf{e}, \end{aligned} \tag{3.3}$$

where $\mathbf{H}^{\dagger} = \left(\mathbf{H}^{\mathrm{T}}\mathbf{H}\right)^{-1}\mathbf{H}^{\mathrm{T}}$. Accordingly, it follows that the covariance of $\mathbf{x}$ is

$$\begin{aligned} \mathbb{E}\left[\left(\mathbf{x} - \mathbf{x}^{true}\right)\left(\mathbf{x} - \mathbf{x}^{true}\right)^{\mathrm{T}}\right] &= \mathbf{H}^{\dagger^{-1}}\mathbb{E}\left(\mathbf{e}\mathbf{e}^{\mathrm{T}}\right)\mathbf{H}^{\dagger^{-\mathrm{T}}} \\ \mathrm{Cov}\left(\mathbf{x}\right) &= \nu^2\mathbf{I}\left(\mathbf{H}^{\dagger^{\mathrm{T}}}\mathbf{H}^{\dagger}\right)^{-1}. \end{aligned} \tag{3.4}$$

taking the 2-norm of the covariance, we get,

$$\left\|\mathrm{Cov}\left(\mathbf{x}\right)\right\|_2 = \nu^2/\sigma_n^2, \tag{3.5}$$

where σ_n is the smallest singular value of $\mathbf{H}^{\dagger^{\mathrm{T}}}\mathbf{H}^{\dagger}$. Obviously, if $\mathbf{H}^{\dagger^{\mathrm{T}}}\mathbf{H}^{\dagger}$ is very ill-conditioned and the smallest singular value is much smaller than that of the noise variance, the norm of the covariance of $\mathbf{x}$ will be very large and sensitive to observation noise in $\mathbf{y}$. Clearly, here we assumed that the variance of the noise is smaller than that of the observations, otherwise the entire information of $\mathbf{y}^{true}$ will be buried in $\mathbf{y}$. Therefore, not only an underdetermined linear system but also an overdetermined one can be ill-posed due to the ill-conditioning of the the measurement operator (see, *Hansen*, 2010).

3.2 Regularization

3.2.1 Tikhonov Regularization

Regularization is a methodology for narrowing down the solution of an ill-posed inverse problem to a unique and stable one. The Tikhonov regularization by *Tikhonov et al.* (1977) is probably one of the most well-known and successful regularization of all time. Specifically, the basic form of the Tikhonov regularization to solve the linear system of equation in (4.1) is the following:

$$\underset{\mathbf{x}}{\text{minimize}} \left\{ \left\|\mathbf{y} - \mathbf{H}\mathbf{x}\right\|_2^2 + \lambda \left\|\mathbf{x}\right\|_2^2 \right\}, \tag{3.6}$$

where $\|\mathbf{x}\|_2 = \left(\sum_i^m x_i^2\right)^{1/2}$. Here, the regularization parameter is a non-negative parameter that controls the contribution of the two terms in the solution of (3.6). The first term $\|\mathbf{y} - \mathbf{H}\mathbf{x}\|_2^2$ expresses the fidelity of the solution to the observations while the second term $\lambda \|\mathbf{x}\|_2^2$ measures the regularity of the solution. Obviously, when we send λ to zero, we solve a simple least squares and only minimize the mean squared error. In this case, the solution only follows the observations without respecting any specific underlying regularity. For larger values of λ, we impose more regularity on the solution. The incorporation of this term refers to our prior knowledge about the possible ill-conditioning of the problem and the adverse effects of the observation noise on the solution. Therefore, the hope is to constrain the norm of the solution to suppress the adverse noise effects. Proper selection of λ can provide a good balance between these two terms and allows us to obtain a solution with sufficient regularity and fidelity to the observations.

It is worth nothing that the problem in (4.6) is the Lagrangian function of the following constrained optimization,

$$\begin{aligned} &\underset{\mathbf{x}}{\text{minimize}} \, \|\mathbf{y} - \mathbf{H}\mathbf{x}\|_2^2 \\ &\text{s.t.} \quad \|\mathbf{x}\|_2^2 \leq \text{const.} \end{aligned} \tag{3.7}$$

Setting the derivative of (3.6) to zero for obtaining the stationary point of the Tikhonov regularized least squares, we get the following solution:

$$\hat{\mathbf{x}} = \left(\mathbf{H}^{\mathrm{T}}\mathbf{H} + \lambda \mathbf{I}\right)^{-1} \mathbf{H}^{\mathrm{T}}\mathbf{y}. \tag{3.8}$$

The above solution is obviously unique for any non-negative λ and does not require any rank or dimensionality assumption on $\mathbf{H}$. In a more general setting, one may express the Tikhonov regularization in the following general form

$$\underset{\mathbf{x}}{\text{minimize}} \left\{ \|\mathbf{y} - \mathbf{H}\mathbf{x}\|_2^2 + \lambda \|\Phi\mathbf{x}\|_2^2 \right\}, \tag{3.9}$$

where $\mathbf{\Phi} \in \mathbb{R}^{n \times m}$ is an appropriately chosen transformation which typically produces a derivative measure of $\mathbf{x}$. If $\mathbf{\Phi}$ is invertible and letting $\mathbf{c} = \mathbf{\Phi}\mathbf{x}$, then the solution to the above problem is

$$\underset{\mathbf{c}}{\text{minimize}} \left\{ \left\|\mathbf{y} - \mathbf{H}\mathbf{\Phi}^{-1}\mathbf{c}\right\|_2^2 + \lambda \|\mathbf{c}\|_2^2 \right\}. \tag{3.10}$$

Note that while $\mathbf{\Phi}$ represents a derivative operator, the multiplication with $\mathbf{\Phi}^{-1}$ is an integration, which yields additional smoothness in the regularized solution, compared to the choice of $\mathbf{\Phi} = \mathbf{I}$. Therefore, typically the above general form of regularization is called

smoothing norm Tikhonov regularization. Various choices of $\mathbf{\Phi}$ might be considered, where the two common choices of $\mathbf{\Phi}$ are the following rectangular matrices

$$\Phi_1 = \begin{bmatrix} -1 & 1 & \cdots & 0 \\ \vdots & \ddots & \ddots & \vdots \\ 0 & \cdots & -1 & 1 \end{bmatrix} \in \mathbb{R}^{(m-1)\times m}, \tag{3.11}$$

and

$$\Phi_2 = \begin{bmatrix} 1 & -2 & 1 & \cdots & 0 \\ \vdots & \ddots & \ddots & \ddots & \vdots \\ 0 & \cdots & 1 & -2 & 1 \end{bmatrix} \in \mathbb{R}^{(m-2)\times m}. \tag{3.12}$$

These matrices represent approximations to the first and second order derivative operators. For a catalog of derivative matrices and their incorporation in regularization, the reader is referred to *Hansen* (2010, p. 175).

3.2.2 Non-smooth Regularization

It turns out that the smoothing Tikhonov or ℓ_2-norm regularization penalizes drastically the existing jumps and isolated discontinuities of the underlying state variable of interest. Therefore, the solutions of the this smoothing norm regularization are often overly smooth representation of the true state $\mathbf{x}$. For environmental scientists these sharp transitions typically encode environmental extreme events which are very important for hazard estimation, prediction and mitigation practices.

To be more specific, let us consider a piecewise linear function of the following form:

$$f(t) = \begin{cases} 0, & 0 \le t < \frac{1}{2}(1-h) \\ \frac{t}{h} - \frac{1-h}{2h}, & \frac{1}{2}(1-h) \le t \le \frac{1}{2}(1+h) \\ 1, & \frac{1}{2}(1+h) < t \le 1 \end{cases}, \tag{3.13}$$

as shown in Figure 3.1. It can be demonstrated that the smoothing norms associated with the ℓ_1 and ℓ_2-norms of the first order derivative $f^{(1)}(t)$ satisfy:

$$\left\| f^{(1)} \right\|_1 = \int_0^1 \left| f^{(1)}(t) \right| \, dt = \int_0^h \frac{1}{h} \, dt = 1 \tag{3.14}$$

while

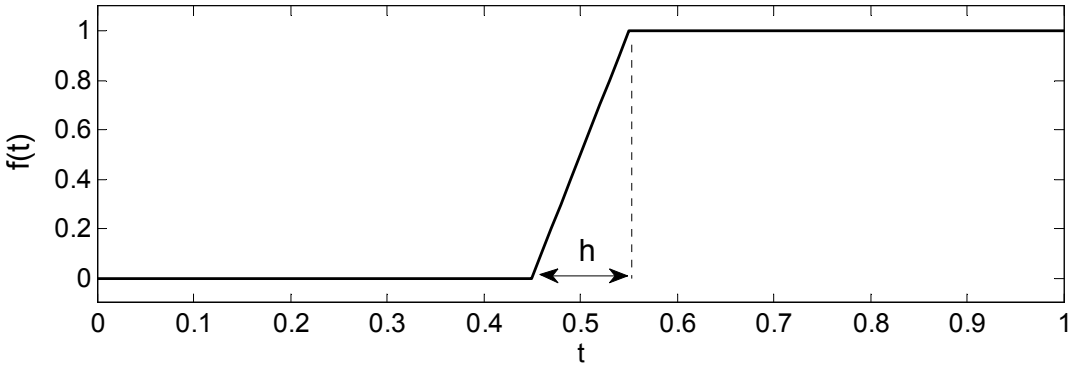

Figure 3.1: A piecewise linear function $f(t)$ with a slope $f^{(1)} = 1/h$ at the non-horizontal part. Notice that the steepness of the gradient depends on the value of h. For this function the $\left\|f^{(1)}\right\|_1$ is constant and independent of h while $\left\|f^{(1)}\right\|_2^2 = 1/h$ goes to infinity as h goes to zero (i.e., for a very steep gradient). As a result, the ℓ_2-norm solutions do not allow steep gradients, while the ℓ_1-norm does.

$$\left\|f^{(1)}\right\|_2^2 = \int_0^1 \left|f^{(1)}(t)\right|^2 dt = \int_0^h \frac{1}{h^2}\, dt = \frac{1}{h}. \tag{3.15}$$

It is observed that the smoothing ℓ_1-norm is independent of the slope of the middle part of $f(t)$ while the smoothing ℓ_2-norm is inversely proportional to h and, as such, it severely penalizes sharp transitions (small h). In other words, due to the excessive penalty over sharp transitions, the ℓ_2-norm of $f^{(1)}$ will produce a very smooth solution. Clearly, this is not desirable in solving inverse problems that we know as a priori that the input state variable of interest exhibits sharp and isolated like discontinuities (see, *Hansen*, 2010).

Therefore, having the above simple arguments, for preservation of jump and isolated singularities, we can imagine that the ℓ_1-norm regularization seems more advantageous than that of the ℓ_2-norm regularization. To this end, another choice of regularization can be stated as follows:

$$\underset{\mathbf{x}}{\text{minimize}} \left\{ \|\mathbf{y} - \mathbf{H}\mathbf{x}\|_2^2 + \lambda \|\Phi\mathbf{x}\|_1 \right\}, \tag{3.16}$$

where $\|\mathbf{x}\|_1 = \sum_i^m |x_i|$.

From statistical point of view, often the variable of interest is non-Gaussian while its distribution under a proper transformation can be well parameterized with the family of the Generalized Gaussian Density (GGD), that is $p(\mathbf{x}) \propto \exp\left(-\lambda \|\mathbf{x}\|_p^p\right)$, where p and λ are both non-negative. Clearly, the family of GGD spans a wide spectrum of probability density functions that includes Gaussian ($p = 2$) and Laplace ($p = 1$) densities as special cases, Figure (3.2). Obviously, in this family of density functions, the tail is ticker than the Gaussian case for $p < 2$.

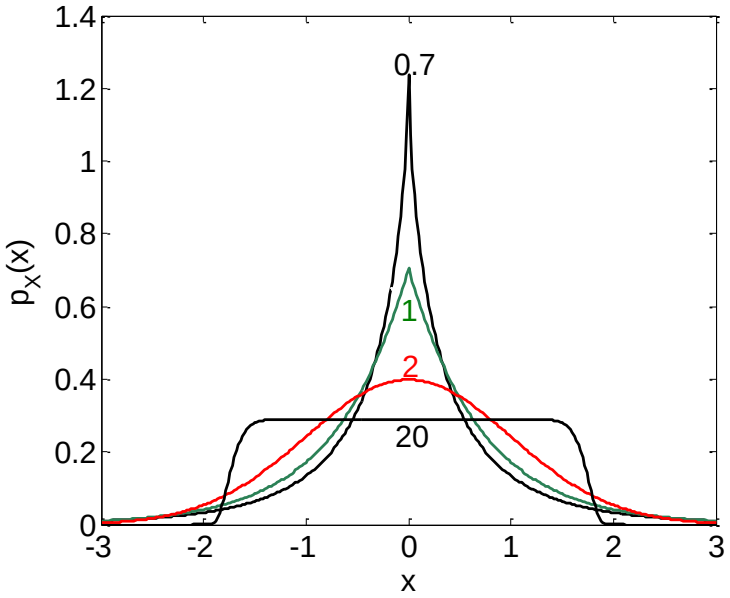

Figure 3.2: One dimensional Generalized Gaussian Density (GDD), $p_X(x) \propto \exp\left(-\lambda |x|^p\right)$ with different tail parameter $p = 20,\ 2,\ 1,\ 0.7$.

Therefore, using the ℓ_1-norm regularization is equivalent to consider the Laplace density to explain the distribution of $\mathbf{x}$ in the real or transformed domain. Specifically, let us define the maximum a posteriori (MAP) estimator as follows:

$$\hat{\mathbf{x}} = \underset{\mathbf{x}}{\operatorname{argmax}} \left\{ p\left(\mathbf{x}|\mathbf{y}\right) \right\}, \tag{3.17}$$

where the observations are related to the state variable of interest though the following observation model:

$$\mathbf{y} = \mathbf{H}\mathbf{x} + \mathbf{v}, \tag{3.18}$$

with $\mathbf{v} \sim \mathcal{N}\left(0,\ \sigma_r^2 \mathbf{I}\right)$. Using the Bayes' rule, one can obtain

$$\hat{\mathbf{x}} = \underset{\mathbf{x}}{\operatorname{argmin}} \left\{ -\log\ p\left(\mathbf{y}|\mathbf{x}\right) - \log\ p\left(\mathbf{x}\right) \right\}, \tag{3.19}$$

for which it is straightforward to conclude that the ℓ_1-norm regularization in (3.16) is the maximum a posterior (MAP) estimator. In this MAP estimator the prior density is explained by the multivariate Laplace density $p\left(\mathbf{x}\right) \propto \exp\left(-\lambda \left\|\mathbf{\Phi}\mathbf{x}\right\|_1\right)$, where the log-likelihood is $p\left(\mathbf{y}|\mathbf{x}\right) \propto \exp\left(-\left\|\mathbf{y} - \mathbf{H}\mathbf{x}\right\|_2^2\right)$. Therefore, from statistical point of view, the choice of ℓ_1-norm regularization and proper selection of the transformation $\mathbf{\Phi}$ may be considered as a statistical model selection problem in response to the underlying heavy tailed structure of the state variable of interest.

Another related important concept that has received a great deal of attention in the past decade is the so-called *sparsity*. By Definition a vector is sparse when the number of its

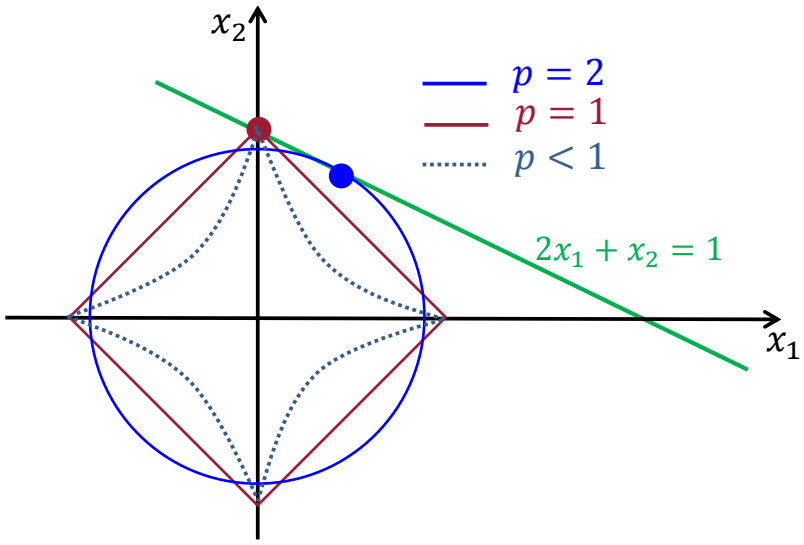

Figure 3.3: Geometry of ℓ_p-norm regularization and sparsity. In general, the ℓ_p-norm regularization promotes sparsity for $p \leq 1$. Theoretically, the sparsest solution can be obtained for $p = 0$; however, this norm is discontinuous and gives rise to Non-deterministic Polynomial-time hard complexity (NP-hard). Thus, the ℓ_1-norm regularization can be considered as the best convex relaxation of the ℓ_0-norm to promote sparsity.

nonzero elements is much smaller than that of its observational dimension. More specifically, a vector $\mathbf{x} \in \mathbb{R}^m$ is sparse if $\|\mathbf{x}\|_0 \ll n$, where $\mathbf{y} \in \mathbb{R}^n$ and ℓ_0-norm denotes the number of non-zero elements of $\mathbf{x}$. Therefore, if as a priori, we know that the solution of a system of equation is sparse, naturally, we need to solve the following general form of the regularized least-squares

$$\underset{\mathbf{x}}{\text{minimize}} \left\{ \|\mathbf{y} - \mathbf{H}\mathbf{x}\|_2^2 + \lambda \|\Phi\mathbf{x}\|_0 \right\}. \tag{3.20}$$

However, the ℓ_0-norm[1] is discontinuous and can not be tackled through the domain of smooth and convex optimization. It turns out that in general, the ℓ_p-norm regularization tends to produce sparser solutions than that of the Tikhonov regularization for $p < 2$. However, the ℓ_p-norm is not convex for $p < 1$. Consequently, ℓ_1-norm regularization can be considered as the closest convex relaxation of the ℓ_0-norm to induce the desired sparsity on the solution of a linear system (Figure 3.3). A middle ground that allows us to incorporate sparsity while staying in the domain of convex optimization.

Intuitively, the concept of sparsity is very related to the statistical interpretation of the prior distribution of $\mathbf{x}$ using the GGD density. Choosing a heavy tailed symmetric GGD density implies that a large number of the elements of the state variable of interest $\mathbf{x}$ are

[1]The term ℓ_0-norm is misleading, as this function does not satisfy the axiomatic requirements of a norm. Formally $\|\mathbf{x}\|_0 = \lim_{p\to 0} \sum_{i=1}^m |x_i|^p = \#\{i : x_i \neq 0\}$ obeys the triangle inequality $\|\mathbf{x}+\mathbf{z}\|_0 \leq \|\mathbf{x}\|_0 + \|\mathbf{z}\|_0$ while homogeneity property is not met: for $t \neq 0$, $\|t\mathbf{x}\|_0 = \|\mathbf{x}\|_0 \neq t\|\mathbf{x}\|_0$. Nevertheless, we proceed the discussion in this document and use the term ℓ_0-norm for notational convenience.

nearly zero while a few of them are significantly non-zero and form the tail. This relaxed interpretation of sparsity often called *compressibility* (*Elad*, 2010).

Chapter 4

Variational Data Assimilation via Sparse Regularization

4.1 Background

In this subsection, we briefly review the recently proposed regularized variational data assimilation (RVDA) methodology and its implications with particular emphasis on the smoothing ℓ_1-norm regularization.

As is evident, when the Hessian (i.e., $\underline{\mathbf{H}}^{\mathrm{T}}\underline{\mathbf{R}}^{-1}\underline{\mathbf{H}}+\mathbf{B}^{-1}$) in the classic VDA cost function in (2.86) is ill-conditioned, the VDA solution is likely to be unstable with large estimation uncertainty. Typically, the ill-conditioning of the Hessian is due to observation noise and the structure of the observation operator. Therefore, it is clear that a well-conditioned background covariance $\mathbf{B}$ can improve the overall condition number of the Hessian and stabilize the solution. Inspired by the well-known relationship between the Tikhonov regularization and spectral filtering (e.g., *Golub et al.*, 1999), *Johnson et al.* (2005b,a) proposed to reformulate the classic VDA problem analogous to the standard form of the Tikhonov regularization (*Tikhonov et al.*, 1977). Accordingly, using a change of variable $\mathbf{z}_0 = \mathbf{C}_{\mathrm{B}}^{-1/2}\left(\mathbf{x}_0 - \mathbf{x}_0^b\right)$, letting $\mathbf{B} = \sigma_b^2\mathbf{C}_{\mathrm{B}}$ and $\underline{\mathbf{R}} = \sigma_r^2\underline{\mathbf{C}}_{\mathrm{R}}$, where $\mathbf{C}_{\mathrm{B}}$ and $\underline{\mathbf{C}}_{\mathrm{R}}$ are the correlation matrices, the classic variational cost function was proposed to be reformulated as follows:

$$\mathcal{J}_{4D}(\mathbf{z}_0) = \|\mathbf{f} - \mathbf{G}\mathbf{z}_0\|_2^2 + \mu\,\|\mathbf{z}_0\|_2^2\,. \tag{4.1}$$

where the ℓ_2-norm is $\|\mathbf{x}\|_2 = \left(\Sigma_{i=1}^m x_i^2\right)^{1/2}$, $\mu = \sigma_r^2/\sigma_b^2$, $\mathbf{G} = \underline{\mathbf{C}}_{\mathrm{R}}^{-1/2}\underline{\mathbf{H}}\mathbf{C}_{\mathrm{B}}^{1/2}$, and $\mathbf{f} = \underline{\mathbf{C}}_{\mathrm{R}}^{-1/2}\left(\underline{\mathbf{y}} - \underline{\mathbf{H}}\mathbf{x}_0^b\right)$. Hence, by solving

$$\mathbf{z}_0^a = \underset{\mathbf{z}_0}{\operatorname{argmin}}\left\{\mathcal{J}_{4D}(\mathbf{z}_0)\right\},$$

the analysis can be obtained as, $\mathbf{x}_0^a = \mathbf{x}_0^b + \mathbf{C}_{\mathrm{B}}^{1/2}\mathbf{z}_0^a$. Having the above reformulated problem, (*Johnson et al.*, 2005a) provided new insights into the stabilizing role of the background error covariance matrix on the solution of the classic VDA problem.

To tackle data assimilation of sharp fronts, following the above reformulation, *Freitag et al.* (2012) suggested to add the smoothing ℓ_1-norm regularization as follows:

$$\mathbf{z}_0^a = \underset{\mathbf{z}_0}{\operatorname{argmin}} \left\{ \mathcal{J}_{4D}(\mathbf{z}_0) + \lambda \left\| \mathbf{\Phi} \left(\mathbf{C}_{\mathrm{B}}^{1/2}\mathbf{z}_0 + \mathbf{x}_0^b \right) \right\|_1 \right\}, \tag{4.2}$$

where the ℓ_1-norm is $\|\mathbf{x}\|_1 = \Sigma_{i=1}^m |x_i|$; the non-negative λ is called the regularization parameter; and $\mathbf{\Phi}$ is proposed to be an approximate first-order derivative operator as follows:

$$\mathbf{\Phi} = \begin{bmatrix} -1 & 1 & & 0 \\ & \ddots & \ddots & \\ 0 & & -1 & 1 \end{bmatrix} \in \mathbb{R}^{(m-1)\times m}.$$

Notice that problem (3.2) is a non-smooth optimization as the derivative of the cost function does not exist at the origin. *Freitag et al.* (2012) recast this problem into a quadratic programing (QP) with both equality and inequality constraints where the dimension of the proposed QP is three times larger than that of the original problem. It is also worth noting that, the reformulations in (4.1) and (3.2) assume that the error covariance matrices are stationary (i.e., $\mathbf{B} = \sigma_b^2\mathbf{C}_{\mathrm{B}}$, $\mathbf{R} = \sigma_r^2\mathbf{C}_{\mathrm{R}}$) and the error variance is distributed uniformly across all of the problem dimensions, while without loss of generality, a covariance matrix $\mathbf{B} \in \mathbb{R}^{m\times m}$ can be decomposed as $\mathbf{B} = \operatorname{diag}(\mathbf{s})\ \mathbf{C}_{\mathrm{B}}\ \operatorname{diag}(\mathbf{s})$, where $\mathbf{s} \in \mathbb{R}^m$ is the vector of standard deviations (*Barnard et al.*, 2000). Therefore, while one can have an advantage in stability of computation in the proposed formulation in (4.1) and (3.2), the assumptions might be restrictive in practice.

In the subsequent sections, we present a unified framework to regularize the VDA problem in a properly chosen transform domain or a pre-selected basis (e.g., wavelet, Fourier, DCT). The presented formulation includes smoothing $\ell_1$and ℓ_2-norm regularization as two especial cases and does not require any explicit assumption about the stationarity of the error covariance matrices. We present a solution method, which recasts the proposed regularized VDA problem into a QP with lower dimension and simpler constraints compared to the presented solution method by *Freitag et al.* (2012). Some results are presented via assimilating low-resolution and noisy observations into the linear advection-diffusion equation in a 4D-Var setting.

4.1.1 A Unified Framework for Regularized Variational Data Assimilation in Transform Domains

In a more general setting, to regularize the solution of the classic VDA problem, one may constrain the magnitude of the analysis in the norm sense as follows:

$$\begin{aligned} \mathbf{x}_0^a &= \underset{\mathbf{x}_0}{\operatorname{argmin}} \left\{ \mathcal{J}_{4D}(\mathbf{x}_0) \right\} \\ &\text{s.t.} \quad \left\| \mathbf{\Phi} \mathbf{x}_0 \right\|_p^p \leq \text{const.} \end{aligned} \tag{4.3}$$

where $\mathbf{\Phi} \in \mathbb{R}^{m \times m}$ is any appropriately chosen linear transformation, and the ℓ_p-norm is $\|\mathbf{x}\|_p = (\Sigma \, |x_i|^p)^{1/p}$ with $p > 0$. By constraining the ℓ_p-norm of the analysis, we implicitly make the solution more stable. In other words, we bound the magnitude of the analysis state and reduce the instability of the solution due to the potential ill-conditioning of the classic cost function. Using the theory of Lagrange multipliers, the above constrained problem can be turned into the following unconstrained one:

$$\mathbf{x}_0^a = \underset{\mathbf{x}_0}{\operatorname{argmin}} \left\{ \frac{1}{2} \left\| \underline{\mathbf{y}} - \underline{\mathbf{H}} \mathbf{x}_0 \right\|_{\underline{\mathbf{R}}^{-1}}^2 + \frac{1}{2} \left\| \mathbf{x}_0^b - \mathbf{x}_0 \right\|_{\mathbf{B}^{-1}}^2 + \lambda \left\| \mathbf{\Phi} \mathbf{x}_0 \right\|_p^p \right\}. \tag{4.4}$$

where the non-negative λ is the Lagrange multiplier. As is evident, when λ tends to zero the regularized analysis tends to the classic analysis in (2.86), while large values are expected to produce more stable solutions but with less fidelity to the observations and background state. Therefore, in problem (4.4), the regularization parameter λ plays an important trade-off role and ensures that the magnitude of the analysis is sufficiently constrained in the norm sense while keeping it sufficiently close to observations and background state. Notice that although in special cases there are some heuristic approaches to find an optimal regularization parameter (e.g., *Hansen and O'Leary*, 1993; *Johnson et al.*, 2005b), typically this parameter is selected empirically based on the problem at hand.

It is important to note that, from the probabilistic point of view, the regularized problem (4.4) can be viewed as the maximum a posteriori (MAP) Bayesian estimator. Indeed, the constraint of regularization refers to the *prior* knowledge about the probabilistic distribution of the state as $p(\mathbf{x}) \propto \exp\left(-\lambda \left\| \mathbf{\Phi} \mathbf{x} \right\|_p^p\right)$. In other words, we implicitly assume that under the chosen transformation $\mathbf{\Phi}$ the state of interest can be well explained by the family of multivariate Generalized Gaussian Density (e.g., *Nadarajah*, 2005) which includes the multivariate Gaussian ($p = 2$) and Laplace ($p = 1$) densities as special cases. As is evident, because the prior term is not Gaussian, the posterior density of the above estimator does not remain in the Gaussian domain and thus characterization of the a posteriori covariance is not straightforward in this case.

From an optimization view point, the above regularized variational data assimilation (RVDA) problem is convex with a unique global solution (analysis) when $p \geq 1$; otherwise, it may

suffer from multiple local minima. For the special case of the Gaussian prior ($p = 2$) the problem is smooth and resembles the well-known smoothing norm Tikhonov regularization (*Tikhonov et al.*, 1977; *Hansen*, 2010). However, for the case of the Laplace prior ($p = 1$) the problem is non-smooth, and it has received a great deal of attention in recent years for solving sparse ill-posed inverse problems (see, *Elad*, 2010, and references there in). It turns out that the ℓ_1-norm regularization promotes sparsity in the solution. In other words, using this regularization, it is expected that the number of non-zero elements of $\mathbf{\Phi}\mathbf{x}_0^a$ be significantly less than the observational dimension. Therefore, if we know a priori that a specific $\mathbf{\Phi}$ projects a large number of elements of the state variable of interest onto (near) zero values, the ℓ_1-norm is a proper choice of the regularization term that can yield improved estimates of the analysis state (e.g., *Chen et al.*, 2001; *Candes and Tao*, 2006; *Elad*, 2010).

In the subsequent sections, we focus on the 4D-Var problem under the ℓ_1-norm regularization as follows:

$$\mathbf{x}_0^a = \underset{\mathbf{x}_0}{\operatorname{argmin}} \left\{ \frac{1}{2} \left\| \underline{\mathbf{y}} - \underline{\mathbf{H}}\mathbf{x}_0 \right\|_{\bar{\mathbf{R}}^{-1}}^2 + \frac{1}{2} \left\| \mathbf{x}_0^b - \mathbf{x}_0 \right\|_{\mathbf{B}^{-1}}^2 + \lambda \left\| \mathbf{\Phi}\mathbf{x}_0 \right\|_1 \right\}. \tag{4.5}$$

It is important to note that the presented formulation in (4.5) shares the same solution with the problem in (3.2) while in a more general setting, it allows us to use non-stationary error covariance matrices without the need for additional computational cost to obtain their square roots, as needed in problem (3.2).

4.1.1.1 Solution Method via Quadratic Programing

Due to the separability of the ℓ_1-norm, one of the most well-known methods (see, *Chen et al.*, 1998; *Figueiredo et al.*, 2007) can be used to recast the ℓ_1-norm RVDA problem in (4.5) to a constrained quadratic programming. To this end, let us expand the ℓ_1-norm regularized variational data assimilation (ℓ_1-RVDA) problem in (4.5) as follows:

$$\underset{\mathbf{x}_0}{\text{minimize}} \quad \left\{ \frac{1}{2}\mathbf{x}_0^{\mathrm{T}} \left(\mathbf{B}^{-1} + \underline{\mathbf{H}}^{\mathrm{T}}\mathbf{R}^{-1}\underline{\mathbf{H}} \right) \mathbf{x}_0 - \left(\mathbf{B}^{-1}\mathbf{x}_0^b + \underline{\mathbf{H}}^{\mathrm{T}}\mathbf{R}^{-1}\underline{\mathbf{y}} \right)^{\mathrm{T}} \mathbf{x}_0 + \lambda \left\| \mathbf{\Phi}\mathbf{x}_0 \right\|_1 \right\}. \tag{4.6}$$

Here, let us assume that $\mathbf{c}_0 = \mathbf{\Phi}\mathbf{x}_0$, where $\mathbf{x}_0$ and $\mathbf{c}_0$ are in $\mathbb{R}^m$, then the above problem can be rewritten as:

$$\underset{\mathbf{z}_0}{\text{minimize}} \quad \left\{ \frac{1}{2}\mathbf{c}_0^{\mathrm{T}}\mathbf{Q}\mathbf{c}_0 + \mathbf{b}^{\mathrm{T}}\mathbf{c}_0 + \lambda \left\| \mathbf{c}_0 \right\|_1 \right\}, \tag{4.7}$$

where, $\mathbf{Q} = \mathbf{\Phi}^{-\mathrm{T}} \left(\mathbf{B}^{-1} + \underline{\mathbf{H}}^{\mathrm{T}}\mathbf{R}^{-1}\underline{\mathbf{H}} \right) \mathbf{\Phi}^{-1}$ and $\mathbf{b} = -\mathbf{\Phi}^{-\mathrm{T}} \left(\mathbf{B}^{-1}\mathbf{x}_0^b + \underline{\mathbf{H}}^{\mathrm{T}}\mathbf{R}^{-1}\underline{\mathbf{y}} \right)$.

Split $\mathbf{c}_0$ into its positive $\mathbf{u}_0 = \max(\mathbf{c}_0, 0)$ and negative $\mathbf{v}_0 = \max(-\mathbf{c}_0, 0)$ components such that $\mathbf{c}_0 = \mathbf{u}_0 - \mathbf{v}_0$. as a result we get,

$$\begin{aligned} \underset{\mathbf{x}_0}{\text{minimize}} \quad & \left\{ \frac{1}{2} (\mathbf{u}_0 - \mathbf{v}_0)^{\mathrm{T}} \mathbf{Q} (\mathbf{u}_0 - \mathbf{v}_0) + \mathbf{b}^{\mathrm{T}} (\mathbf{u}_0 - \mathbf{v}_0) + \lambda 1_m^{\mathrm{T}} (\mathbf{u}_0 + \mathbf{v}_0) \right\} \\ & \text{subject to} \quad \mathbf{u}_0 \succcurlyeq 0, \, \mathbf{v}_0 \succcurlyeq 0 \end{aligned} \tag{4.8}$$

Stacking $\mathbf{u}_0$ and $\mathbf{v}_0$ in $\mathbf{w}_0 = [\mathbf{u}_0^{\mathrm{T}}, \, \mathbf{v}_0^{\mathrm{T}}]^{\mathrm{T}}$, the more standard QP formulation of the problem is immediately followed as:

$$\begin{aligned} \underset{\mathbf{w}_0}{\text{minimize}} \quad & \left\{ \frac{1}{2} \mathbf{w}_0^{\mathrm{T}} \begin{bmatrix} \mathbf{Q} & -\mathbf{Q} \\ -\mathbf{Q} & \mathbf{Q} \end{bmatrix} \mathbf{w}_0 + \left(\lambda \mathbf{1}_{2m} + \begin{bmatrix} \mathbf{b} \\ -\mathbf{b} \end{bmatrix} \right)^{\mathrm{T}} \mathbf{w}_0 \right\}. \\ & \text{s.t.} \quad \mathbf{w}_0 \succcurlyeq 0, \end{aligned} \tag{4.9}$$

Clearly, given the solution $\hat{\mathbf{w}}_0$ of (4.9), one can easily retrieve $\hat{\mathbf{c}}_0$ and thus the analysis state is $\mathbf{x}_0^a = \mathbf{\Phi} \hat{\mathbf{c}}_0$. The dimension of the QP representation (4.9) is twice that of the original ℓ_1-RVDA problem (4.5). However, using iterative first order gradient based methods, which are often the only practical option for large-scale data assimilation problems, it is easy to see that the effect of this dimensionality enlargement is minor on the overall cost of the problem. Because, one can easily see that obtaining the gradient of the cost function in (4.9) only requires to compute

$$\begin{bmatrix} \mathbf{Q} & -\mathbf{Q} \\ -\mathbf{Q} & \mathbf{Q} \end{bmatrix} \mathbf{w}_0 = \begin{bmatrix} \mathbf{Q} (\mathbf{u}_0 - \mathbf{v}_0) \\ -\mathbf{Q} (\mathbf{u}_0 - \mathbf{v}_0) \end{bmatrix},$$

which mainly requires matrix-vector multiplication in $\mathbb{R}^m$ (see; e.g., *Figueiredo et al.*, 2007).

The constraint of the QP problem (4.9) is simpler than the formulation suggested by (*Freitag et al.*, 2012) and allows us to use efficient and convergent gradient projection methods (e.g., *Bertsekas*, 1976; *Serafini et al.*, 2005; *Figueiredo et al.*, 2007), suitable for large-scale VDA problems. The dimension of the above problem seems twice that of the original problem; however, because of the existing symmetry in this formulation, the computational burden remains at the same order as the original classic problem (see, appendix A). Another important observation is that, choosing an orthogonal transformation (e.g., orthogonal wavelet, DCT, Fourier) for $\mathbf{\Phi}$ is very advantageous computationally, as in this case $\mathbf{\Phi}^{-1} = \mathbf{\Phi}^{\mathrm{T}}$.

Conceptually, adding relevant regularization terms, we enforce the analysis to follow a certain regularity and become more stable (*Hansen*, 2010). Here, by regularity, we refer to a certain degree of smoothness in the analysis state. For instance if we think of $\mathbf{\Phi}$ as

a first order derivative operator, using the smoothing ℓ_2-norm regularization ($\lambda \left\| \mathbf{\Phi x}_0 \right\|_2^2$), we enforce the energy of the solution's increments to be minimal, which naturally imposes more smoothness. Therefore, using the smoothing ℓ_2-norm regularization in a derivative space, is naturally suitable for continuous and smooth physical states. On the other hand, for piece-wise smooth physical states with isolated singularities and jumps, it turns out that the use of the smoothing ℓ_1-norm regularization ($\lambda \left\| \mathbf{\Phi x}_0 \right\|_1$) in a derivative domain is very advantageous. Using this norm in derivative space, we implicitly constrain the total variation of the solution which prevents imposing extra smoothness on the solution. Proper selection of the smoothing norm and $\mathbf{\Phi}$ may fall into the category of statistical model selection which is briefly explained in the following subsections and Appendix A.

As briefly explained previously, more stability of the solution comes from the fact that we constrain the magnitude of the solution by adding the regularization term and preventing the solution to blow up due to the inversion of observations and background error (see, e.g., *Hansen*, 1998; *Johnson et al.*, 2005a). In ill-conditioned classic VDA problems, it is easy to see that the inverse of the Hessian in (2.87) may contain very large elements which spoil the analysis. However, by regularization and making the problem well-posed, we shrink the size of the elements of the covariance matrix and reduce the estimation error. We need to emphasize that this improvement in the analysis error covariance, naturally comes at the cost of introducing a small bias in the regularized solution whose magnitude can be kept small by proper selection of the regularization parameter λ (see, e.g., *Neumaier*, 1998).

It is important to note that, for the smoothing ℓ_1-norm regularization in (4.9), it is easy to show that the regularization parameter is bounded as, $0 < \lambda < \left\| \mathbf{b} \right\|_\infty$, where the infinity-norm is $\left\| \mathbf{x} \right\|_\infty = \max\left(\left| x_1 \right|, \ldots, \left| x_m \right| \right)$. For those values of λ greater than the upper bound, clearly the analysis state in (4.9) is the zero vector with maximum sparsity.

To derive this upper bound, we follow a similar approach as suggested for example by *Kim et al.* (2007). Obviously, $\mathbf{c}_0^a$ is a minimizer of problem (4.7) if and only if its cost function $\mathcal{J}_{R4D}\left(\mathbf{c}_0 \right)$ is sub-differentiable at $\mathbf{c}_0^a$ and thus

$$0 \in \partial \mathcal{J}_{R4D}(\mathbf{c}_0^a),$$

where, $\partial \mathcal{J}_{R4D}(\mathbf{c}_0^a)$ is the sub-differential set at the solution point or analysis coefficients at in the selected basis. Given that

$$\partial \mathcal{J}_{R4D}(\mathbf{c}_0^a) = \mathbf{Q}\mathbf{c}_0^a + \mathbf{b} + \lambda \partial \left(\left\| \mathbf{c}_0^a \right\|_1 \right),$$

we have

$$-\mathbf{Q}\mathbf{c}_0^a - \mathbf{b} \in \lambda \partial \left(\left\| \mathbf{c}_0^a \right\|_1 \right).$$

and thus for $\mathbf{c}_0^a = \mathbf{0}_m$, $\mathbf{0}_m = [0, \ldots, 0]^{\mathrm{T}} \in \mathbb{R}^m$, one can obtain the following vector

inequality

$$-\lambda \mathbf{1}_m \preceq -\mathbf{b} \preceq \lambda \mathbf{1}_m,$$

which implies that $\lambda \geq \|\mathbf{b}\|_\infty$. Therefore for λ must be less than $\|\mathbf{b}\|_\infty$ to obtain nonzero analysis coefficients in problem (4.6).

To solve the QP problem in (4.9) for large dimensional problems, one can use the efficient Gradient projection method explained in (see, *Bertsekas*, 1999, pp. 228), which is explained in the next subsection.

4.1.2 Gradient Projection Method

Gradient projection (GP) method is an efficient and convergent optimization method to solve convex optimization problems over convex sets (see, *Bertsekas*, 1999, pp. 228). This method is of particular interest, especially, when the constraints form a convex set $\mathcal{C}$ with simple projection operator. The cost function $\mathcal{J}_{R4D}(\mathbf{w}_0)$ in (2.8) is a quadratic function that need to be minimized on non-negative orthant $\mathcal{C} = \{\mathbf{w}_0 |\ w_{0,i} \geq 0\ \forall\, i = 1, \ldots, 2m\}$ as follows:

$$\begin{aligned} \hat{\mathbf{w}}_0 \quad &= \quad \text{argmin } \{\mathcal{J}_{R4D}(\mathbf{w}_0)\} \\ &\qquad \text{s.t. } \mathbf{w}_0 \succeq 0. \end{aligned} \tag{4.10}$$

For this particular problem, the GP method amounts obtaining the following fixed point:

$$\mathbf{w}_0^* = \left[\mathbf{w}_0^* - \beta \nabla \mathcal{J}_{R4D}(\mathbf{w}_0^*)\right]^+, \tag{4.11}$$

where β is a stepsize along the descent direction and for every element of $\mathbf{w}_0$

$$[w_0]^+ = \begin{cases} 0 & \text{if } w_0 \leq 0 \\ w_0 & \text{otherwise,} \end{cases} \tag{4.12}$$

denotes the Euclidean projection operator onto the non-negative orthant. As is evident, the fixed point can be obtained iteratively as

$$\mathbf{w}_0^{k+1} = \left[\mathbf{w}_0^k - \beta^k \nabla \mathcal{J}_{R4D}(\mathbf{w}_0^k)\right]^+. \tag{4.13}$$

Thus, if the descent at step k is feasible, that is $\mathbf{w}_0^k - \beta^k \nabla \mathcal{J}_{R4D}(\mathbf{w}_0^k) \succeq 0$, the GP iteration becomes an ordinary unconstrained steepest descent method, otherwise the result is mapped back onto the feasible set by the projection operator in (4.12). In effect, the GP method finds iteratively the closest feasible point in the constraint set to the solution of the original unconstrained minimization.

In our study, the stepsize β^k was selected using the *Armijo rule,* or the so-called *backtracking line search*, that is a convergent and very effective stepsize rule. This stepsize rule depends on two constants $0 < \xi < 0.5$, $0 < \varsigma < 1$ and assumed to be $\beta^k = \varsigma^{m_k}$, where m_k is the smallest non-negative integer for which

$$\mathcal{J}_{R4D}\left(\mathbf{w}_0^k - \beta^k \nabla \mathcal{J}_{R4D}(\mathbf{w}_0^k)\right) \leq \mathcal{J}_{R4D}(\mathbf{w}_0^k) - \xi \beta^k \nabla \mathcal{J}_{R4D}(\mathbf{w}_0^k)^{\mathrm{T}} \nabla \mathcal{J}_{R4D}(\mathbf{w}_0^k). \qquad (4.14)$$

In our experiments, described in the next section, the backtracking parameters are set to $\xi = 0.2$ and $\varsigma = 0.5$ (see, *Boyd and Vandenberghe*, 2004, pp.464 for more explanation). In our coding, the iterations terminate if $\frac{\left\|\mathbf{w}_0^k - \mathbf{w}_0^{k-1}\right\|_2}{\left\|\mathbf{w}_0^{k-1}\right\|_2} \leq 10^{-5}$ or the number of iterations exceeds 100.

Chapter 5

Results of Sparse promoting VDA

5.1 Examples on Linear Advection Diffusion Equation

5.1.1 Problem Statement

The advection diffusion equation is a parabolic partial differential equation with a drift and has fundamental applications in various areas of applied sciences and engineering. This equation is indeed a simplified version of the general Navier-Stocks equation for a divergence free and incompressible Newtonian fluid where the pressure gradient is negligible. In a general form, this equation for a quantity of $\mathbf{x}(s,\, t)$ is

$$\begin{aligned} \frac{\partial \mathbf{x}(s,\, t)}{\partial t} + a(s,\, t)\nabla \mathbf{x}(s,\, t) &= \epsilon \nabla^2 \mathbf{x}(s,\, t), \\ \mathbf{x}(s,\, 0) &= \mathbf{x}_0(s), \end{aligned} \tag{5.1}$$

where $a(s,\, t)$ represents the velocity and $\epsilon \geq 0$ denotes the viscosity constant.

The linear ($a = \text{const.}$) and inviscid form ($\epsilon = 0$) of (5.1) has been the subject of modeling, numerical simulation, and data assimilation studies of advective atmospheric and oceanic flows and fluxes. For example, *Lin et al.* (1998) argued that the mechanism of rain-cell regeneration can be well explained by a pure advection mechanism, *Jochum and Murtugudde* (2006) found that Tropical Instability Waves (TIWs) need to be modeled by horizontal advection without involving any temperature mixing length. The nonlinear inviscid form (e.g., Burgers' equation) has been used in the shallow water equation and has been subject of oceanic and tidal data assimilation studies (e.g., *Bennett and McIntosh*, 1982; *Evensen*, 1994b). The linear and viscid form ($\epsilon > 0$), has fundamental applications in modeling of atmospheric and oceanic mixing (e.g., *Smith and Marshall*, 2009; *Lanser and Verwer*, 1999; *Jochum and Murtugudde*, 2006, chap. 6); land-surface moisture and heat transport (e.g., *Afshar and Marino*, 1978; *Hu and Islam*, 1995; *Peters-Lidard et al.*, 1997; *Liang et al.*,

1999); surface water quality modeling (e.g., *Chapra*, 2008, chap. 8), and subsurface mass and heat transfer studies (e.g., *Fetter*, 1994).

Here, we restrict our consideration only to the linear form and present a series of test problems to demonstrate the effectiveness of the ℓ_1-norm RVDA in a 4D-Var setting. It is well understood that the general solution of the linear viscid form of (5.1) relies on the principle of superposition of linear advection and diffusion. In other words, the solution at time t is obtained via shifting the initial condition by at, followed by a convolution with the fundamental Gaussian kernel as follows:

$$\mathcal{D}(s,\, t) = (4\pi\epsilon t)^{-1/2} \exp\left(\frac{-\,|s|^2}{4\epsilon t}\right), \tag{5.2}$$

where the standard deviation is $\sqrt{2\epsilon t}$. As is evident, the linear shift of size at also amounts to obtaining the convolution of the initial condition with a Kronecker delta function as follows:

$$\mathcal{A}\,(s - at) = \begin{cases} 1 & s = at \\ 0 & \text{otherwise} \end{cases}. \tag{5.3}$$

5.1.2 Assimilation Set Up and Results

5.1.2.1 Prognostic Equation and Observation Model

It is well understood that (circular) convolution in discrete space can be constructed as a (circulant) Toeplitz matrix-vector product (e.g., *Chan and Jin*, 2007). Therefore, in the context of a discrete advection-diffusion model, the temporal diffusivity and spatial linear shift of the initial condition can be expressed in a matrix form by $\mathbf{D}_{0,i}$ and $\mathbf{A}_{0,i}$, respectively. In effect, $\mathbf{D}_{0,i}$ represents a Toeplitz matrix, for which its rows are filled with discrete samples of the Gaussian Kernel in (5.2), while the rows of $\mathbf{A}_{0,i}$ contain a properly positioned Kronecker delta function.

Thus, for our case, the underlying prognostic equation, i.e., $\mathbf{x}_i = \mathbf{M}_{0,i}\,\mathbf{x}_0$, may be expressed as follows:

$$\mathbf{x}_i = \mathbf{A}_{0,i}\mathbf{D}_{0,i}\,\mathbf{x}_0. \tag{5.4}$$

In this study, the low-resolution constraints of the sensing system are modeled using a linear smoothing filter followed by a down-sampling operation. Specifically, we consider the following time-invariant linear measurement operator

$$\mathbf{H} = \frac{1}{4}\begin{bmatrix} 1\,1\,1\,1 & 0\,0\,0\,0 & \cdots & 0\,0\,0\,0 \\ 0\,0\,0\,0 & 1\,1\,1\,1 & \cdots & 0\,0\,0\,0 \\ \vdots & \vdots & \vdots & \vdots \\ 0\,0\,0\,0 & 0\,0\,0\,0 & \cdots & 1\,1\,1\,1 \end{bmatrix} \in \mathbb{R}^{n\times m}, \tag{5.5}$$

which maps the higher-dimensional state to a lower-dimensional observation space. In effect, each observation point is then an average and noisy representation of the four adjacent points of the true state.

5.1.2.2 Initial States

To demonstrate the effectiveness of the proposed ℓ_1-norm regularization in (2.12), we consider four different initial conditions which exhibit sparse representation in the wavelet and DCT domains (Figure 5.1). In particular, we consider: (a) a flat top-hat, which is a composition of zero-order polynomials and can be sparsified theoretically using the first order Daubechies wavelet (DB01) or the Haar basis; (b) a quadratic top-hat which is a composition of zero and second order polynomials and theoretically can be well sparsified by wavelets with vanishing moments of order greater than three (*Mallat*, 2009, pp.284); (c) a window sinusoid; and (d) a squared exponential function which exhibits sparse behavior in the DCT basis. All of the initial states are assumed to be in $\mathbb{R}^{1024}$ and are evolved in time with a viscosity coefficient $\epsilon = 4\,[\mathrm{L}^2/\mathrm{T}]$ and velocity $a = 1\,[\mathrm{L}/\mathrm{T}]$. The assimilation interval is assumed to be between 0 and $T = 500[\mathrm{T}]$, where the observations are sparsely available over this interval at every 125[T] time steps (Figure 5.1 and 5.2).

5.1.2.3 Observation and Background Error

The observations and background error are one of the most important components of a data assimilation system that determines the quality and information content of the analysis. Clearly, the nature and behavior of the errors are problem-dependent and need to be carefully investigated in a case by case study. It needs to be stressed that from a probabilistic point of view, the presented formulation for the ℓ_1-norm RVDA assumes that both of the error components are unimodal and can be well explained by the class of Gaussian covariance models. Here, for observation error, we only consider a stationary white Gaussian measurement error, $\mathbf{v} \sim \mathcal{N}(0, \mathbf{R})$, where $\mathbf{R} = \sigma_r^2\mathbf{I}$ (Figure 5.2).

However, inspired by (*Gaspari and Cohn*, 1999; *Johnson et al.*, 2005b,a; *Freitag et al.*, 2012), the first and second order auto-regressive (AR) Gaussian Markov processes, are also considered for mathematical simulation of a possible spatial correlation in the background error; see *Gaspari and Cohn* (1999) for very detailed discussion about the error covariance models for data assimilation studies.

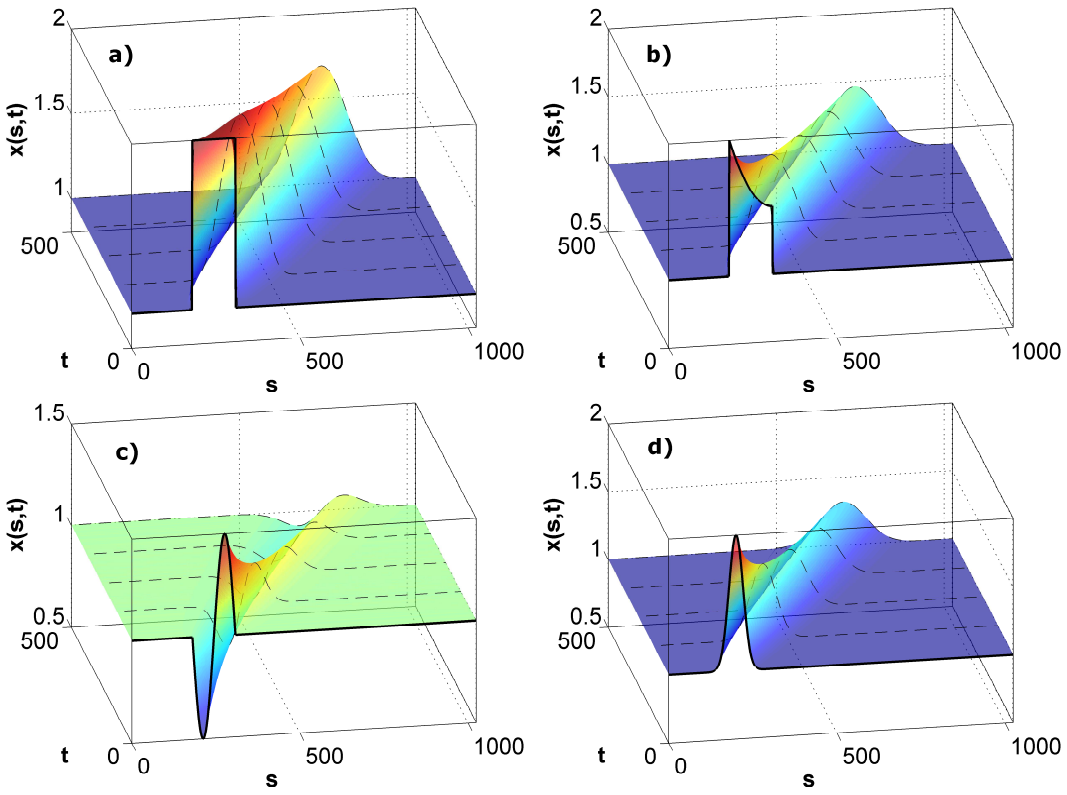

Figure 5.1: Initial conditions and their evolutions with linear advection diffusion equation: (a) flat top-hat, (b) quadratic top-hat, (c) periodic window sinusoid, and (d) squared-exponential. The first two initial conditions (a, b) exhibit sparse representation in the wavelet domain while the next two (c, d) show nearly sparse representation (the high-frequencies due to the discontinuity in derivative decay sufficiently fast) in the discrete cosine domain (DCT). Initial conditions are evolved under the linear advection-diffusion equation (5.1) with $\epsilon = 4\,[\mathrm{L}^2/\mathrm{T}]$ and $a = 1\,[\mathrm{L}/\mathrm{T}]$. The broken lines show the time instants where the low-resolution and noisy observations are available in the assimilation interval.

The AR(1), also known as the Ornestein-Ulenbeck process in infinite dimension, has an exponential covariance function $\rho(\tau) \propto e^{-\alpha|\tau|}$. In this covariance function, τ denotes the lag either in space or time, and the parameter α determines the decay rate of the correlation. The inverse of the correlation decay rate $l_c = 1/\alpha$ is often called the characteristic correlation length of the process. The covariance function of the AR(1) model has been studied very well in the context of stochastic process (e.g., *Durrett*, 1999) and estimation theory (e.g., *Levy*, 2008). For example, it is shown by *Levy* (2008, p. 298) that the eigenvalues are monotonically decreasing which may give rise to a very ill-conditioned covariance matrix in the discrete space, especially for small α or large correlation length. The covariance function of the AR(2) is more complicated than the AR(1); however, it has been shown that in special cases, its covariance function can be explained by $\rho(\tau) \propto e^{-\alpha|\tau|}\,(1 + \alpha\,|\tau|)$ (*Gaspari and Cohn*, 1999; *Stein*, 1999, p. 31). Note that, both of these covariance models are stationary and also isotropic as they are only a function of the magnitude of the correlation

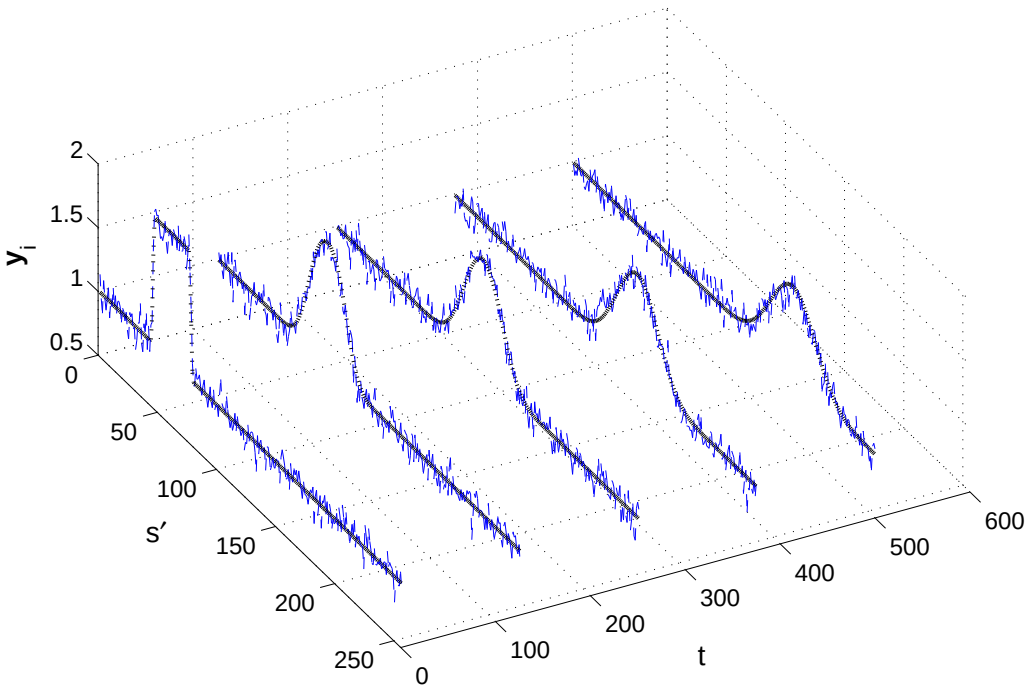

Figure 5.2: A sample representation of the available low-resolution (dotted lines) and noisy observations (broken lines) in every 125 [T] time steps in the assimilation window for the flat top-hat initial condition. Here, the observation error covariance is set to $\mathbf{R} = \sigma_r^2\mathbf{I}$ with $\sigma_r = 0.08$ equivalent to SNR $= 20\log\left(\sigma_{\mathbf{x}_0}/\sigma_r\right) \approx 12$ dB.

lag (*Rasmussen and Williams*, 2006, pp. 82). Consequently, the discrete background error covariance is a Hermitian Teoplitz matrix and can be decomposed into a scalar standard deviation and a correlation matrix as $\mathbf{B} = \sigma_b^2\mathbf{C}_b$, where

$$\mathbf{C}_b = \begin{bmatrix} \rho(0) & \rho(1) & \cdots & \rho(m) \\ \rho(1) & \rho(0) & \ddots & \vdots \\ \vdots & \ddots & \ddots & \rho(1) \\ \rho(m) & \cdots & \rho(1) & \rho(0) \end{bmatrix} \in \mathbb{R}^{m\times m}.$$

For the same values of α the correlation length, it is clear that the AR(2) correlation function decays slower than the AR(1). Figure 5.3 shows empirical estimation of the condition number of the reconstructed correlation matrices at different dimensions ranging from m =4-to-1024. As is evident, the error covariance of the AR(2) has larger condition number for the same values of the decay rate α. Clearly, as the background error plays a very important role on the overall condition number of the Hessian in the cost function in (2.86), an ill-conditioned background error covariance makes the solution more unstable with larger uncertainty around the obtained analysis.

Figure 5.4 shows a sample path and sample correlation of the chosen error models for

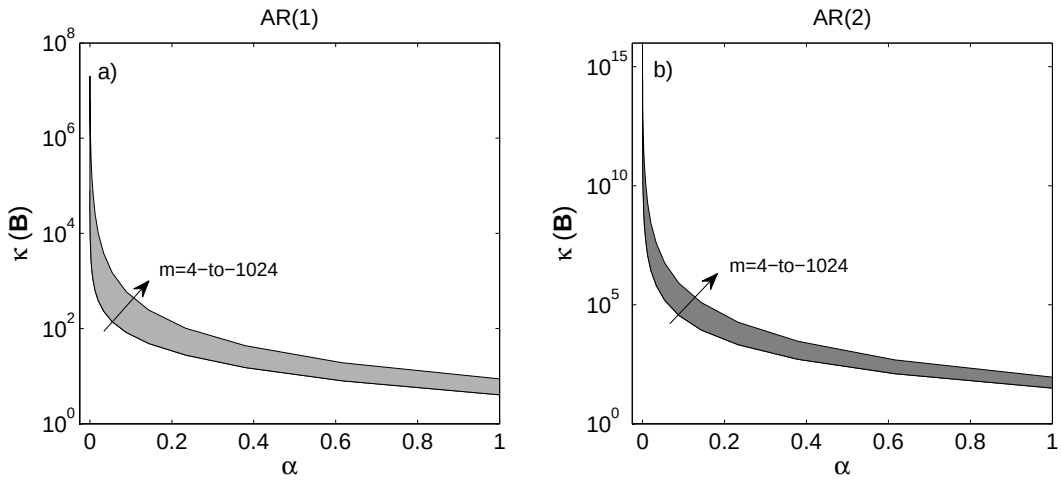

Figure 5.3: Empirical condition numbers of the background error covariance matrices as a function of the correlation decay rate (α) and problem dimension (m) for the AR(1) in (a) and AR(2) in (b). The parameter α varies along the x-axis and m varies along the different curves of the condition numbers with values between 4 and 1024. We recall that $\kappa(\mathbf{B})$ is the ratio between the largest and smallest singular values of $\mathbf{B}$. In (a) the covariance matrix is $\mathbf{B}_{ij} = e^{-\alpha|i-j|}$ and in (b) $\mathbf{B}_{ij} = e^{-\alpha|i-j|}(1+\alpha|i-j|)$, $1 \leq i, j \leq m$. It is seen that the condition numbers of the AR(2) model are significantly larger than those of the AR(1) model for the same values of the correlation decay rates.

the background error. Generally speaking, a correlated error contains large-scale (low-frequency) components that can corrupt main spectral components of the true state at the same frequency range. Therefore, this type of errors can become a part of the large-scale characteristic features of the initial state and their removal is naturally more difficult than that of the white error via a data assimilation methodology.

5.1.3 Results of Assimilation Experiments

In this subsection, we present the results of the proposed regularized data assimilation as expressed in (4.5). We first present the results for the white background error and then discuss the correlated error scenarios. As previously explained, the first two initial conditions exhibit sharp transitions and are naturally sparse in the wavelet domain. For those initial states (Figure 5.1a, b) we have used classic orthogonal wavelet transformation by *Mallat* (1989). Indeed, the columns of $\mathbf{\Phi} \in \mathbb{R}^{1024\times1024}$ in this case contain the chosen wavelet basis that allow us to decompose the initial state of interest into its wavelet representation coefficients, as $\mathbf{c} = \mathbf{\Phi x}$ (forward wavelet transform). On the other hand, due to the orthogonality of the chosen wavelet $\mathbf{\Phi\Phi}^{\mathrm{T}} = \mathbf{I}$, rows of $\mathbf{\Phi}^{\mathrm{T}}$ contain the wavelet basis that allows us to reconstruct the initial state from its wavelet representation coefficients, i.e., $\mathbf{x} = \mathbf{\Phi}^{\mathrm{T}}\mathbf{c}$. We used a full level of decomposition without any truncation of wavelet decomposition levels to produce a fully sparse representation of the initial state. For example, in our case where

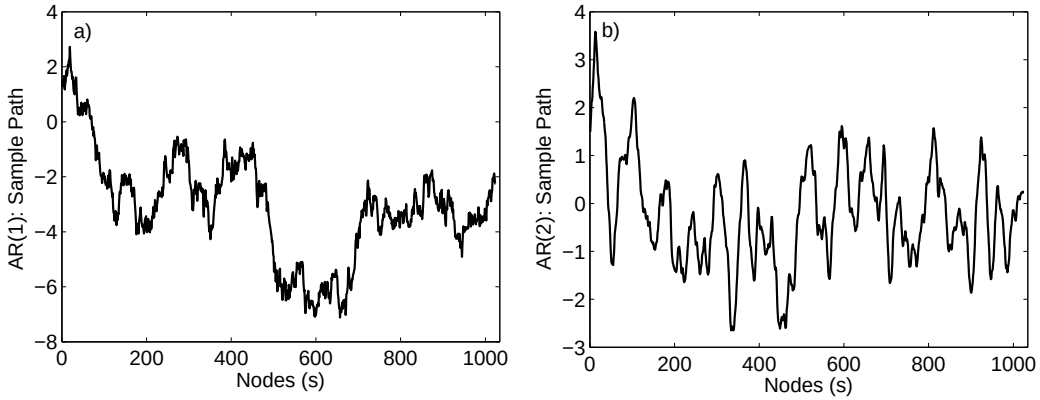

Figure 5.4: Sample paths of the used correlated background error: (a) the sample path for the AR(1) covariance matrix with $\alpha^{-1} = 150$, and (b) the sample path for the AR(2) covariance matrix with $\alpha^{-1} = 25$. The paths are formed by $\mathbf{Le}$, where $\mathbf{L}$ is the lower triangular component of the background error covariance matrix obtained via Cholesky factorization $\mathbf{B} = \mathbf{L}\mathbf{L}^{\mathrm{T}}$, and $\mathbf{e} \sim \mathcal{N}(0, \mathbf{I})$ denotes i.i.d. samples drawn from the standard white Gaussian distribution. It is seen that for very small α, the sample paths exhibit large scale oscillatory behavior that can potentially corrupt low-frequency components of the underlying state.

$\mathbf{x} \in \mathbb{R}^{1024}$, we have used ten levels of decomposition.

For the last two initial states (Figure 5.1c, d) we use DCT transformation (e.g., *Rao and Yip*, 1990) which expresses the state of interest by a linear combination of the oscillatory cosine functions at different frequencies. It is very well understood that this basis has a very strong compaction capacity to capture the energy content of sufficiently smooth states and sparsely represent them via a few cosine elementary waveforms. Note that, this transformation is also orthogonal ($\mathbf{\Phi}\mathbf{\Phi}^{\mathrm{T}} = \mathbf{I}$) and contrary to the Fourier transformation, the expansion coefficients are real.

5.1.3.1 White Background Error

For the white background and observation error covariance matrices ($\mathbf{B} = \sigma_b^2\mathbf{I}$, $\mathbf{R} = \sigma_r^2\mathbf{I}$), we considered $\sigma_b = 0.10$ (SNR $\cong$ 10.5 dB) and $\sigma_r = 0.08$ (SNR $\cong$ 12 dB), respectively. Some results are shown in Figure 5.5 for the selected initial conditions. It is clear that the ℓ_1-norm regularized solution markedly outperforms the classic 4D-Var solutions in terms of the selected metrics. Indeed, in the regularized analysis the error is sufficiently suppressed and filtered, while characteristic features of the initial state are well-preserved. On the other hand, classic solutions typically over-fitted and followed the background state rather than extracting the true state. As a result, we can argue that for the white error covariance the classic 4D-Var has very weak filtering effect which is an essential component of an ideal data assimilation scheme. This over-fitting may be due to the redundant (over-determined) formulation of the classic 4D-Var, see (*Hawkins*, 2004) for a general explanation

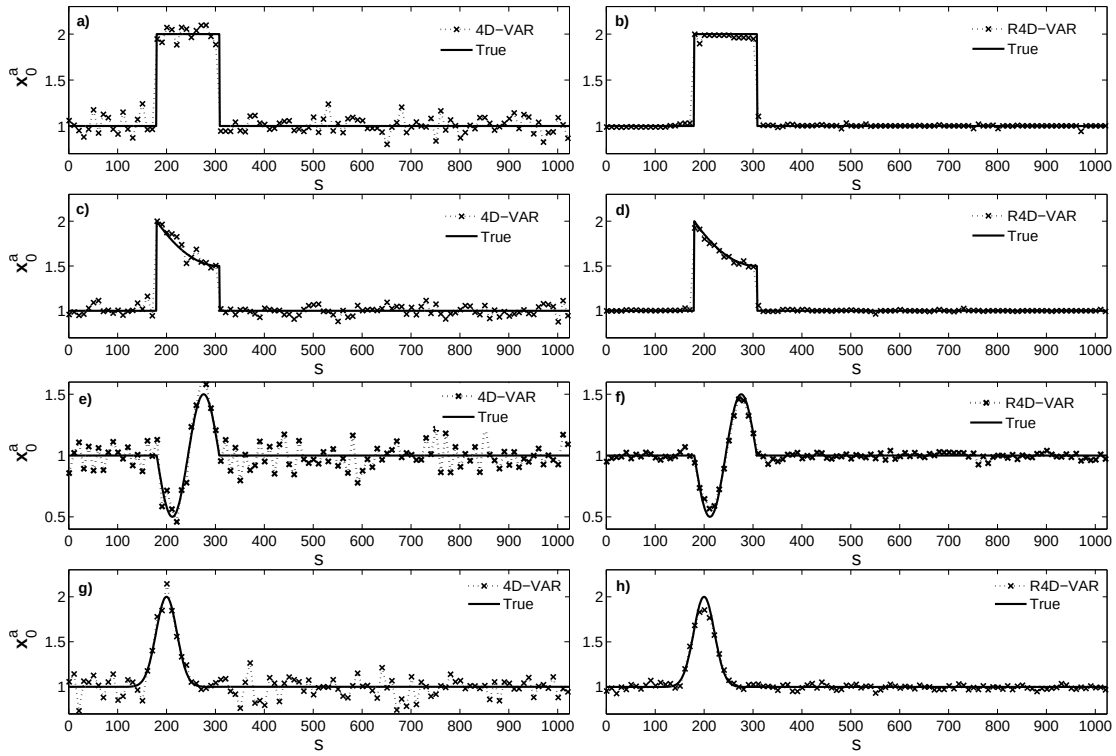

Figure 5.5: The results of the classic 4D-Var (left panel) versus the results of ℓ_1-norm R4D-Var (right panel) for the tested initial conditions in a white Gaussian error environment. The solid lines are the true initial conditions and the crosses represent the recovered initial states or the analysis. In general, the results of the classic 4D-Var suffer from overfitting while the background and observation errors are suppressed and the sharp transitions and peaks are effectively recovered in the regularized analysis.

on overfitting problems in statistical estimators and also see *Daley* (1993, p.41).

The average of the results for 30 independent runs is reported in Table 5.1. Three different lump quality metrics are examined as follows:

$$\begin{aligned} \mathrm{MSE}_r &= \left\|\mathbf{x}_0^t - \mathbf{x}_0^a\right\|_2 / \left\|\mathbf{x}_0^t\right\|_2 \\ \mathrm{MAE}_r &= \left\|\mathbf{x}_0^t - \mathbf{x}_0^a\right\|_1 / \left\|\mathbf{x}_0^t\right\|_1 \\ \mathrm{BIAS}_r &= \left|\bar{\mathbf{x}}_0^t - \bar{\mathbf{x}}_0^a\right| / \left|\bar{\mathbf{x}}_0^t\right| \end{aligned} \tag{5.6}$$

namely, relative mean squared error (MSE_r); relative mean absolute error (MAE_r); and relative Bias (BIAS_r). In (5.6) $\mathbf{x}_0^t$ denotes the true initial condition,$\mathbf{x}_0^a$ is the analysis, and upper bar denote the expected value. It is seen that based on the selected lump quality metrics, the ℓ_1-norm R4D-Var significantly outperforms the classic 4D-Var. In general, the MAE_r metric is improved more than the MSE_r metric in the presented experiments. The best improvement is obtained for the top-hat initial condition (IC1), where the sparsity is very strong compared to the other initial conditions. In other words, the ℓ_1-norm R4D-Var

White Background Error						
	MSE_r		MAE_r		BIAS_r	
	R4D-Var	4D-Var	R4D-Var	4D-Var	R4D-Var	4D-Var
IC1	0.0188	0.0690	0.0099	0.0589	0.0016	0.0004
IC2	0.0152	0.0515	0.0083	0.0414	0.0030	0.0016
IC3	0.0296	0.0959	0.0229	0.0771	0.0038	0.0022
IC4	0.0316	0.0899	0.0235	0.0728	0.0018	$4.26\text{e}-5$

Table 5.1: Expected values of the MSE_r, MAE_r, and BIAS_r, defined in (5.6), for 30 independent runs. The background and observation errors are white ($\mathbf{B} = \sigma_b^2\mathbf{I}$, $\mathbf{R} = \sigma_r^2\mathbf{I}$), where $\sigma_b = 0.10$ (SNR $\cong$ 10.5 dB) and $\sigma_r = 0.08$ (SNR $\cong$ 12 dB). The initial conditions are: IC1 (flat top-hat), IC2 (quadratic top-hat), IC3 (window sinusoid), and IC4 (squared-exponential) and the results are reported for both the classic 4D-Var and the regularized 4D-Var (R4D-Var).

is more effective for stronger sparsity of the initial state. In effect, the MSE_r metric is improved almost three orders of magnitude, while the MAE_r improvement reaches up to six orders of magnitude in the IC1 initial condition. We need to note that although the trigonometric functions can be sparsely represented in the DCT domain, here we used a window sinusoid for the IC3, which suffers from discontinuities over the edges and can not be perfectly sparsified in the DCT domain. However, we see that even in a weaker sparsity, the results of the ℓ_1-norm R4D-Var are still much better than then classic solution.

5.1.3.2 Correlated background error

In this part, the background error $\mathbf{B} = \sigma_b^2\mathbf{C}_b$ is considered to be correlated. As previously discussed, typically longer correlation length creates ill-conditioning in the background error covariance matrix and makes the problem more unstable. On the other hand, the correlated background error covariance imposes smoothness on the analysis (see, *Gaspari and Cohn*, 1999), improves filtering effects, and makes the classic solution to be less prone to overfitting. In this subsection, we examine the effect of correlation length on the solution of data assimilation and compare the results of the sparsity promoting R4D-Var with the classic 4D-Var. Here, we do not apply any preconditioning as the goal is to emphasize on the stabilizing role of the ℓ_1-norm regularization. In addition, for brevity, the results are only reported for the top-hat and window sinusoid initial condition, which are solved in the wavelet and DCT domains, respectively.

a) Results for the AR(1) background error

As is evident, in this case, the background state is defined by adding AR(1) correlated error to the true state (5.6a, d) which is known to us for these experimental studies. Figure 5.6 demonstrates that in the case of correlated error the classic 4D-Var is less prone to overfitting compared to the case of the uncorrelated error in Figure 5.5. Typically in the top-hat

initial condition (IC1) with sharp transitions, the classic solution fails to capture those sharp jumps and becomes spoiled around the jumps (Figure 5.6b). For the trigonometric initial condition (IC3), the classic solution is typically overly smooth and can not capture the peaks (Figure 5.6e). These deficiencies in classic solutions typically become more pronounced for larger correlation lengths and thus more ill-conditioned problems. On the other hand, the ℓ_1-norm R4D-Var markedly outperforms the classic method by improving the recovery of the sharp transitions in IC1 and peaks in IC3 (Figure 5.6).

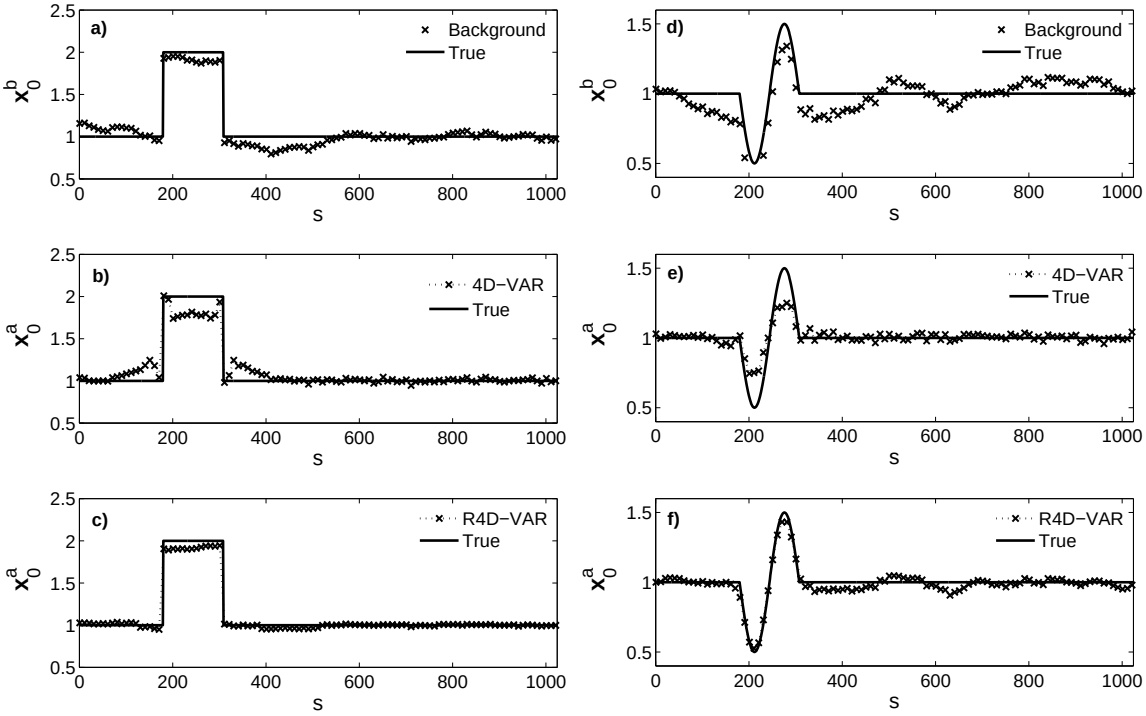

Figure 5.6: Comparison of the results of the classic 4D-Var (b, e) and ℓ_1-norm R4D-Var (c, f) for the top-hat initial (left panel) and window sinusoid (right panel) initial conditions, respectively. The background states in (a) and (d) are defined by adding correlated errors using an AR(1) covariance model of $\rho(\tau) \propto e^{-\alpha|\tau|}$, where $\alpha = 1/250$. The results show that the ℓ_1-norm R4D-Var improves recovery of sharp jumps and peaks and results in a more stable solution compared to the classic 4D-Var; see Figure 5.7 for quantitative results.

We examined a relatively wide range of applicable correlation lengths by choosing a set of different values of $\alpha^{-1} \in \{1,\ 10,\ 25,\ 50,\ 250,\ 1000\}$, which correspond to decadal variations ranging from 10^1 to 10^6 in the condition number $\kappa(\mathbf{B})$ of the background error covariance matrices (see Figure 5.3a). The assimilation results using different correlation lengths are demonstrated in Figure 5.7. To have a robust conclusion about comparison of the proposed R4D-Var with the classic 4D-Var, the plots in this figure demonstrate the expected values of the quality metrics for 30 independent runs.

It can be seen that for small error correlation lengths ($\alpha^{-1} \lesssim 25$), the improvement of the R4D-Var is very significant while in the medium range ($25 \lesssim \alpha^{-1} \lesssim 50$) the classic solution becomes more competitive and closer to the regularized analysis. As previously mentioned, this improvement in the classic solutions is mainly due to the smoothing effect of the background covariance matrix. However, for larger correlation lengths ($\alpha^{-1} \gtrsim 50$), the differences of the two methods are more drastic as the classic solutions become more unstable and fail to capture the underlying structure of the initial state of interest. In general, we see that the MSE_r and MAE_r metrics are improved for all examined background error correlation lengths. As expected, the regularized solutions are slightly biased compared to classic solutions; however, the magnitude of the bias is not significant compared to the mean value of the initial state (see Figure 5.7). Figure 5.7 also shows a very important outcome of regularization which implies that the R4D-Var is almost insensitive to the studied range of correlation length and thus condition number of the problem. This confirms the stabilizing role of regularization and needs to be further studied for large scale and operational data assimilation problems. Another important observation is that, for extremely correlated background error, the classic R4D-Var may produce analysis with larger bias than the proposed R4D-Var (Figure 5.7c). This unexpected result might be due to the presence of spurious bias in the background state coming from a strongly correlated error. In other words, a strongly correlated error may shift the mean value of the background state significantly and create a large bias in the solution of the classic 4D-Var. In this case, the improved performance of the R4D-Var may be due to its stronger stability and filtering properties.

b) Results for the AR(2) background error

The AR(2) model is suitable for errors with higher order Markovian structure compared to the AR(1) model. As is seen in Figure (5.4), the condition number of the AR(2) covariance matrix is much larger than the AR(1) for the same values of the correlation parameter α in the studied covariance models. Here, we limited our experiments to fewer characteristic correlation lengths of $\alpha^{-1} = \{1, 5, 25, 50\}$. We limited our considerations to $\alpha^{-1} \lesssim 50$, because for larger values (slower correlation decay rates) the condition number of $\mathbf{B}$ exceeds 10^8 and almost both methods failed to obtain the analysis without any preconditioning effort.

In our case study, for $\alpha^{-1} \lesssim 25$, where $\kappa(\mathbf{B}) \lesssim 10^6$, the proposed R4D-Var outperforms the 4D-Var similar to what have been explained for the AR(1) error in the previous sub-section. However, we found that for $25 \lesssim \alpha^{-1} \lesssim 50$, where $10^6 \lesssim \kappa(\mathbf{B}) \lesssim 10^8$, without proper preconditioning, the used conjugate gradient algorithm fails to obtain the analysis state in the 4D-Var (Table 5.2). On the other hand, due to the role of the proposed regularization, the R4D-Var remained sufficiently stable; however, its effectiveness deteriorated compared

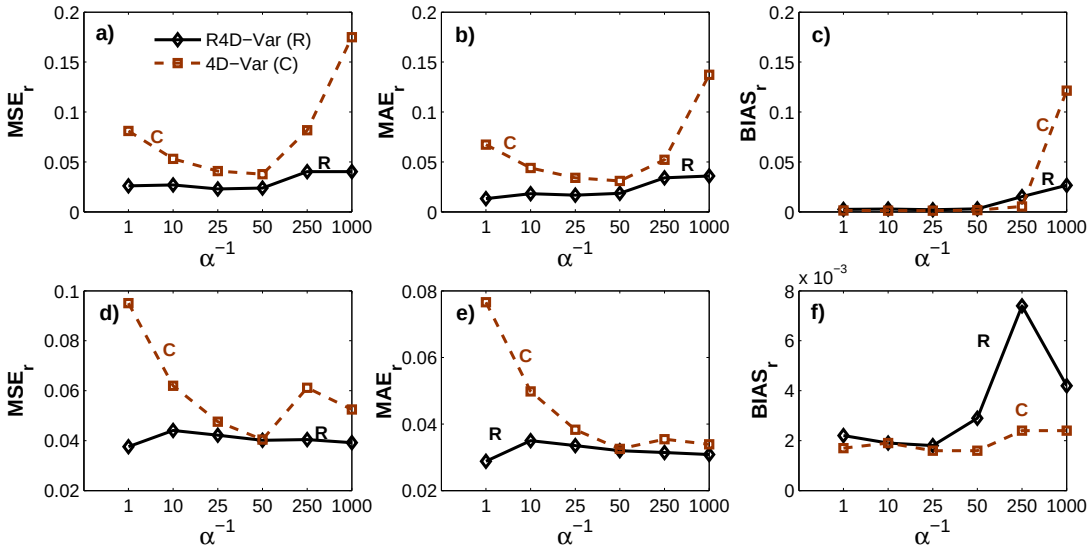

Figure 5.7: Comparison of the results of the proposed ℓ_1-norm R4D-Var (solid lines) and the classic 4D-Var (broken lines) under the AR(1) background error for different correlation characteristic length scales (α^{-1}). (a-c) The chosen quality metrics for the top-hat initial condition (IC1), and (d-f) the metrics for the window sinusoid initial condition (IC3). These results, averaged over 30 independent runs, demonstrate significant improvements in recover of the analysis state by the proposed ℓ_1-norm R4D-Var compared to the classic 4D-Var.

to the cases where the condition numbers were lower. This observation verifies the known role of the proposed regularization for improving the condition number of the variational data assimilation problem.

AR(2) – Background Error							
	α^{-1}	MSE_r		MAE_r		BIAS_r	
		R4D-Var	4D-Var	R4D-Var	4D-Var	R4D-Var	4D-Var
IC1	1	0.0254	0.0754	0.0162	0.0629	0.0023	0.0016
	5	0.0328	0.0643	0.0212	0.0534	0.0043	0.0018
	25	0.0722	NaN	0.0608	NaN	0.0187	NaN
	50	0.0742	NaN	0.0582	NaN	0.0268	NaN
IC3	1	0.0363	0.0887	0.0272	0.0715	0.0029	0.0012
	5	0.0708	0.0906	0.0571	0.0529	0.0106	0.0017
	25	0.0877	NaN	0.0710	NaN	0.0243	NaN
	50	0.0898	NaN	0.0747	NaN	0.0361	NaN

Table 5.2: Expected values of the MSE_r, MAE_r, and BIAS_r, defined in (5.6), for 30 independent runs. The background and observation errors are modeled by the first order auto-regressive ($\mathbf{B} = \sigma_b^2 \mathbf{C}_B$) and white ($\mathbf{R} = \sigma_r^2 \mathbf{I}$) Gaussian processes, where $\sigma_b = 0.10$ (SNR $\cong$ 10.5 dB) and $\sigma_r = 0.08$ (SNR $\cong$ 12 dB). The parameter α denotes the correlation decay rate in the AR(2) covariance function $\rho(\tau) \propto e^{-\alpha|\tau|}(1 + \alpha|\tau|)$. The studied initial conditions are: IC1 (flat top-hat), and IC3 (window sinusoid) and the results are reported for both the classic 4D-Var and the regularized 4D-Var (R4D-Var).

5.1.3.3 Selection of the regularization parameters

As previously explained, the regularization parameter λ plays a very important role in making the analysis sufficiently faithful to the observations and to the background state while preserving the underlying regularity of the analysis. To the best of our knowledge, no general purpose algorithm exists which will produce an exact and closed form solution for the selection of the regularization parameter, especially for the proposed ℓ_1-norm regularization (see, *Hansen*, 2010, chap.5). Here, we chose the regularization parameter λ by trial and error based on a minimum mean squared error criterion (Figure 5.8). As a rule of thumb, we found that in general $\lambda \lesssim 0.05 \|\mathbf{b}\|_\infty$ yields reasonable results. We also realized that under similar error signal-to-noise ratio, the selection of λ depends on some important factors such as, the pre-selected basis, and especially the degree of ill-conditioning of the problem.

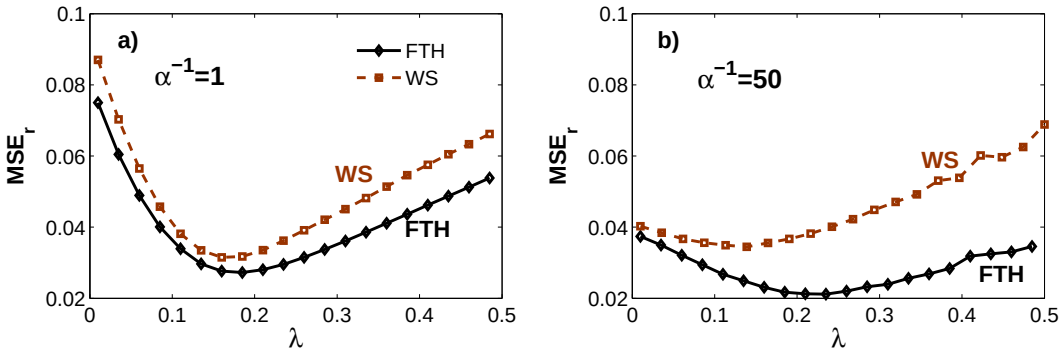

Figure 5.8: The relative mean squared error versus the regularization parameter obtained for the AR(1) background error for different characteristic correlation length (a) $\alpha^{-1} = 1$, and (b) $\alpha^{-1} = 50$. IC1 and IC2 refer to the top-hat and window sinusoid initial conditions, respectively. See Table (5.1) and (5.2) for more information and definitions.

Chapter 6

Conclusions

We have discussed the concept of sparse regularization in variational data assimilation and examined a simple but important application of the proposed problem formulation to the advection-diffusion equation, relevant to land surface heat and mass flux studies. In particular, we extended the classic formulations by leveraging sparsity for solving data assimilation problems in wavelet and spectral domains. The basic claim is that if the underlying state of interest exhibits sparsity in a pre-selected basis, this prior information can serve to further constrain and improve the quality of the analysis cycle and thus the forecast skill. We demonstrated that the regularized variational data assimilation (RVDA) not only shows better interpolation properties but also exhibits improved filtering attributes by effectively removing small scale noisy features that possibly do not satisfy the underlying governing physical laws. Furthermore, it is argued that the ℓ_1-norm RVDA is more robust to the possible ill-conditioning of the data assimilation problem and leads to more stable analysis compared to the classic methods.

We explained that, from the statistical point of view, this prior knowledge speaks for the spatial intrinsic non-Gaussian structure of the state variable of interest which can be well parameterized and modeled in a properly chosen basis. We discussed that selection of the sparsifying basis can be seen as a statistical model selection problem which can be guided by studying the distribution of the representation coefficients.

Further research needs to be devoted to developing methodologies to: (a) characterize the analysis covariance, especially using ensemble based approaches; (b) automatize the selection of the regularization parameter and study its impact on various applications of data assimilation problems; (c) apply the methodology in an incremental setting to tackle non-linear observation operators (*Courtier et al.*, 1994); and (d) study the role of preconditioning on the background error covariance for very ill-conditioned data assimilation problems in regularized variational data assimilation settings.

Furthermore, a promising area of future research is that of developing and testing ℓ_1-norm

RVDA to tackle non-linear measurement and model equations in a hybrid variational-ensemble data setting. Basically, a crude framework can be cast as follows: (1) given the analysis and its covariance at previous time step, properly generate an ensemble of analysis state; (2) use the analysis ensembles to generate forecasts or background ensembles via the model equation and then compute the background ensemble mean and covariance; (3) given the background ensembles, obtain observation ensembles via the observation equation and then obtain the ensemble observation covariance; (4) solve an ℓ_1-norm RVDA problem for each ensemble to obtain ensemble analysis states at present time; (5) compute the ensemble analysis mean and covariance and use them to forecast the next time step; and (6) repeat the recursion.

Bibliography

Afshar, A., and M. A. Marino (1978), Model for simulating soil-water content considering evapotranspiration, *Journal of Hydrology*, *37*(3–4), 309 – 322, doi:10.1016/0022-1694(78)90022-7.

Ambadan, J. T., and Y. Tang (2009), Sigma-point Kalman filter data assimilation methods for strongly nonlinear systems, *J. Atmos. Sci.*, *66*(2), 261–285.

Anderson, J. L. (2001), An Ensemble Adjustment Kalman Filter for Data Assimilation, *Mon. Wea. Rev.*, *129*(12), 2884–2903, doi:10.1175/1520-0493(2001)129<2884:AEAKFF>2.0.CO;2.

Arulampalam, M. S., S. Maskell, N. Gordon, and T. Clapp (2002), A tutorial on particle filters for online nonlinear/non-Gaussian Bayesian tracking, *IEEE Trans. Signal. Proces.*, *50*(2), 174–188.

Bai, Z., J. Demmel, J. Dongarra, A. Ruhe, and H. Van Der Vorst (1987), *Templates for the solution of algebraic eigenvalue problems: a practical guide*, vol. 11, SIAM, Philadelphia.

Barnard, J., R. McCulloch, and X. Meng (2000), Modeling covariance matrices in terms of standard deviations and correlations, with application to shrinkage, *Stat. Sinica*, *10*(4), 1281–1312.

Bateni, S. M., and D. Entekhabi (2012), Surface heat flux estimation with the ensemble Kalman smoother: Joint estimation of state and parameters, *Water Resour. Res.*, *48*(8), doi:10.1029/2011WR011542.

Bennett, A. F., and P. C. McIntosh (1982), Open Ocean Modeling as an Inverse Problem: Tidal Theory, *J. Phys. Oceanogr.*, *12*(10), 1004–1018, doi:10.1175/1520-0485(1982)012<1004:OOMAAI>2.0.CO;2.

Bergthórsson, P., and B. R. Döös (1955), Numerical Weather Map Analysis1, *Tellus*, *7*(3), 329–340.

Bertsekas, D. (1976), On the Goldstein-Levitin-Polyak gradient projection method, *IEEE Trans. Automat. Contr.*, *21*(2), 174 – 184, doi:10.1109/TAC.1976.1101194.

Bertsekas, D. P. (1999), *Nonlinear Programming*, 2nd ed., 794 pp., Athena Scientific, Belmont, MA.

Boyd, S., and L. Vandenberghe (2004), *Convex optimization*, 716 pp., Cambridge University Press, New York.

Burgers, G., P. Jan van Leeuwen, and G. Evensen (1998), Analysis scheme in the ensemble Kalman filter, *Monthly weather review*, *126*(6), 1719–1724.

Candes, E., and T. Tao (2006), Near-Optimal Signal Recovery From Random Projections: Universal Encoding Strategies?, *IEEE Trans. Inform. Theory.*, *52*(12), 5406–5425, doi: 10.1109/TIT.2006.885507.

Chan, R. H.-F., and X.-Q. Jin (2007), *An Introduction to Iterative Toeplitz Solvers*, SIAM, Philadelphia.

Chapra, S. C. (2008), *Surface Water Quality Modeling*, Waveland Press, Inc. IL, USA.

Chen, S., D. Donoho, and M. Saunders (2001), Atomic Decomposition by Basis Pursuit, *SIAM rev.*, *43*(1), 129–159.

Chen, S. S., D. L. Donoho, and M. A. Saunders (1998), Atomic decomposition by basis pursuit, *SIAM J. Sci. Comput.*, *20*, 33–61.

Courtier, P., J.-N. Thépaut, and A. Hollingsworth (1994), A strategy for operational implementation of 4D-VAR, using an incremental approach, *Quart. J. Roy. Meteor. Soc.*, *120*(519), 1367–1387, doi:10.1002/qj.49712051912.

Cressman, G. (1959), An operational objective analysis system, *Monthly Weather Review*, *87*(10), 367–374.

Daley, R. (1993), *Atmospheric data analysis*, 472 pp., Cambridge University Press.

Doucet, A., S. Godsill, and C. Andrieu (2000), On sequential Monte Carlo sampling methods for Bayesian filtering, *Statistics and Computing*, *10*(3), 197–208, doi:10.1023/A: 1008935410038.

Doucet, A., N. De Freitas, and N. Gordon (2001), *Sequential Monte Carlo Methods in Practice*, Springer-Verlag, New York.

Durrett, R. (1999), *Essentials of Stochastic Processes*, Springer-Verlag, N.Y.

Ebtehaj, A. M., and E. Foufoula-Georgiou (2013), On Variational Downscaling, Fusion and Assimilation of Hydro-meteorological States: A Unified Framework via Regularization, *Water Resour. Res*, doi:10.1002/wrcr.20424, in press.

Elad, M. (2010), *Sparse and Redundant Representations: From Theory to Applications in Signal and Image Processing*, 376 pp., Springer Verlag.

Evensen, G. (1994a), Sequential data assimilation with a nonlinear quasi-geostrophic model using Monte Carlo methods to forecast error statistics, *J. Geophys. Res.*, *99*(C5), 10,143–10,162.

Evensen, G. (1994b), Inverse methods and data assimilation in nonlinear ocean models, *Physica D: Nonlinear Phenomena*, *77*(1–3), 108 – 129, doi:10.1016/0167-2789(94)90130-9, <ce:title>Special Issue Originating from the 13th Annual International Conference of the Center for Nonlinear Studies Los Alamos, NM, USA, 17–21 May 1993 </ce:title>.

Evensen, G. (2003), The ensemble Kalman filter: Theoretical formulation and practical implementation, *Ocean dynamics*, *53*(4), 343–367.

Fetter, C. (1994), *Applied Hydrogeology*, Prentice Hall, New Jersey, USA, Fourth Edition.

Figueiredo, M., R. Nowak, and S. Wright (2007), Gradient Projection for Sparse Reconstruction: Application to Compressed Sensing and Other Inverse Problems, *IEEE J. Sel. Topics Signal Process.*, *1*(4), 586–597, doi:10.1109/JSTSP.2007.910281.

Freitag, M. A., N. K. Nichols, and C. J. Budd (2012), Resolution of sharp fronts in the presence of model error in variational data assimilation, *Quart. J. Roy. Meteor. Soc.*, doi:10.1002/qj.2002.

Gandin, S. (1966), Objective analysis of meteorological fields. Translated from the Russian. Jerusalem (Israel Program for Scientific Translations), 1965., *Quart. J. Roy. Meteor. Soc.*, *92*(393), 447–447, doi:10.1002/qj.49709239320.

Gaspari, G., and S. E. Cohn (1999), Construction of correlation functions in two and three dimensions, *Quart. J. Roy. Meteor. Soc.*, *125*(554), 723–757, doi:10.1002/qj.49712555417.

Ghil, M. (1997), Advances in sequential estimation for atmospheric and oceanic flows, *J. Meteor. Soc. Japan*, *75*, 289–304.

Ghil, M., S. Cohn, J. Tavantzis, K. Bube, and E. Isaacson (1981), Applications of Estimation Theory to Numerical Weather Prediction, in *Dynamic Meteorology: Data Assimilation Methods*, *Applied Mathematical Sciences*, vol. 36, edited by L. Bengtsson, M. Ghil, and E. Källén, pp. 139–224, Springer New York, doi:10.1007/978-1-4612-5970-1_5.

Gilchrist, B., and G. Cressman (1954), An Experiment in Objective Analysis, *Tellus*, *6*(4), 309–318, doi:10.1111/j.2153-3490.1954.tb01126.x.

Golub, G., P. Hansen, and D. O'Leary (1999), Tikhonov regularization and total least squares, *SIAM J. Matrix Anal. Appl.*, *21*(1), 185–194.

Gordon, N., D. Salmond, and A. F. M. Smith (1993), Novel approach to nonlinear/non-Gaussian Bayesian state estimation, *IEE PROC-F*, *140*(2), 107–113.

Hamill, T. M. (2006), *Ensemble-based atmospheric data assimilation*, chap. 6, pp. 124–156, Cambridge University Press.

Hamill, T. M., and J. S. Whitaker (2005), Accounting for the error due to unresolved scales in ensemble data assimilation: A comparison of different approaches, *Mon. Weather Rev.*, *133*(11), 3132–3147.

Hamill, T. M., J. S. Whitaker, and C. Snyder (2001), Distance-dependent filtering of background error covariance estimates in an ensemble Kalman filter, *Monthly Weather Review*, *129*(11), 2776–2790.

Han, E., V. Merwade, and G. C. Heathman (2012), Application of data assimilation with the Root Zone Water Quality Model for soil moisture profile estimation in the upper Cedar Creek, Indiana, *Hydrol. Process.*, *26*(11), 1707–1719, doi:10.1002/hyp.8292.

Hansen, P. (1998), *Rank-deficient and discrete ill-posed problems: numerical aspects of linear inversion*, vol. 4, Society for Industrial Mathematics (SIAM), Philadelphia.

Hansen, P. (2010), *Discrete inverse problems: insight and algorithms*, vol. 7, Society for Industrial & Applied Mathematics (SIAM), Philadelphia, PA, USA.

Hansen, P., and D. O'Leary (1993), The use of the L-curve in the regularization of discrete ill-posed problems, *SIAM J Sci Comput*, *14*(6), 1487–1503.

Hawkins, D. M. (2004), The problem of overfitting, *J. Chem. Inf. Comput. Sci.*, *44*(1), 1–12.

Houtekamer, P., L. Lefaivre, J. Derome, H. Ritchie, and H. Mitchell (1996), A system simulation approach to ensemble prediction, *Mon. Weather Rev.*, *124*(6), 1225–1242.

Houtekamer, P. L., and H. L. Mitchell (1998), Data assimilation using an ensemble Kalman filter technique, *Mon. Weather Rev.*, *126*(3), 796–811.

Houtekamer, P. L., and H. L. Mitchell (2001), A sequential ensemble Kalman filter for atmospheric data assimilation, *Monthly Weather Review*, *129*(1), 123–137.

Houtekamer, P. L., H. L. Mitchell, G. Pellerin, M. Buehner, M. Charron, L. Spacek, and B. Hansen (2005), Atmospheric data assimilation with an ensemble Kalman filter: Results with real observations, *Mon. Weather Rev.*, *133*(3), 604–620.

Hu, Z., and S. Islam (1995), Prediction of Ground Surface Temperature and Soil Moisture Content by the Force-Restore Method, *Water Resources Research*, *31*(10), 2531–2539, doi:10.1029/95WR01650.

Hunt, B., E. Kostelich, and I. Szunyogh (2007), Efficient data assimilation for spatiotemporal chaos: A local ensemble transform Kalman filter, *Physica D: Nonlinear Phenomena*, *230*(1), 112–126.

Ide, K., P. Courtier, M. Gill, and A. Lorenc (1997), Unified notation for data assimilation: Operational, sequential, and variational, *J. Meteo. Soc. Japan*, *75*, 181–189.

Jochum, M., and R. Murtugudde (2006), Temperature advection by tropical instability waves, *J. Phys. Oceanogr.*, *36*(4), 592–605.

Johnson, C., B. J. Hoskins, and N. K. Nichols (2005a), A singular vector perspective of 4D-Var: Filtering and interpolation, *Quart. J. Roy. Meteor. Soc.*, *131*(605), 1–19, doi: 10.1256/qj.03.231.

Johnson, C., N. K. Nichols, and B. J. Hoskins (2005b), Very large inverse problems in atmosphere and ocean modelling, *Int. J. Numer. Meth. Fl.*, *47*(8-9), 759–771, doi:10. 1002/fld.869.

Julier, S., and J. Uhlmann (2002), Reduced sigma point filters for the propagation of means and covariances through nonlinear transformations, in *American Control Conference, 2002. Proceedings of the 2002*, vol. 2, pp. 887–892 vol.2, doi:10.1109/ACC.2002.1023128.

Julier, S., and J. Uhlmann (2004), Unscented filtering and nonlinear estimation, *Proceedings of the IEEE*, *92*(3), 401–422, doi:10.1109/JPROC.2003.823141.

Julier, S. J., and J. K. Uhlmann (1997), New extension of the Kalman filter to nonlinear systems, in *AeroSense, Simul. and Control 3*.

Kalman, R. E. (1960), A new approach to linear filtering and prediction problems, *J Basic eng-T ASME*, *82*(1), 35–45.

Kalman, R. E., and R. S. Bucy (1961), New results in linear filtering and prediction theory, *J. Basic eng-T ASME*, *83*(3), 95–108.

Kalnay, E. (2003), *Atmospheric modeling, data assimilation, and predictability*, 341 pp., Cambridge University Press, New York.

Kepert, J. D. (2009), Covariance localisation and balance in an ensemble Kalman filter, *Quart. J. Roy. Meteor. Soc.*, *135*(642), 1157–1176.

Kim, S.-J., K. Koh, M. Lustig, S. Boyd, and D. Gorinevsky (2007), An Interior-Point Method for Large-Scale l1-Regularized Least Squares, *IEEE J. Sel. Topics Signal Process.*, *1*(4), 606–617, doi:10.1109/JSTSP.2007.910971.

Kumar, P., and A. L. Kaleita (2003), Assimilation of near-surface temperature using extended Kalman filter, *Adv. Water Resour.*, *26*(1), 79 – 93, doi:10.1016/S0309-1708(02)00098-2.

Lanser, D., and J. Verwer (1999), Analysis of operator splitting for advection–diffusion–reaction problems from air pollution modelling, *Journal of Computational and Applied Mathematics*, *111*(1–2), 201 – 216, doi:10.1016/S0377-0427(99)00143-0.

Levy, B. C. (2008), *Principles of Signal Detection and Parameter Estimation*, 1 ed., 639 pp., Springer Publishing Company, New York, USA, doi:10.1007/978-0-387-76544-0.

Liang, X., E. F. Wood, and D. P. Lettenmaier (1999), Modeling ground heat flux in land surface parameterization schemes, *J. Geophys. Res.*, *104*(D8), 9581–9600.

Lin, Y.-L., R. L. Deal, and M. S. Kulie (1998), Mechanisms of cell regeneration, development, and propagation within a two-dimensional multicell storm, *J. Atmos. Sci.*, *55*(10), 1867–1886.

Lorenc, A. (1981), A global three-dimensional multivariate statistical interpolation scheme, *Mon. Weather Rev.*, *109*, 701–721.

Lorenc, A. C. (1986), Analysis methods for numerical weather prediction, *Quart. J. Roy. Meteor. Soc.*, *112*(474), 1177–1194, doi:10.1002/qj.49711247414.

Lorenz, E. N. (1963a), Deterministic Nonperiodic Flow, *J. Atmos. Sci.*, *20*(2), 130–141, doi:10.1175/1520-0469(1963)020<0130:DNF>2.0.CO;2.

Lorenz, E. N. (1963b), The Predictability of hydrodynamic flows, *Trans. NY Acad. Sci. Series II*, *25*(4 Series II), 409–432, doi:10.1111/j.2164-0947.1963.tb01464.x.

Lorenz, E. N. (1965), A study of the predictability of a 28-variable atmospheric model, *Tellus*, *17*(3), 321–333.

Mallat, S. (1989), A theory for multiresolution signal decomposition: the wavelet representation, *IEEE Trans. Pattern Anal. Mach. Intell.*, *11*(7), 674–693, doi:10.1109/34.192463.

Mallat, S. (2009), *A wavelet tour of signal processing: the sparse way*, 3rd ed., 805 pp., Elsevier /Academic Press.

Miller, R., M. Ghil, and F. Gauthiez (1994), Advanced data assimilation in strongly nonlinear dynamical systems, *J. Atmos. Sci.*, *51*(8), 1037–1037.

Moradkhani, H., K.-L. Hsu, H. Gupta, and S. Sorooshian (2005a), Uncertainty assessment of hydrologic model states and parameters: Sequential data assimilation using the particle filter, *Water Resour. Res.*, *41*(5), W05,012–.

Moradkhani, H., S. Sorooshian, H. Gupta, and P. Houser (2005b), Dual state–parameter estimation of hydrological models using ensemble Kalman filter, *Adv. Water Resour.*, *28*(2), 135–147.

Nadarajah, S. (2005), A generalized normal distribution, *J. Appl. Stat.*, *32*(7), 685–694.

Neumaier, A. (1998), Solving Ill-Conditioned and Singular Linear Systems: A Tutorial on Regularization, *SIAM Rev.*, *40*(3), 636–666, doi:10.1137/S0036144597321909.

Ott, E., B. Hunt, I. Szunyogh, A. Zimin, E. Kostelich, M. Corazza, E. Kalnay, D. Patil, and J. Yorke (2004), A local ensemble Kalman filter for atmospheric data assimilation, *Tellus A*, *56*(5), 415–428, doi:10.1111/j.1600-0870.2004.00076.x.

Panofsky, H. (1949), Objective Weather-map analysis, *J. Appl. Meteor.*, *6*, 386–392.

Peters-Lidard, C. D., M. S. Zion, and E. F. Wood (1997), A soil-vegetation-atmosphere transfer scheme for modeling spatially variable water and energy balance processes, *J. Geophys. Res.*, *102*(D4), 4303–4324, doi:10.1029/96JD02948.

Pitt, M. K., and N. Shephard (1999), Filtering via Simulation: Auxiliary Particle Filters, *J. Am. Stat. Assoc.*, *94*(446), 590–599, doi:10.1080/01621459.1999.10474153.

Platzman, G. W. (1967), A retrospective view of Richardson's book on weather prediction, *Bull. Amer. Meteor. Soc.*, *48*, 514–550.

Rabier, F., H. Järvinen, E. Klinker, J.-F. Mahfouf, and A. Simmons (2000), The ECMWF operational implementation of four-dimensional variational assimilation. I: Experimental results with simplified physics, *Quart. J. Roy. Meteor. Soc.*, *126*(564), 1143–1170.

Rao, K., and P. Yip (1990), *Discrete Cosine Transform: Algorithms, Advantages, Applications*, Boston: Academic Press.

Rasmussen, C., and C. Williams (2006), *Gaussian processes for machine learning*, vol. 1, MIT press Cambridge, MA.

Ristic, B., S. Arulampalm, and N. Gordon (2004), *Beyond the Kalman filter: Particle filters for tracking applications*, Artech House Publishers.

Sasaki, Y. (1970a), Some basic formalisms in numerical variational analysis, *Mon. Weather Rev.*, *98*(12), 875–883.

Sasaki, Y. (1970b), Numerical variational analysis formulated under the constraints as determined by the longwave equations and a low-pass filter, *Mon. Wea. Rev.*, *98*(12), 884–898, doi:10.1175/1520-0493(1970)098<0884:NVAFUT>2.3.CO;2.

Serafini, T., G. Zanghirati, and L. Zanni (2005), Gradient projection methods for quadratic programs and applications in training support vector machines, *Optim. Methods Softw.*, *20*(2-3), 353–378, doi:10.1080/10556780512331318182.

Simon, D. (2006), *Optimal state estimation: Kalman, H [infinity] and nonlinear approaches*, John Wiley and Sons.

Smith, K. S., and J. Marshall (2009), Evidence for Enhanced Eddy Mixing at Middepth in the Southern Ocean, *J. Phys. Oceanogr.*, *39*(1), 50–69, doi:10.1175/2008JPO3880.1.

Stein, M. L. (1999), *Interpolation of Spatial Data*, Springer-Verlag, New York.

Szunyogh, I., E. Kostelich, G. Gyarmati, E. Kalnay, B. Hunt, E. Ott, E. Satterfield, and J. Yorke (2008), A local ensemble transform Kalman filter data assimilation system for the NCEP global model, *Tellus A*, *60*(1), 113–130.

Thépaut, J.-N., R. N. Hoffman, and P. Courtier (1993), Interactions of Dynamics and Observations in a Four-Dimensional Variational Assimilation, *Mon. Wea. Rev.*, *121*(12), 3393–3414, doi:10.1175/1520-0493(1993)121<3393:IODAOI>2.0.CO;2.

Tibshirani, R. (1996), Regression Shrinkage and Selection via the Lasso, *J. R. Stat. Soc. Ser. B Stat. Methodol.*, *58*(1), 267–288.

Tikhonov, A., V. Arsenin, and F. John (1977), *Solutions of ill-posed problems*, Winston & Sons. Washington, DC.

Uhlmann, J. (1995), Dynamic Map Building and Localization: New Theoretical Foundations, Ph.D. thesis, University of Oxford.

van Leeuwen, P. J. (2009), Particle Filtering in Geophysical Systems, *Mon. Wea. Rev.*, *137*(12), 4089–4114, doi:10.1175/2009MWR2835.1.

van Leeuwen, P. J. (2010), Nonlinear data assimilation in geosciences: an extremely efficient particle filter, *Q.J.R. Meteorol. Soc.*, *136*(653), 1991–1999.

Wan, E., and R. Van der Merwe (2000), The unscented Kalman filter for nonlinear estimation, in *Adaptive Systems for Signal Processing, Communications, and Control Symposium 2000. AS-SPCC. The IEEE 2000*, pp. 153–158, doi:10.1109/ASSPCC.2000.882463.

Zhou, Y., D. McLaughlin, and D. Entekhabi (2006), Assessing the performance of the ensemble Kalman filter for land surface data assimilation, *Mon. Weather Rev.*, *134*(8), 2128–2142.

Appendix A

Probabilistic View to the Variational Data Assimilation

This subsection reinterprets the above variational data assimilation methodologies from the two perspectives of the statistical inferences: the frequentist and Bayesian. The importance of this subsection becomes more apparent while we move into the discussion of the regularization and its applications to the problem of variational data assimilation.

A.1 The Frequentist View

As previously explained, the frequentist view draws inference from data either from empirical observations or physical modeling considerations. In this view to the VDA, the unknown state of interest $\mathbf{x}_0 \in \mathbb{R}^m$ is considered to be deterministic and *non-random*. However, the available information, including the observations and the background state, is assumed to be random. In other words, the observation model is assumed to be equation (2.1) and the background $\mathbf{x}_0^b$ is considered a random realization of the unknown (deterministic) state $\mathbf{x}_0$ as

$$\mathbf{x}_0^b = \mathbf{x}_0 + \mathbf{w}, \tag{A.1}$$

where the error $\mathbf{w}$ is assumed to be a zero mean Gaussian density $\mathbf{w} \sim \mathcal{N}(0, \mathbf{B})$, uncorrelated with the observation error $\bar{\mathbf{v}} \sim \mathcal{N}(0, \underline{\mathbf{R}})$. Notice that, in this interpretation, the unknown true state is considered as the center of the forecast and the background is just a random realization of it. By augmenting observation and background model in (2.1) and (A.1), respectively; we obtain

$$\begin{bmatrix} \underline{\mathbf{y}} \\ \mathbf{x}_0^b \end{bmatrix} = \begin{bmatrix} \underline{\mathbf{H}} \\ \mathbf{I} \end{bmatrix} \mathbf{x}_0 + \begin{bmatrix} \bar{\mathbf{v}} \\ \mathbf{w} \end{bmatrix}. \tag{A.2}$$

Thus, from a frequentist point of view, the augmented *likelihood function* or the probability to be maximized in order to obtain the most likely state (an estimate), $\hat{\mathbf{x}}^{\mathrm{ML}} \in \mathbb{R}^m$, is that for both the observation $\bar{\mathbf{y}}$ and the background state $\mathbf{x}_0^b$, given the true initial state $\mathbf{x}_0$:

$$\hat{\mathbf{x}}_0^{\mathrm{ML}} = \underset{\mathbf{x}_0}{\operatorname{argmax}} \left\{ p\left(\underline{\mathbf{y}},\, \mathbf{x}_0^b | \mathbf{x}_0\right) \right\}. \tag{A.3}$$

The argument of the above problem which maximizes the likelihood function is called the maximum likelihood (ML) estimator.

Considering the observations and background errors are independent, and also take into account monotonicity of the logarithm function, the ML estimator is reformulated as

$$\begin{aligned} \hat{\mathbf{x}}_0^{\mathrm{ML}} &= \underset{\mathbf{x}_0}{\operatorname{argmin}} \left\{ -\log\, p\left(\underline{\mathbf{y}},\, \mathbf{x}_0^b | \mathbf{x}_0\right) \right\}, \\ &= \underset{\mathbf{x}_0}{\operatorname{argmin}} \left\{ -\log\, p\left(\underline{\mathbf{y}} | \mathbf{x}_0\right) - \log\, p\left(\mathbf{x}_0^b | \mathbf{x}_0\right) \right\}, \end{aligned}$$

where the observation log-likelihood function is:

$$-\log\, p(\bar{\mathbf{y}}|\mathbf{x}_0) \propto \frac{1}{2}(\underline{\mathbf{y}} - \underline{\mathbf{H}}\mathbf{x}_0)^{\mathrm{T}} \underline{\mathbf{R}}^{-1} (\underline{\mathbf{y}} - \underline{\mathbf{H}}\mathbf{x}_0), \tag{A.4}$$

and we have,

$$-\log\, p(\mathbf{x}_0^b|\mathbf{x}_0) \propto \frac{1}{2}(\mathbf{x}_0^b - \mathbf{x}_0)^{\mathrm{T}} \mathbf{B}^{-1} (\mathbf{x}_0^b - \mathbf{x}_0).$$

Consequently, the ML estimator reduces to the minimization of the classic VDA cost function given in (1.4).

Having the ML interpretation, allows us to exploit the theoretical developments about the asymptotic distribution of the analysis. Given that the background and available observations are unbiased, it can be concluded that the analysis covariance meets the Cramér-Rao lower bound as

$$\mathbb{E}\left[\left(\mathbf{x}_0^a - \mathbf{x}_0\right) \left(\mathbf{x}_0^a - \mathbf{x}_0\right)^{\mathrm{T}} \right] = \mathbf{J}^{-1}\left(\mathbf{x}_0\right), \tag{A.5}$$

where $\mathbf{x}_0$ is the unknown true state, and $\mathbf{J}\left(\mathbf{x}_0\right)$ is the Fisher information matrix (see, *Levy*, 2008, pp.138). Recalling that the Fisher information is the expected value of the negative of the Hessian of the log-likelihood function

$$\mathbf{J}\left(\mathbf{x}_0\right) = -\mathbb{E}\left[\nabla_{\mathbf{x}_0}^2 \log\, p\left(\underline{\mathbf{y}},\, \mathbf{x}_0^b | \mathbf{x}_0\right) \right],$$

we get

$$\mathbf{J}\left(\mathbf{x}_0\right) = \underline{\mathbf{H}}^{\mathrm{T}} \underline{\mathbf{R}}^{-1} \underline{\mathbf{H}} + \mathbf{B}^{-1}, \tag{A.6}$$

which its inverse is the covariance of the analysis. Therefore, we can say that the analysis in the VDA is also an *efficient estimator*, meaning that it attains the lowest possible mean squared error among all feasible unbiased estimators. Here, it is clear that if the

inverse of the error covariance metrics ($\mathbf{B}^{-1}$and $\underline{\mathbf{R}}^{-1}$), or the concentration matrices, are ill-conditioned; it is likely that the analysis covariance matrix has very large elements giving rise to large estimation uncertainty and solution instability.

A.2 The Bayesian View

In the Bayesian view, probability is a measure of uncertainty. In this sense, not only observations $\mathbf{y} \in \mathbb{R}^n$ but also the initial state of interest $\mathbf{x}_0 \in \mathbb{R}^m$ is considered probabilistic (random), even though it might be a deterministic quantity; randomness simply represents the limits of our knowledge.

Consequently, in this view, the most likely state is obtained by maximizing the posterior probability, which is the probability of the true state $\mathbf{x}_0$ conditioned on the observational knowledge $\bar{\mathbf{y}}$:

$$\hat{\mathbf{x}}_0^{\mathrm{MAP}} = \underset{\mathbf{x}_0}{\operatorname{argmax}} \left\{ p\left(\mathbf{x}_0 | \underline{\mathbf{y}}\right) \right\}. \tag{A.7}$$

The argument of the above maximization, which is the most likely state of the posterior probability, is called the maximum a posteriori estimator (MAP).

Using the Bayes theorem, monotonicity of the logarithm and ignoring $p\left(\underline{\mathbf{y}}\right)$ which is constant with respect to $\mathbf{x}_0$, we obtain the MAP estimator as follows:

$$\hat{\mathbf{x}}_0^{\mathrm{MAP}} = \underset{\mathbf{x}_0}{\operatorname{argmin}} \left\{ -\log p\left(\underline{\mathbf{y}} | \mathbf{x}_0\right) - \log p(\mathbf{x}_0) \right\}. \tag{A.8}$$

This estimator consists of the two terms: the observations log-likelihood term as also found in the ML estimator defined in (A.4), and *a priori* information about the *probability distribution* of the unknown state of interest $p(\mathbf{x}_0)$. The latter is simply called the *prior*, which represents our subjective and limited knowledge about the true state. The prior needs to be characterized either in a form of full distribution as adopted for the general Bayesian estimation, or just by the mean and covariance as adopted for a suboptimal linear Bayesian estimation (*Levy*, 2008, pp.125). As previously mentioned, the full density of any arbitrary initial state is unknown to us; however, its mean and covariance may be characterized using the background state $\mathbf{x}_0^b \in \mathbb{R}^m$ and its error covariance $\mathbf{B} \in \mathbb{R}^{m \times m}$. In other words, we implicitly assume

$$\mathbf{x}_0 = \mathbf{x}_0^b + \mathbf{w}, \tag{A.9}$$

where $\mathbb{E}\left[\mathbf{x}_0\right] = \mathbf{x}_0^b$ and $\mathbf{w} \sim \mathcal{N}\left(0, \mathbf{B}\right)$ is uncorrelated with the observation error $\bar{\mathbf{v}} \sim \mathcal{N}\left(0, \bar{\mathbf{R}}\right)$. Having the mean and covariance, implies that the prior can be approximated by following Gaussian density:

$$-\log p(\mathbf{x}_0) \underset{\sim}{\propto} \frac{1}{2}(\mathbf{x}_0 - \mathbf{x}_0^b)^{\mathrm{T}} \mathbf{B}^{-1} (\mathbf{x}_0 - \mathbf{x}_0^b). \tag{A.10}$$

By substituting equations (A.4) and (A.10) in (A.8), the MAP estimator reduces to the solution of the classic VDA cost function given in (1.4).

As we see, having the Gaussian approximation for the unknown prior in the VDA problem, the Bayesian MAP estimator can not go beyond the frequentist ML approach. In the next Section, we explain the recently proposed regularized VDA problem and its link to the MAP estimator. From this perspective, we will argue that we can incorporate prior knowledge about the non-Gaussian manifestation of the unknown initial state in the derivative space or any appropriately chosen domain, which typically leads to a more accurate and stable analysis.